



**HAL**  
open science

# Prognosis and Maintenance Modelling for Wind Turbines

Jinrui Ma

► **To cite this version:**

Jinrui Ma. Prognosis and Maintenance Modelling for Wind Turbines. Other. Université de Technologie de Troyes, 2019. English. NNT : 2019TROY0016 . tel-03619049

**HAL Id: tel-03619049**

**<https://theses.hal.science/tel-03619049>**

Submitted on 24 Mar 2022

**HAL** is a multi-disciplinary open access archive for the deposit and dissemination of scientific research documents, whether they are published or not. The documents may come from teaching and research institutions in France or abroad, or from public or private research centers.

L'archive ouverte pluridisciplinaire **HAL**, est destinée au dépôt et à la diffusion de documents scientifiques de niveau recherche, publiés ou non, émanant des établissements d'enseignement et de recherche français ou étrangers, des laboratoires publics ou privés.

Thèse  
de doctorat  
de l'UTT

**Jinrui MA**

# Prognosis and Maintenance Modelling for Wind Turbines



**Champ disciplinaire :**  
Sciences pour l'Ingénieur

2019TROY0016

Année 2019

---

---

# THESE

*pour l'obtention du grade de*

## DOCTEUR

de l'UNIVERSITE DE TECHNOLOGIE DE TROYES

EN SCIENCES POUR L'INGENIEUR

**Spécialité : OPTIMISATION ET SURETE DES SYSTEMES**

*présentée et soutenue par*

**Jinrui MA**

*le 27 juin 2019*

---

---

**Prognosis and Maintenance Modelling for Wind Turbines**

---

---

## JURY

M. P.-E. LABEAU	PROFESSEUR	Président
M. C. BERENGUER	PROFESSEUR DES UNIVERSITES	Rapporteur
M. J. VATN	PROFESSOR	Rapporteur
M. R. SUEUR	INGENIEUR CHERCHEUR	Examineur
Mme M. FOULADIRAD	PROFESSEURE DES UNIVERSITES	Directrice de thèse
M. A. GRALL	PROFESSEUR DES UNIVERSITES	Directeur de thèse

Université de Technologie de Troyes

Spécialité: OPTIMISATION ET SURETE DES SYSTEMES

# **Prognosis and Maintenance Modelling for Wind Turbines**

**Jinrui MA**



## Acknowledgements

First and foremost, I would like to express my deep gratitude to Professor Mitra Fouladirad and Professor Antoine Grall, my Ph.D supervisors, for their enthusiastic encouragement, patient guidance and expert advice throughout my Ph.D project, also for their kindness during the four years.

Special thanks should be given to Professor Christophe Bérenguer and Professor Jørn Vatn for their acceptance as the reviewers of the the thesis, for their useful critiques and comments helping me to improve the manuscript. I would also like to thank the president of my Ph.D defense committee Professor Pierre-Etienne Labeau as well as Mr. Roman Sueur, who are the examiners of the thesis. Thanks for their questions and discussions during the Ph.D defense.

My grateful thanks are also extended to my colleagues in the laboratory of M2S (Modélisation et Sûreté des Systèmes) for their scientific discussions and encouragements, I would like to thank the secretaries of doctoral school and the secretaries of department ROSAS. I wish to thank my friends for their accompany, encouragement and the happy moments with them, especially, Nan Zhang, Binbin Wang and Yurui Han.

I wish to thank my parents for their support throughout my study. Many thanks to my husband Jianbo for helping me achieve my dreams.

Thanks to all the people who I met in France.

Jinrui MA



## Abstract

Nowadays, more and more wind turbines are erected on-shore or off-shore to generate electrical energy from wind. Since the valuable big-size wind turbines automatically operate under harsh environment, undesirable downtime occurs as a consequence of high failure caused by the environment. Therefore, the research about the reliability of wind turbine attract a lot of attention.

The main component studied in this thesis is the hydraulic pitch system which is a crucial component for variable-speed wind turbines. Three subjects are addressed in this thesis: the hydraulic pitch system deteriorating modelling, the remaining useful life estimation of the hydraulic pitch system, and its maintenance policy. The methods proposed in the thesis are not only limited to the hydraulic pitch system, but also can be extended to the dynamic systems that operate under various environment. The main contribution of the thesis is that the influence of the environment (wind speed) is always taken into account. A continuous long-term wind speed model is proposed as a research byproduct in the thesis. A wind turbine simulator with deteriorating hydraulic pitch system is established to carry out the numerical simulations.

This thesis can be considered as an application about stochastic processes on the field of wind energy. Such as the wind speed model based on a two-level Markov chain embedded diffusion processes, the deterioration process of hydraulic pitch system modeled by a gamma process and Markov chain. On these basis, the remaining useful life and the unavailability of wind turbine are discussed.

**Key words:** Wind turbines, Winds-Speed, Stochastic processes, Service life (Engineering), Maintenance



## Résumé

De plus en plus d'éoliennes sont exploitées pour produire de l'énergie électrique. Les éoliennes de grande taille fonctionnent de manière automatique dans des conditions environnementales souvent difficiles. Il en résulte des dégradations et des défaillances provoquant des arrêts indésirables. En conséquence, les recherches sur la fiabilité des éoliennes attirent beaucoup d'attention. Le principal composant étudié dans cette thèse est un composant crucial pour les éoliennes à vitesse variable : le système hydraulique d'orientation des pales.

Trois sujets sont abordés : la modélisation de la détérioration du système hydraulique de contrôle de l'angle de tangage, l'estimation de sa durée de vie utile restante et une politique de maintenance. La principale contribution de la thèse est la prise en compte de l'influence de l'environnement caractérisé par la vitesse du vent. Un modèle continu à long terme d'évolution de la vitesse du vent est proposé. Un simulateur d'éolienne avec système hydraulique de contrôle de tangage se détériorant est établi pour effectuer les simulations numériques.

Cette thèse illustre l'intérêt des processus stochastiques pour la modélisation dans le domaine de l'énergie éolienne. Le modèle de vitesse du vent s'appuie sur une chaîne de Markov à deux niveaux avec diffusion intégrée. Le processus de détérioration du système hydraulique de contrôle est modélisé par un processus gamma couplé à une chaîne de Markov. Sur cette base, la durée de vie et l'indisponibilité de l'éolienne sont modélisées, évaluées et utilisées pour l'aide à la décision de maintenance.

**Mots-clés :** Eoliennes; Vents – Vitesse; Entretien; Processus stochastiques; Durée de vie (ingénierie)



## General introduction

Since the Paris Agreement has been signed among the 195 members of the United Nations Framework Convention on Climate Change (UNFCCC), an increasing number of countries have announced their plans to reduce the emission of  $CO_2$  and to develop alternative clean energy like wind energy, solar energy, and tidal energy, etc. In recent years, due to the ability of its worldwide exploitation and the rapid technical development of wind turbines, the clean and renewal wind energy is occupying a large section of the energy market. In Europe, the wind energy production in 2016 reached 13489.9 MW and the estimated electricity production from wind power in the Europe Union (EU) in 2016 is 302.7 TWh [1]. By 2030, wind energy could cover almost 30% of EU's electricity demand [2]. However, because of the inherent randomness of wind speed, the wind power industry faces enormous challenges in practice that makes the comprehensive and efficient development of wind power industry being considerably restricted.

One of the main issues to enhance the wind power development is the wind forecasting in short and long-term for different geographical sites. Wind speed modelling is crucial to study the reliability of the wind turbines, to estimate the remaining useful life (RUL) of their key components, to give an accurate output power forecasting, control strategy optimization, etc.

As a wind turbine operates in a harsh and varying environment, wind turbines have higher failure rate compared with other gas/steam turbines used in the energy industry. The study about the reliability of wind turbine is always attractive, for wind turbines are expected to service more than decades, even two decades. However, the operation and maintenance (O&M) costs of wind power which accounts for 20%-30% of the cost for a wind turbine project, are higher than desirable. Additionally, with the extension of wind farm to offshore, the influence of environment (such as the wide wind speed range of operation, the inherent characteristic of wind speed/wave), brings new challenges to this topic. The continuous changeable operational environment makes wind turbine withstand constantly changing loads, leading to gradual changes in the critical components' performance (blade, pitch system, bearing, gearbox et etc.). In other words, the deterioration of performance over time results in failures. Hence, it is necessary to monitor the deterioration process, estimate the current health status and predict the remaining useful life (RUL) for critical wind turbine components. Prediction and health management (PHM) is one of the useful strategies to improve the reliability of system and reduce the OM cost. The RUL prediction according to the information provided by condition monitoring system (CMS) is a key procedure of PHM, due to its important role in maintenance policy decision and operation optimization. To appropriately organize maintenance schedule in long-term and budget maintenance cost, it is necessary study the unavailability of wind turbine.

In **Chapter 1**, a brief review of the literature on the evolutions of wind turbine is presented. The existing wind speed model, condition monitoring, deterioration model, maintenance and maintenance policies and stochastic processes are introduced, respectively

In **Chapter 2**, we devote to realize a wind turbine simulator that combines a deteriorating hydraulic pitch system. As the 5-MW baseline wind turbine developed by the National Renewable Energy Laboratory (NREL) is the base of the work, an introduction about it will be given firstly, followed by an introduction about pitch control system (control strategy and pitch actuator). Then a method about the deteriorated hydraulic system modelling is arranged. Finally, this chapter ends with the wind turbine simulator realization method in the environment of Matlab/simulink<sup>®</sup>.

In **Chapter 3**, a continuous wind speed generation method based on a 2-level Markov chain and stochastic differential equations (SDEs) is proposed. Two SDEs are discussed in this model framework. This model is capable of generating wind speed with different time scales. For example, a one-second step wind speed generation can be performed during 10 minutes or for a few hours based on SDEs. In line with the short time generation, a long-term generation for a few months or years can be generated based on the outer Markov chain. The developed model is particularly suitable to be merged with the deterioration model of wind turbine's key component, like blade-pitch system. Furthermore, this model could be applied for studies of wind turbine's power system like the dynamic behavior of generator. This chapter is a part of a global modeling framework which allows jointly short-term wind speed generation for closed-loop control of wind turbine and long-term wind speed prognosis for the estimations about the remaining useful lifetime and the unavailability.

In **Chapter 4**, RUL estimation methods for different timescales are proposed. According to the historical climate data, windy season appears in a certain season and wind speed has its distribution over a year. Hence, we can consider that the environment (wind speed) where wind turbines operate have a stationary distribution. A RUL estimation methods based on the stationary distribution is discussed. Moreover, we proposed a N-step RUL estimation model by means of matrix, which is a speed and less computational consumption method.

It should be kept in mind that the operational environment of wind turbine is various and harsh so that the maintenance can not be carried out whenever we want. Therefore, a random maintenance delay exists according to the environment condition. To prevent failure caused by the deterioration during the maintenance delay, it is necessary to propose an alarm threshold. When the deterioration level exceeds the threshold, maintenance can be prepared and once the environment condition allows to maintain, it can be carried out immediately. Therefore, in **Chapter 5**, we discuss the unavailability model considering the maintenance delay for wind turbine.

In **Chapter 6**, the conclusions are made and future perspectives are discussed.

# Contents

<b>Acknowledgements</b>	<b>i</b>
<b>Abstract</b>	<b>iii</b>
<b>Résumé</b>	<b>iii</b>
<b>General introduction</b>	<b>v</b>
<b>1 State-of-the-art</b>	<b>1</b>
1.1 Main components of wind turbine . . . . .	1
1.2 Wind turbine operation . . . . .	3
1.3 Wind turbine development tendency . . . . .	4
1.4 Wind turbine reliability, wind influence and wind speed model . . .	8
1.4.1 Wind turbine reliability and wind influence . . . . .	8
1.4.2 Wind speed model . . . . .	11
1.4.2.1 Time series models . . . . .	11
1.4.2.2 Artificial Intelligence model . . . . .	13
1.5 Prognostics and health management for wind turbine . . . . .	13
1.5.1 Condition monitoring . . . . .	14
1.5.1.1 Condition monitoring technology for wind turbine .	14
1.5.2 Deterioration phenomena of wind turbine components . . . .	16
1.5.3 Remaining useful life estimation . . . . .	17
1.5.4 Maintenance and maintenance policies . . . . .	18
1.5.4.1 Maintenance actions . . . . .	18

1.5.4.2	Maintenance policies with corrective policy . . . . .	19
1.6	Mathematical tools for wind speed and deterioration modelling: stochastic processes . . . . .	21
1.6.1	Markov chain . . . . .	21
1.6.2	Gamma process . . . . .	22
1.6.3	Wiener process . . . . .	23
1.6.4	Ornstein-Uhlenbeck process . . . . .	24
1.6.5	Regenerative process . . . . .	25
1.7	Conclusions . . . . .	25
<b>2</b>	<b>Wind turbine simulator</b>	<b>27</b>
2.1	Introduction . . . . .	27
2.2	NREL 5-MW baseline wind turbine and its pitch control system . . . . .	27
2.2.1	NREL 5-MW baseline wind turbine properties . . . . .	27
2.2.2	Pitch control system . . . . .	30
2.2.2.1	Pitch control strategy . . . . .	32
2.3	Hydraulic pitch system: principle and failures . . . . .	32
2.3.1	Principle of hydraulic pitch system . . . . .	32
2.3.2	Failures of hydraulic pitch system . . . . .	33
2.4	Deteriorating hydraulic pitch system modelling . . . . .	34
2.4.1	Fault-free hydraulic pitch system model . . . . .	34
2.4.2	Parameters for deteriorated hydraulic pitch system . . . . .	34
2.4.3	Response of deteriorated hydraulic pitch system . . . . .	35
2.4.4	Deteriorated hydraulic pitch system model considering wind speed influence . . . . .	36
2.5	Realization with Matlab/simulink . . . . .	37
2.6	Deterioration indicator for hydraulic pitch system . . . . .	38
2.7	Conclusion . . . . .	39

<b>3</b>	<b>Wind speed model</b>	<b>40</b>
3.1	Introduction . . . . .	40
3.2	Wind Model description . . . . .	42
3.2.1	General description . . . . .	42
3.2.2	Markov chain embedded with SDE . . . . .	44
3.2.3	OU process for wind generation . . . . .	47
3.2.3.1	OU process for class 1 . . . . .	48
3.2.3.2	OU process for class 2 . . . . .	48
3.2.3.3	Markov chain model for two switching wind class . . . . .	49
3.3	Wind speed generation procedure . . . . .	49
3.3.1	Experimental dataset . . . . .	49
3.3.2	Wind speed generation . . . . .	49
3.3.2.1	Generation of macroscopic wind speed using Markov chain model . . . . .	51
3.3.2.2	Continuous generation of wind speed using SDE . . . . .	51
3.4	Application and comparison . . . . .	55
3.4.1	Wind turbine simulator . . . . .	55
3.4.2	Comparative Discussion . . . . .	57
3.5	Conclusion . . . . .	59
<b>4</b>	<b>Hydraulic pitch system remaining useful life estimation</b>	<b>60</b>
4.1	Introduction . . . . .	62
4.2	Simplification and model description for the deteriorating system . . . . .	64
4.2.1	Model for operational environment states . . . . .	66
4.2.2	Model for the deterioration indicator under various operational environment state . . . . .	66
4.3	Remaining useful life prediction . . . . .	67
4.3.1	Case 1: RUL estimation for a long period $\tau$ . . . . .	67
4.3.2	Case 2: RUL estimation considering the current operational environment state . . . . .	69

4.3.2.1	One-step forward RUL prediction . . . . .	70
4.3.2.2	Two-step forward RUL prediction . . . . .	70
4.3.2.3	Approximation of the N-step forward RUL prediction: algebraic expression . . . . .	71
4.4	Numerical results and analysis . . . . .	73
4.4.1	Parameters estimation . . . . .	74
4.4.2	Numerical results for indicators prediction . . . . .	76
4.4.2.1	N-step prediction when N is small . . . . .	77
4.4.3	Numerical results for remaining useful life prediction . . . . .	79
4.4.4	Discussions . . . . .	81
4.5	Conclusions . . . . .	82
<b>5</b>	<b>Unavailability model</b>	<b>83</b>
5.1	Motivation . . . . .	83
5.2	Simplifications, assumptions and maintenance policy . . . . .	84
5.2.1	Operational environment simplification . . . . .	84
5.2.2	Maintenance policy . . . . .	84
5.2.3	Stationary assumption . . . . .	85
5.3	Asymptotic unavailability model for wind turbine . . . . .	86
5.3.1	Hitting time in the alarm threshold $\mathbb{E}(\sigma_A)$ . . . . .	87
5.3.2	Maintenance delay $\mathbb{E}(\tau)$ . . . . .	88
5.3.3	Unavailable period caused by maintenance or failure $\mathbb{E}((\sigma_A + \tau - \sigma_F)\mathbb{1}_{\{\sigma_F \leq \sigma_A + \tau\}})$ . . . . .	90
5.4	Approximation of the asymptotic unavailability . . . . .	91
5.5	Numerical experiment . . . . .	92
5.6	Conclusion . . . . .	94
<b>6</b>	<b>Conclusion and perspective</b>	<b>96</b>
6.1	Conclusions . . . . .	96
6.2	Perspective . . . . .	97

<b>7</b>	<b>Résumé de Thèse en Français</b>	<b>99</b>
7.1	Introduction . . . . .	99
7.1.1	Fiabilité des éoliennes et influence du vent . . . . .	102
7.2	Modèle de génération de la vitesse du vent . . . . .	105
7.2.1	Description du modèle de vent . . . . .	105
7.2.1.1	Description générale . . . . .	105
7.2.1.2	Chaîne de Markov intégrée avec SDE . . . . .	106
7.2.1.3	Processus d'OU pour la production d'énergie éolienne	108
7.2.1.4	Modèle de chaîne de Markov pour deux classes de vent de commutation . . . . .	109
7.2.2	Procédure de génération de la vitesse du vent . . . . .	110
7.3	Estimation de la durée de vie utile résiduelle . . . . .	111
7.3.1	Simplification et description du modèle pour le système en détérioration . . . . .	111
7.3.2	Prévision de la durée de vie utile restante . . . . .	113
7.3.2.1	Cas1 : Estimation RUL pour une étiquette assez longue $\tau$ . . . . .	114
7.3.2.2	Cas 2 : Estimation RUL tenant compte de l'état actuel de l'environnement opérationnel . . . . .	115
7.3.2.3	Prédiction RUL en deux étapes . . . . .	116
7.4	Modèle d'indisponibilité pour éolienne . . . . .	117
7.4.1	Simplifications, hypothèses et politique de maintenance . . . . .	117
7.4.1.1	Simplification de l'environnement opérationnel . . . . .	117
7.4.1.1.a	Maintenance policy . . . . .	118
7.4.1.2	Hypothèse stationnaire . . . . .	118
7.4.2	Modèle d'indisponibilité asymptotique pour les éoliennes . . . . .	119
7.4.3	Temps d'activation dans le seuil d'alarme $\mathbb{E}(\sigma_A)$ . . . . .	120
7.4.4	Maintenance attente $\mathbb{E}(\tau)$ . . . . .	120
7.4.5	Temps indisponible dû à un entretien ou à une panne . . . . .	121

<b>Bibliography</b>	<b>122</b>
---------------------	------------



# List of Tables

- 1.1 Evolution of wind turbine rated power . . . . . 7
- 1.2 Basic SCADA parameters . . . . . 15
- 2.1 General properties of the NREL 5-MW baseline wind turbine . . . . . 28
- 2.2 Blade structural properties . . . . . 28
- 2.3 Hub and nacelle properties . . . . . 29
- 2.4 Drivetrain properties . . . . . 29
- 2.5 Drivetrain properties . . . . . 29
- 2.6 Wind turbine control aims with respect to wind speed . . . . . 31
- 3.1 Example for Markov chain state space . . . . . 44
- 3.2 Transition probability for SSM . . . . . 49
- 3.3 Estimation of Transition Probability Matrix . . . . . 51
- 3.4 Estimated value for SDE . . . . . 52
- 4.1 Switches among different operational status for a wind turbine ( $\surd$  means that the switch between the two status is possible, while  $\times$  means not possible ) . . . . . 63
- 4.2 Parameters of gamma process that are piecewise constant and related to the operational environments . . . . . 67
- 4.3 The states of operational environment . . . . . 75
- 4.4 Parameters for deterioration model related to different operational environments . . . . . 76
- 4.5 Proportion time in each operational state . . . . . 76
- 4.6 Parameters for case 1 . . . . . 76

4.7	1-step prediction results for $D_t, (t=0,10,20,30,40,50)$ . . . . .	77
4.8	1-step, 3-step and 5-step prediction results according to $D_0$ . . . . .	79
5.1	Parameters for deterioration model related to different operational environments . . . . .	93
5.2	Probability of system stays in each operational environment state . . . . .	93
5.3	Unavailability of system corresponding to different alarm threshold $L_A$ . . . . .	94
7.1	Évolution de la puissance nominale des éoliennes . . . . .	100
7.2	Probabilité de transition pour SSM . . . . .	110
7.3	Paramètres du procédé gamma qui sont constants par morceaux et en relation avec les environnements opérationnels . . . . .	113

# List of Figures

- 1.1 Structure of wind turbine with gearbox (Source: [3]) . . . . . 2
- 1.2 Structure of directive wind turbine (Source: [4]) . . . . . 2
- 1.3 Gedser wind turbine, 200 kW, D = 24 m, Denmark 1957 (Source: [5]) 5
- 1.4 TVIND wind turbine, 2 MW, D = 54 m, Denmark 1977 (Source: [6]) 6
- 1.5 Evolution of wind turbine size and power (Source: [7]) . . . . . 7
- 1.6 Expected cumulative installed capacity until 2020 . . . . . 8
- 1.7 Average rate of failure VS wind turbine component (Source [8]) . . 9
- 1.8 Rate of failure VS hours lost per failure:Sweden(SWE), Finland(FIN),  
(DEU) and Germany(DEU-LKW) (Source [8]) . . . . . 9
- 1.9 Average monthly Failure Rate and WEI for each of the 12 months  
over the Survey period 1994-2004(source: [9]) . . . . . 10
- 1.10 Summary of cross-correlograms of subcomponent failure rates to  
WEI, 1994-2004 (source: [9]) . . . . . 10
- 1.11 Maintenance types . . . . . 19
  
- 2.1 Operation ranges and control of a variable speed wind turbine with  
a power control by pitch system . . . . . 30
- 2.2 Flowchart of the baseline control pitch system for NREL 5-MW  
wind turbine . . . . . 32
- 2.3 Diagram for a hydraulic pitch actuator . . . . . 33
- 2.4 Wind turbine behavior according to the wind speed . . . . . 35
- 2.5 Transition among the operational states of variable-speed wind turbine 36
- 2.6 A sample for APR value . . . . . 37
- 2.7 Wind turbine simulator with a deteriorating hydraulic pitch system 38

3.1	Wind speed series . . . . .	42
3.2	Wind speed generation model — 2-level Markov chain model embedded with SDE . . . . .	43
3.3	Three classes of wind speed fluctuation PDF (Source: [10] ) . . . . .	46
3.4	symmetrical PDF . . . . .	46
3.5	dissymmetrical PDF . . . . .	47
3.6	bimodal PDF . . . . .	47
3.7	Steps for wind speed generation . . . . .	50
3.8	Hourly average wind speed generation (m/s) . . . . .	51
3.9	10 sec. wind speed generation of class 1 . . . . .	52
3.10	10 minutes speed generation of class 1 . . . . .	53
3.11	10 sec. wind speed generation of class 2 . . . . .	53
3.12	10 minutes speed generation of class 2 . . . . .	54
3.13	Probability density function of real data and simulated data . . . . .	54
3.14	Wind speed simulation with Markov chain embedded with diffusion processes . . . . .	55
3.15	10 minutes average wind speed data during 30 days . . . . .	56
3.16	wind turbine simulator model . . . . .	56
3.17	Output power and pitch angle of NREL 5MW wind turbine . . . . .	57
3.18	Comparison example . . . . .	58
4.1	Operation ranges and control of a variable speed wind turbine with a power control by pitch system . . . . .	61
4.2	Diagram for the explanation about a deteriorating system operating under various operational environment . . . . .	65
4.3	Illustration of one-step forward prediction . . . . .	70
4.4	Illustration of two-step forward prediction . . . . .	71
4.5	Comparison of the CDFs of deterioration increment . . . . .	74
4.6	(a)Ten trajectories of the deterioration of $\omega_{nD}$ (b)Estimated natural frequency $\hat{\omega}_n$ in $e_8$ . . . . .	75
4.7	Simulated deterioration indicator $D_t$ . . . . .	76

4.8	1-step forward prediction for deterioration indicator Probability density of 1-step prediction for deterioration indicator $D_0, D_{10}, D_{20}, D_{30}, D_{40}$ and $D_{50}$ , respectively . . . . .	78
4.9	1-step, 3-step and 5-step prediction results for the deterioration indicator $D_0$ . . . . .	79
4.10	Predicted probability of system surviving at time T $\mathbb{P}(t = T)$ according to indicators $D_0, D_{10}, D_{20}, D_{30}, D_{40}$ and $D_{50}$ , respectively .	80
4.11	Predicted cumulative probability of system surviving at time T $\mathbb{P}(t = T)$ according to indicators $D_0, D_{10}, D_{20}, D_{30}, D_{40}$ and $D_{50}$ , respectively . . . . .	81
5.1	Two subsets of the operational environment . . . . .	84
5.2	Description of the maintenance policy in case of $\sigma_F \geq \sigma_A + \tau$ . . . . .	85
5.3	Description of the maintenance policy in case of $\sigma_F \leq \sigma_A + \tau$ . . . . .	85
5.4	Original Markov chain . . . . .	89
5.5	Markov chain $Y$ . . . . .	89
5.6	Numerical experiment results of the unavailability according to different alarm threshold $L_A$ . . . . .	94
7.1	Taux de défaillance moyen des composants d'éolienne VS (Source [8])	102
7.2	Taux d'échec VS heures perdues par échec : Suède(SWE), Finlande(FIN), (DEU) et Allemagne(DEU_LKW) (Source [8]) . . . . .	103
7.3	Taux d'échec mensuel moyen et IFE pour chacun des 12 mois de la période de l'enquête 1994-2004(source: [9]) . . . . .	103
7.4	Résumé des corrélogrammes croisés des taux de défaillance des sous-composantes de l'IFE, 1994-2004 (source: [9]) . . . . .	104
7.5	Wind speed generation model — 2-level Markov chain model embedded with SDE . . . . .	106
7.6	Etapas pour la génération de la vitesse du vent . . . . .	110



# Chapter 1

## State-of-the-art

Wind is one of the earliest powers used by man. Wind turbine is developed with human's requirements such as grind grain, pump water, cut lumber, etc. Nowadays, wind turbine is widely known for its utilisation of power generation. To ensure a safe operation, and the reliability of wind turbine becomes a challenge along with the rapid developments of wind turbine.

In this chapter, we will introduce the developments and evolutions of wind turbine, which lead to the challenges about wind turbine's reliability. The reliability of wind turbine is a wide subject that contains different objects, methods and technologies. However, this thesis mainly focuses on one component that is the hydraulic pitch system. We studied its deterioration modelling by the means of stochastic process. Moreover we study its remaining useful life estimation and the unavailability for wind turbine caused by the maintenance of hydraulic pitch system. As the wind turbine totally operates under variable environment, in our opinion, the influence of operational environment (especially the wind speed) should be taken into account in the study. Therefore, in this chapter, we will give a state-of-the-art about the evolution of wind turbine, wind speed model, condition monitoring, deterioration model, maintenance and maintenance policies.

### 1.1 Main components of wind turbine

Wind turbine with gearbox (structure shown in Figure 1.1) and directive-drive wind turbine (structure shown in Figure 1.2) share the commercial wind power market. The latter is also called gearless wind turbine whose rotor is directly connected with a permanent magnet generator. The main components of wind turbine are listed as follows:

- Rotor

It is the heart of a wind turbine which contains the blades and the hub. Blades are used to capture the wind energy and convert it into mechanical energy to force the rotor to rotate. Hub is used to support the blades and is connected to other parts of the wind turbine.

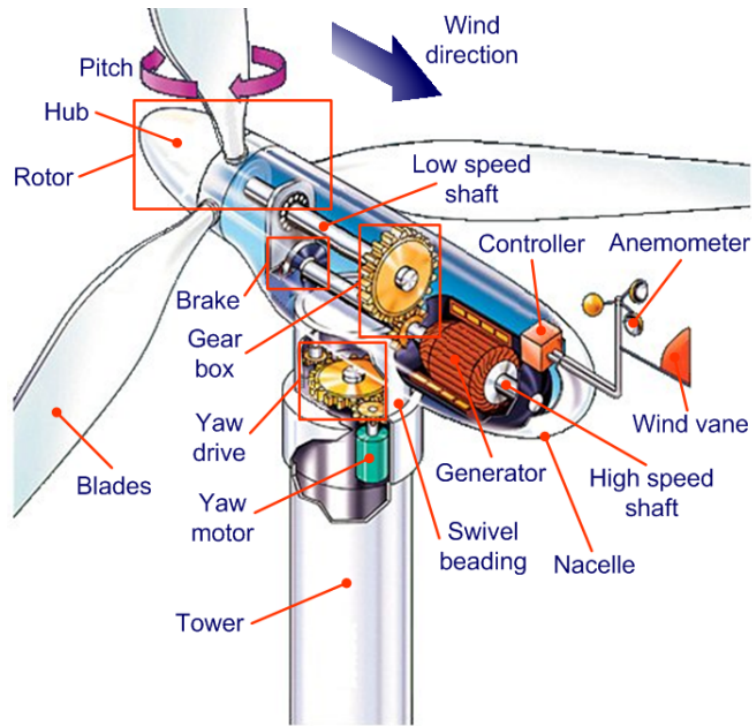


Figure 1.1: Structure of wind turbine with gearbox (Source: [3])

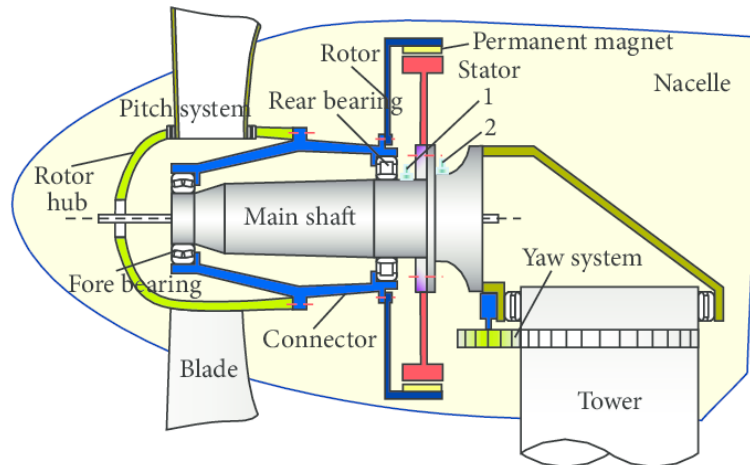


Figure 1.2: Structure of directive wind turbine (Source: [4])

- Pitch system

Pitch system turns the blades in/out of the wind to keep the rotor rotating in a larger wind speed range. It is also an important power adjustment system for variable speed wind turbine. It limits the power generation at the rated output power and helps wind turbine to catch as much as possible wind energy when wind speed is low. It consists of a control system and actuators.

- Nacelle

Nacelle is installed at the top of tower connecting the rotor and the tower.

It covers and protects the components inside itself from different weather conditions.

- Yaw system

Yaw system makes the rotor face into the wind when the wind direction changes. It consists of a control system and actuators.

- Gearbox (Not for directive-drive wind turbine)

It connects the low-speed shaft (connecting to rotor) to the high-speed shaft which connected to the generator.

- Generator

It converts the wind energy to electrical power. The most commonly used generators for wind turbines with gearbox are the synchronous AC generators or the induction generator.

- Anemometer

It is applied to measure the wind speed and sends it to SCADA.

- Tower

Due to surface aerodynamic drag caused by land or water surface, wind velocities increase at higher altitudes. The tower helps the nacelle to stand at a high altitude so that improving the power generation of wind turbine.

## 1.2 Wind turbine operation

The operation of wind turbine is automatically controlled according to the condition of wind. A normal wind turbine operation procedure is as follows:

### 1. System test

The rotor position is checked and changed if necessary, the system is checked for faults. If no irregularities are detected, the wind turbine is ready for operation.

### 2. Idling

The wind turbine stands with braked rotor and is turned into the wind inflow direction by the yaw system. With the wind speed measurement data providing by the anemometer, the system determines when the starting level wind speed has been reached.

### 3. Initiation

The rotor blades are pitched into the wind, and the mechanical rotor brake is released. The rotor starts to rotate.

### 4. Powering up

The rotor speed increases until the synchronization speed of the generator is reached. If the synchronization speed can be maintained constant over a specified period, the generator is then coupled to the grid.

## 5. Power generation

If the generator has successfully started the operation, power is delivered to the power grid.

## 6. Power off

If the wind speed is too strong and exceed the cut-out wind speed, the system is completely stopped by using of the mechanical brake.

# 1.3 Wind turbine development tendency

The initial wind turbines were passive stall-regulated load control, working in a narrow wind speed range. Paul La Cour designed the first wind turbine for the direct current production in 1891 [11]. After the First World War, due to the experience of propeller design for aircraft, the scientific understanding of wind turbine design greatly stepped forward in Europe. With the new theoretical background of wind turbine, many promising methods for the modern wind turbine design emerged. The wind turbine WIME D-30 with a diameter of 30 m and a power of 100 kW operated from 1931 to 1942 in Crimea [12] and produced power into a small 20 MW grid. However, the start of the Second World War ruined these models. With the reconstruction of Europe after the war, the developments of wind turbine attracted again the researchers. Some prototypes of wind turbine were fabricated and provided electricity to the grid. Such as the famous Gedser wind turbine [5], TVIND wind turbine [6], shown in Figure 1.3 and Figure 1.4, respectively. After 1980, the renaissance of the wind energy started tremendously in Europe and the USA. After almost 40 years, wind turbine shares a part of the electricity market. It is necessary to summarise the evolutions about site, size, power, and control of wind turbine so that the research background of this thesis can be unfolded.

- **Evolution of site**

In order to catch as much as possible wind energy, onshore wind turbines are being erected in remote locations with abundant wind resource. Nowadays, offshore wind power has successfully attracted interest in some countries, such as Denmark, China, UK, Netherlands and Germany, because of its excellent wind resource and the avoidance of land-use issues. With the development of support technologies, wind turbines are being erected from shallow water (for fixed foundation wind turbine) to deeper water (for floating wind turbine).

- **Evolution of size**

If the aircraft Airbus A380 with a 79.75 m wingspan is regarded as a giant, commercial wind turbines in our days should be called super-giant, as their rotor's diameters easily exceed 100 m. Referring to the modern wind turbine fabricated after the year 2004 shown in Figure 1.5, their total heights are at



Figure 1.3: Gedser wind turbine, 200 kW,  $D = 24$  m, Denmark 1957 (Source: [5])

least 150 *m*. The power of wind  $P$  that flows through an area  $A$  at a velocity  $v$  is

$$P = \frac{1}{2}\rho Av^3 \quad (1.1)$$

where  $\rho$  is the air density.  $P$  is proportional to the cross-sectional area  $A$ , hence, improving the area of rotor is an efficient way to capture much more energy with the same wind speed  $v$ . The rotor diameter of the newest Siemens offshore wind turbine SG 10.0-193DD is 193 m [13]. Nowadays, the size limit of a wind turbine is unknown. With the ambition for capturing enormous energy, larger wind turbine may appear in the future.

- **Evolution of rated power**

According to Yang et al. [14], wind turbines are becoming larger with higher rated power, as shown in Table 1.1.

- **Evolution of control**

In the beginning, wind turbines were passive stall-regulated load control, fixed-rotational speed, working in a narrow wind speed range. Then, variable-speed wind turbine with active pitch control appeared. The application of blade-pitch control has allowed modern wind turbines to be larger and capable of operating over wider wind speed ranges. However, researchers are



Figure 1.4: TVIND wind turbine, 2 MW,  $D = 54$  m, Denmark 1977 (Source: [6])

trying to develop intelligent blade that can measure wind speed and automatically adapt itself to wind conditions [15]. It is believed that with the intelligent blades, the reliability and efficiency of wind turbine can be enhanced.

- **Evolution of cumulative installed capacity**

According to the report of Wind EUROPE [16], the total cumulative installed capacity in Europe will reach 204 GW in 2020, shown in Figure 1.6.

Therefore, wind turbines are giant machines that automatically operate at remote places or off-shore under harsh and random environment without a human supervisor. As a costly power generator and with increasing contribution to grid, the reliability of wind turbine is an important issue. However, its operation environment, the location of site and size of wind turbine bring a lot of challenges to reliability and maintenance of wind turbine:

- **Challenges caused by site**

The remote site of wind farm may not be accessible all the time. Hence, the maintenance activities for wind turbine only can be carried out during an accessible time period. It requires prediction and planning. The deteriorated components that are likely to fail during the unaccessible time period need to be repaired / replaced in advance to avoid undesirable downtime.

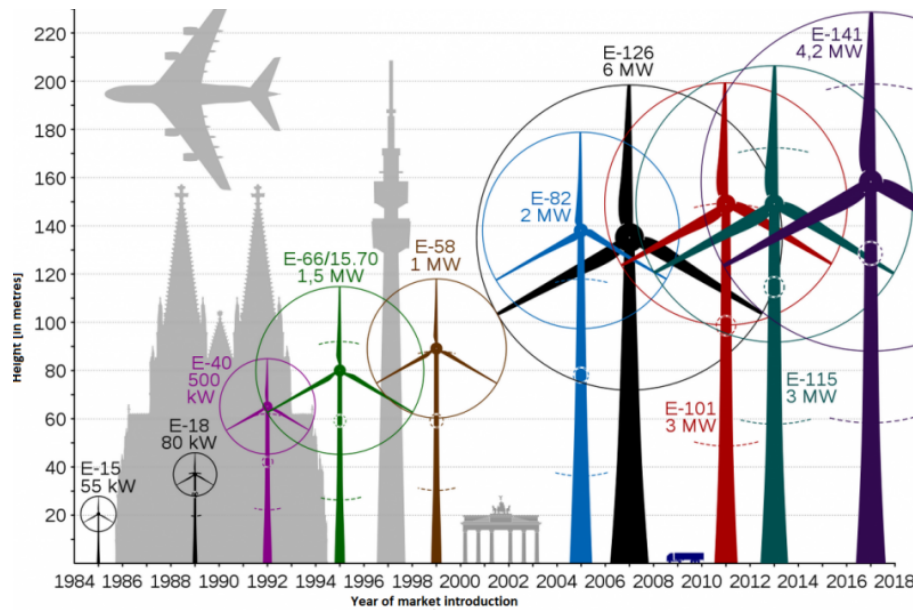


Figure 1.5: Evolution of wind turbine size and power (Source: [7])

Table 1.1: Evolution of wind turbine rated power

Manufacturer	Wind turbine model	Rated power
Repower	M104	3.4 MW
GE	4.0-110	4.0MW
Gamesa	G-128	4.5MW
Enercon	E-126	7MW
Wind Power Ltd	Aerogenerator X	10MW (in development)

- **Challenges caused by size**

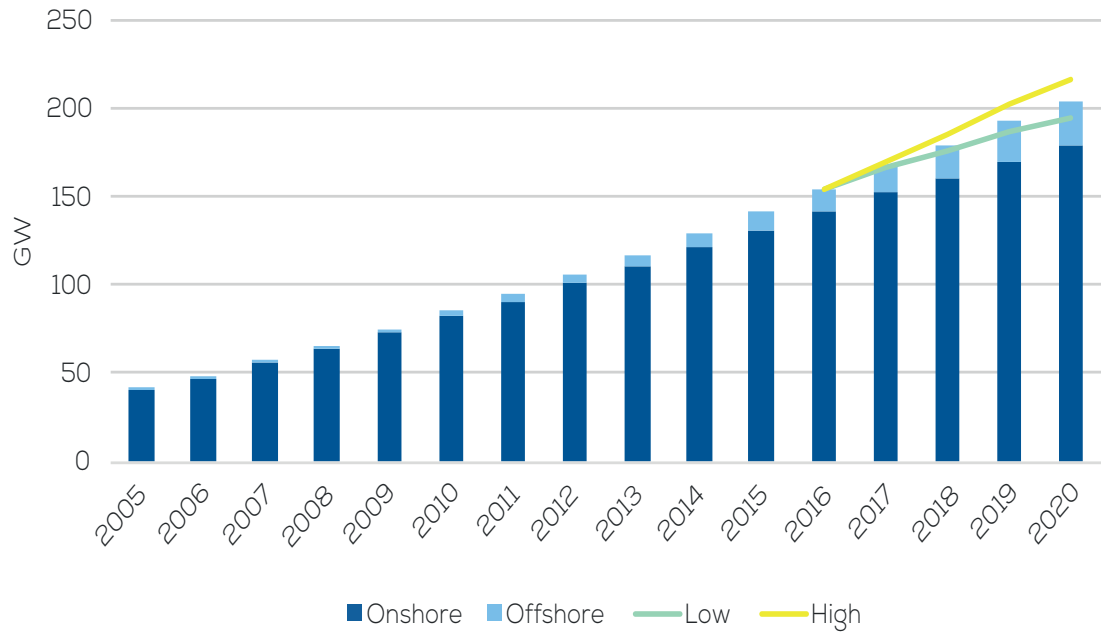
To carry out maintenance activities, the increasing size of wind turbine may need special vehicles or equipments. Besides, the rapid growth in design size that lacks a practical operational experience may cause unexpected failures.

- **Challenges caused by control system**

The control systems used for pitch, generator and converter are more and more sophisticated. However, the electrical and electronic components are showing that they are less reliable than mechanical components. Further more, the existing condition monitoring system are not effective for detecting electrical and electronic failures. The downtime caused by electrical and electronic components failures are more significant in remote location and offshore because of the reduced accessibility.

To improve the reliability of wind turbines, several methods can be considered:

1. Improving wind turbine's design theory and magnification technology.



Source: WindEurope

Figure 1.6: Expected cumulative installed capacity until 2020

2. Developing advanced condition monitoring system for wind turbine.
3. Predicting the remaining useful life of wind turbine, and providing reasonable and economical maintenance schedules for wind turbines in service.

The work of this thesis can be classified into the last method. But it is also an essential part for the advanced condition monitoring system, as the latter need to merge a prognostic module.

## 1.4 Wind turbine reliability, wind influence and wind speed model

### 1.4.1 Wind turbine reliability and wind influence

Many efforts have been made to collect wind turbine reliability data [17, 18, 19, 20, 21, 22, 23].

According to Figure 1.7 and 1.8, blade/pitch, electric and control systems have high failure rates; failure of gearboxes, blades and generators result in higher downtime. J.M. Pinar Pérez et al [8] also concluded that larger wind turbines tended to suffer more failures than smaller ones.

#### Wind influence on reliability

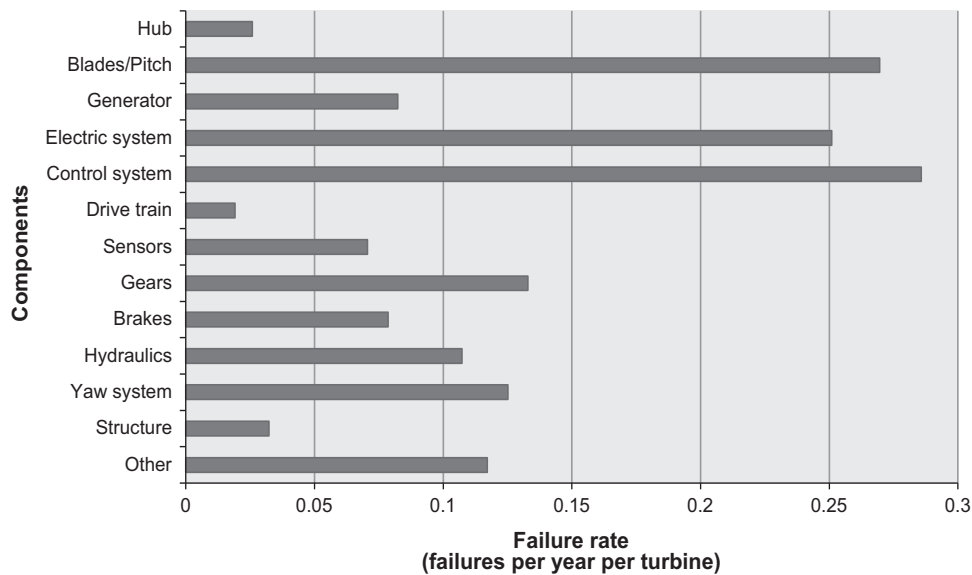


Figure 1.7: Average rate of failure VS wind turbine component (Source [8])

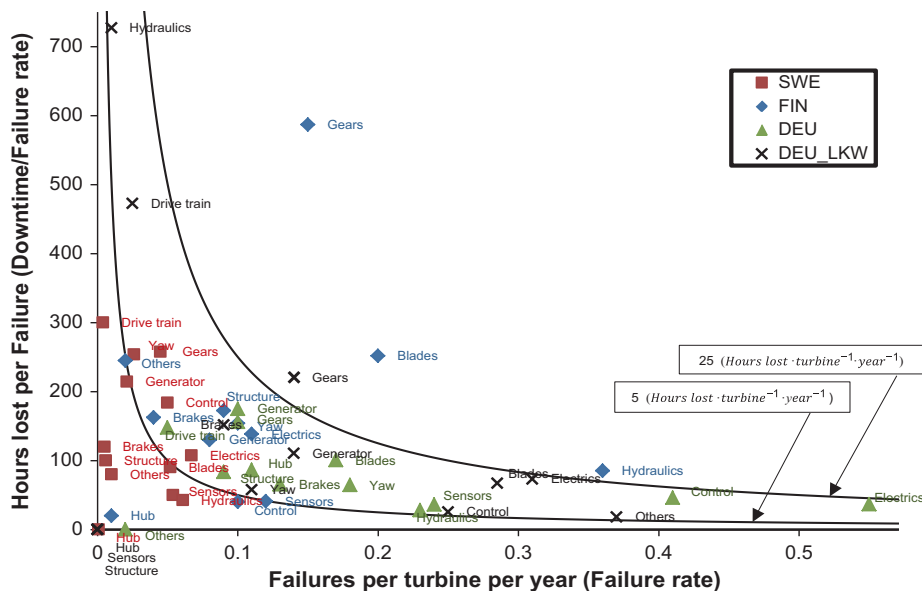


Figure 1.8: Rate of failure VS hours lost per failure:Sweden(SWE), Finland(FIN), (DEU) and Germany(DEU-LKW) (Source [8])

Different from other gas/steam turbines, this regulation is highly affected by wind, especially, the wind speed. P.Tavner et al [9] is concerned with the influence of wind speed on the reliability of wind turbine. This research quantifies the wind speed data as Wind Energy Index (WEI) which is defined as the ratio

$$WEI = \frac{\text{Actual monthly energy production from a collection of wind turbines}}{\text{Long term expected monthly energy production from those turbines in the presence of average weather}}$$

Figure 1.9 shows the relationship between the failure rate and WEI. From this figure and the research result of [19], it is obvious that weather and wind speed

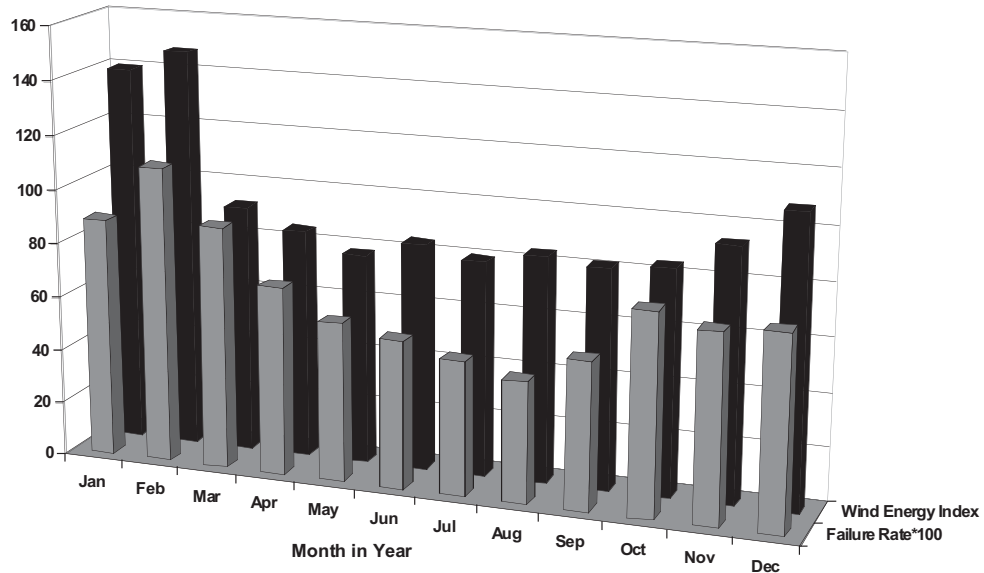


Figure 1.9: Average monthly Failure Rate and WEI for each of the 12 months over the Survey period 1994-2004(source: [9])

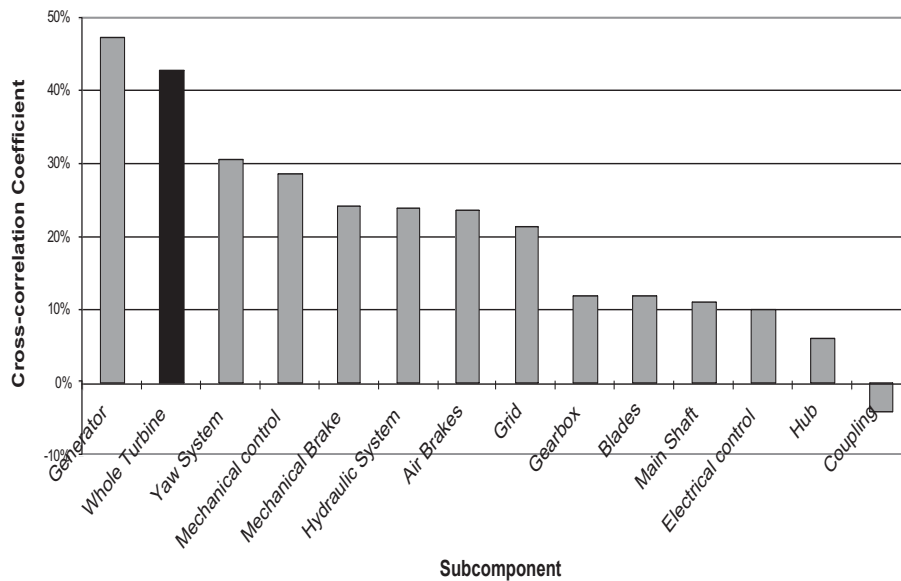


Figure 1.10: Summary of cross-correlograms of subcomponent failure rates to WEI, 1994-2004 (source: [9])

have significant influence on WT components deterioration and failure. Moreover, they point out that some WT components are more affected by wind speed than others, such as hydraulic system, generator, yaw control and mechanical brake (see Figure 1.9). In the opinion of the author, the reason is that these components are not designed with the rapidly changing effects of the wind speed variation. A Chinese report about WT pitch failure affirms that most pitch system failures occur in windy seasons as a consequence of high wind speed variation[24]. The research in [25] shows that different wind speed has different effects on fatigue damage of the gear applied to a wind turbine. This is due to the fact that the gear

stress range is a function of gear rotational speed, which is fundamentally decided by the wind speed.

## 1.4.2 Wind speed model

The literature on wind speed could be classified into three groups: wind characteristics for a specific site, wind speed generation, and wind speed prognosis.

The study of wind characteristics emphasizes the statistical features (average, maximum, minimum and standard deviation) and the probability distribution of wind speed. The Weibull distribution is the most frequently used to fit hourly average wind speed [26, 27, 28, 29, 30]; some studies investigate the daily patterns in wind energy production [31] and the modeling for extreme events [32]. Numerous papers focused on this aspect can be recalled, for instance, refer to [33].

Wind speed generation and wind speed prognosis are two different subjects. However, regarding modelling technique, they have similarities. A great deal of work has been done to model the wind speed. For instance, the accurate but high computationally demanding physical models considers environmental conditions (pressure, temperature, humidity etc.) [34, 35]. The following content will focus on the models/methods based on data that is easy to apply in engineering. And the continuous-time stochastic processes will be detailed later as they are considered for the thesis's work.

### 1.4.2.1 Time series models

For its simplicity, time series models are commonly used to reproduce wind speed data for a particular location depending on available historical measured wind speed data [36, 37, 38]. These models have productive computational capacity but their linear forms restrict their usage. Moreover, the prediction accuracy of these models drops fast when the time horizon is increased [39], and they can not model accurate nonlinear data [40]. Two model are presented more precisely hereafter.

#### Autoregressive Moving Average (ARMA) model

An autoregressive (AR) model with  $p$  autoregressive terms, denoted by  $AR(p)$  is a discrete time stochastic process defined as:

$$x_k = a + \sum_{i=1}^p \alpha_i x_{k-i} + \epsilon_k \quad (1.2)$$

where  $a$  is a constant,  $\alpha_i$  ( $i = 1, 2, \dots, p$ ) are the autoregressive parameters,  $\epsilon_k$  is white noise, and  $x_k$  is the wind speed at time  $k$ . Under the assumption of stationarity, the parameters can be estimated by likelihood maximization method or the Yule-Walker method, and  $p$  can be decided with selection criteria or with the autocorrelation function [41].

AR models assume that the subsequent wind speed is a linear combination of current and past wind speed observations with a residual which is described as a white noise. Hence,  $p$  is the number of previous wind speed data with which the subsequent wind speed correlates,  $\alpha_i$  ( $i = 1, 2, \dots, p$ ) signifies how strong the correlations are. As the wind speed has diurnal and seasonal trend, the trend modelings are necessary. For instance, a square root transformation is applied to an hourly average wind speed sequence, after fitting and modeling a diurnal trend, an AR model was used for the residuals [42].

The AR( $p$ ) models have been widely applied for short-term wind speed prediction. An AR (5) model is used to predicate wind speed at an airport and its prediction results are more precise [43]. Another work points out that the prediction root mean squared error (RMSE) of an AR model which is used to fit a truncated wind speed distribution after removing the diurnal trend are reduced by 16% compared to the accurate model [44].

By adding moving average terms  $q$  to AR( $p$ ) model, one can get the general form of ARMA( $p, q$ ), which is a special form of the ARMA model:

$$x_k = a + \sum_{i=1}^p \alpha_i x_{k-i} + \epsilon_k + \sum_{j=1}^q \beta_j \epsilon_{k-j} \quad (1.3)$$

where the  $\beta_j$  ( $j = 1, 2, \dots, q$ ) are the moving average parameters.

A research finds that an ARMA prediction model based on the hourly mean wind speed can successfully be applied for prediction interval between 1 up to 6 hours ahead with a confidence interval of 95% [45].

A more general time series model is Autogressive Integrated Moving Average (ARIMA) model, which is also used for the purpose of wind speed generation and prediction [46].

### Kalman filter

Like AR models, the Kalman filter predict the wind speed as a linear combination of the past wind speed data and the current. However, instead of using the constant linear coefficients, the Kalman Filter updates them by minimizing the MSE that based on the previous historical data and the accuracy of the last prediction.

In the field of wind speed prediction, for instance, 1-step prediction is illustrated by the following equations:

$$x_k = \mathbf{H}_k \mathbf{A}_k + v_k \quad (1.4)$$

$$\mathbf{A}_{k+1} = \mathbf{\Phi} \mathbf{A}_k + \omega_k \quad (1.5)$$

Equation(1.4) is so called the observation equation. It gives a predicted wind speed value  $x_k$  at time  $k$  as a linear combination of the last  $N$  historical wind speed data, denoted by the  $N \times 1$  vector  $\mathbf{H}_k = (x_{k-1}, x_{k-2}, \dots, x_{k-N})'$ , where  $N$  is the order

of the filter. The  $N \times 1$  vector  $\mathbf{A}_k = (a_{k1}, a_{k2}, \dots, a_{kN})'$  contains the regression coefficients and it varies at each time step.

Equation(1.5) describes the time dependent evolution of  $\mathbf{A}_k$ .  $\Phi$  is a known  $N \times N$  transition matrix, which is generally defined as the identity matrix in applications.  $v_t$  is considered as noise of historical data, it has a normal distribution  $v_k \sim N(0, \Upsilon_k)$ .  $\omega_k$  is the system noise and it is assumed as a normal pdf with mean  $\mathbf{0}$  and covariance matrix  $\mathbf{W}_{k(N \times N)}$ :  $\omega_k \sim N(\mathbf{0}, \mathbf{W}_k)$ .

Literature about the applications of Kalman filter on wind speed prediction can refer to [47, 48, 49].

### 1.4.2.2 Artificial Intelligence model

Artificial Intelligence (AI) models include but not limited to artificial neural networks (ANN) model, fuzzy logic model and hybrid model. Since their ability to learn non-linear relationships from experience, they are popular in recent years. In wind energy field, they are more used for out-put power prediction considering other influence factors, for instance, wind speed [50, 51, 52, 53, 54, 55].

Different ANN models are applied to the short term wind speed prediction of hourly time series which are collected during 7 years. After the examination of different ANNs with different structures, an ANN model with two layers and three neurons is considered as the best one [56]. This research shows that lacking a criterion for ANN structure selection makes it difficult to choose the optimal model quickly.

## 1.5 Prognostics and health management for wind turbine

The concept and framework about Prognostic and health management (PHM) have been developed based on diagnostic techniques, maintenance methods and the requirements of the future condition prediction about a system, such as condition based maintenance (CBM) and preventive maintenance (PM). The PHM approach applied on a system attempts to answer the following questions:

- How is the system now? (Condition monitoring)
- What is the fault and why ? (Diagnosis)
- When will the system fail ? (Remaining useful life)
- Which decision should be taken ? Continue to operate or stop to maintain ? When? (Maintenance policy)

The related research topics about PHM contains but do not limit to condition monitoring, fault diagnosis, deterioration modeling, remaining useful life (RUL)

prediction and maintenance decision-making. Therefore, a brief state-of-the-art about condition monitoring, deterioration model, RUL prediction and maintenance will be given, respectively.

### 1.5.1 Condition monitoring

The condition monitoring for a component is an essential part of PHM. According to the frequency of inspection, it exists two types of monitoring: continuous monitoring and discrete monitoring.

#### Continuous monitoring

This type of monitoring considers that the condition of system provided by the inspection system is always known at any time. It is applied to the system that is particularly critical or the most costly. For instance, vibration, temperature, pressure and rotational speed are continuously inspected for an aero-engine used in civil aviation. It is related to sensors that can be placed on the system with some real time pre-processing possibilities to collect information. The term continuous is to be understood in a broad sense. Even if the collected information is discretized, it refers to a high sampling frequency in relation to system dynamics.

#### Discrete monitoring

Discrete monitoring means that specific action (inspection) or significant time delay are required to collect monitoring information. There are two forms of discrete monitoring, namely, periodical monitoring and non-periodical monitoring.

- **Periodical monitoring** means that the time interval between two consecutive monitorings is a constant denoted as  $\Delta T$ . For instance, in wind energy, 10-mins average wind speed is noted by SCADA as a parameter of wind turbine operation condition.
- **Non-periodical monitoring** in this situation, the inspection sequence cannot be scheduled in advance, because the choice of inspection sequence is based on the available information about the system. The next date of monitoring depends on the current system condition.

However, continuously monitoring is costly or not always necessary in reality. Discrete monitoring also has wide application in engineering field.

#### 1.5.1.1 Condition monitoring technology for wind turbine

According to the survey of [57], the monitoring systems applied to commercial wind turbines are as follows:

1. High frequency ( $>500$  Hz, continuous) Supervisory Control and Data Acquisition (SCADA) system that is initially designed for operating wind turbine safely and efficiently.
2. Continuous monitoring and diagnostic system on drive train with a frequency smaller than 50 Hz.
3. Low frequency ( $<5$  Hz) structural health monitoring system for tower and foundation.

### Supervisory Control and Data Acquisition System

The SCADA system saves the information of wind turbine operation, and indicates the partial condition of wind turbine. Using SCADA data to monitor wind turbines and to optimise maintenance became a high priority in wind power industry. Additionally, it is costless.

Tautz-Weinert et al. summarized 4 groups of the basic SCADA parameters shown in Table 1.2, namely, parameters related to environment, electrical characteristics, control system and temperature of some components [58].

Table 1.2: Basic SCADA parameters

Environmental	Control Variables	Electrical	Temparatures
Wind speed	Pitch angle/rate Pitch commande	Active power output Power factor	Gearbox bearing Gearbox bearing lubricant oil
Wind direction	Yaw angle Rotational speed of rotor	Reactive power Generator voltages	Generator bearing Main bearing
Nacelle temperature	Generator speed Number of stats / stops	Generator phase current Voltage frequency	Rotor / Generator shaft Grid busbar

The SCADA-based condition monitoring system provides the approximate condition of wind turbine.

### Technologies applied to wind turbine condition monitoring

As a part of the state-of-the-art, it is necessary to briefly review the technology applied to wind turbine condition monitoring.

- **Vibration analysis**

It is a well-proven and low-cost technology applied to rotational component monitoring. Vibration analysis is widely used on the inspection of the drive-train, especially, the gearbox blade and shaft [59, 60].

- **Oil analysis**

Oil analysis is important for the bearing and hydraulic system. Through oil clearance analysis, particular failures can be diagnosed, for instance, in the case of excessive the wear, oil analysis can give an indication of wear [61].

- **Ultrasonic test**

Ultrasonic test has been widely used in the crack diagnostic of concrete pillar in the field of construction. It has potential application on the early blade or tower defects detection [62].

- **Shock pulse method**

It can be an alternative online approach applied to bearing failure detection [63]. However, this subject needs future study.

- **Electric effects**

Electrical components such as generator, yaw-motor are typically performed using current and voltage analysis. Discharge measurement are used for grids. A spectral analysis of the stator current is applied to the isolation failure detection [64].

- **Acoustic emission**

When the structure of a metal is changed, the metal releases strain energy and generates elastic waves, it can be analysed by acoustic emission. As a kind of non-destructive testing method, the acoustic emission has been successfully applied to the monitoring of gearbox, bearing and blade of wind turbine [65].

## 1.5.2 Deterioration phenomena of wind turbine components

Wind turbine components, such as gearbox, blade, generator, foundations, are exposed to different forms of deterioration processes (corrosion, fatigue cracking, wear etc). The deterioration of wind turbine is a complex issue, because it depends on both random environmental and physical factors. The prediction of deterioration level is meaningful for reliability analysis, scheduling inspection and maintenance for wind turbine. The deterioration of a component can be modeled by a stochastic process, noted as  $\{D(t), t \geq 0\}$  that represents the level of deterioration at time  $t$ . If no maintenance activity interfered,  $D(t)$  will be monotonically increasing. Stochastic processes are detailed in section 1.6.

A gamma process is applied to the deterioration modeling of wind turbine bearings [66].

A reliability wind turbine assessment model subject to degradation is presented in [67]. The purpose of this model is to plan monitoring and maintenance. The model considered the stochastic nature of the degradation process through the use of appropriate statistical distributions.

M. Shaifiee et al [68] developed a model to describe the cracks deterioration of wind turbine blade subject to stress corrosion cracking and environmental shock. The cracks are initiated on the surface of a blade by point events that modeled with a non-homogeneous Poisson process, and then the cracks propagate along a

direction according to a gamma process. The environmental shocks is modeled by a non-homogenous Poisson process.

### 1.5.3 Remaining useful life estimation

A huge amount of research has been carried out to propose prognostic models which aim to be applied to the RUL prediction of engineering assets [69]. Generally speaking, the methods of RUL prediction in literature can be classified into two groups, one is based on physical model and another one is based on data. Physical based model shows the wind turbine failures by means of the physical law, and it predicts the RUL by solving deterministic equations. The advantage of physical-based model is its accuracy and preciseness for a particular issue. However, when the detailed failure mechanism is complicated, it is difficult to obtain an accurate physical-based model. With the development of condition monitoring technology, and since the information provided by Condition Monitoring System (CMS, it provides information on current status of the dynamic system measured by diagnostic variables and on operational environments.) is highly related to the health condition of system, the data based RUL prediction methods have become popular. The RUL prediction method through stochastic process can be considered as one of the data based methods. The clearly physical interpretation of stochastic processes makes people pay a lot of attention to them. The Weiner process is derived from the description of the Brownian motion; nowadays it is widely applied to predict the lifetime of LED, laser generator, lithium-ion batteries, etc. As the gamma process is monotonous increasing, it matches well the wear process and the growing crack.

The RUL of a system is a random variable. **Firstly**, it depends on the current health condition of the system. Intuitively, the RUL at time  $T$  of a system can be given as follows:

$$RUL_T = \inf\{\tau \geq 0 : \mathcal{X}_{T+\tau} \geq \mathcal{L}\} \quad (1.6)$$

Where,  $\mathcal{L}$  is the divide between not-failed status and failed status of dynamic system, and  $\mathcal{X}_t$  as the current status of this dynamic system at time  $t$ .

The meaning of equation (1.6) is that at time  $T$ , a period  $\tau$  is interesting, as at the end of this period  $\tau$ , the current status of the dynamic system firstly arriving at or passing the divide  $\mathcal{L}$ , from not-failed to failed status. In other words, at the end of  $\tau$ , the dynamic system no longer performs its intended purpose. According to equation (1.6), it seems that the RUL only relates to the status over time and a threshold. However, how to define the status of the system  $\mathcal{X}_t$ ? In engineering field, a common way is monitoring the system via CMS.

**Secondly**, the RUL estimation depends on the monitoring information. Hence, in industry combining the monitoring information, the issue about RUL becomes a conditional probability with formula

$$\mathbb{P}(RUL_T > \tau \mid \mathcal{M}_T) = \mathbb{P}(\mathcal{X}_{T+\tau} \in \mathcal{F} \mid \mathcal{X}_T \notin \mathcal{F}, \mathcal{M}_T) \quad (1.7)$$

Where,  $\mathcal{F}$  is the space related to failed dynamic system and  $\mathcal{M}_t$  is the information up to time  $t$  which is provided by CMS.

To predict the RUL at time  $t$ , health indicators  $D(t)$  that directly indicates the system deterioration at time  $t$  is required, and they can be extracted from the information provided by the CMS. **Finally**, for a deteriorating and discrete inspected dynamic system, with inspected data  $\{M\}_t$  ( $t = 1, 2, \dots$ ), the CDF of  $RUL_T$  is

$$\begin{aligned} F_{RUL_T}(\tau) &= \mathbb{P}(RUL_T > \tau \mid M_1 = m_1, M_2 = m_2, \dots, M_T = m_T) \\ &= \mathbb{P}(T_F > T + \tau \mid M_1 = m_1, M_2 = m_2, \dots, M_T = m_T) \\ &= \mathbb{P}(D(T + \tau) < L \mid M_1 = m_1, M_2 = m_2, \dots, M_T = m_T) \end{aligned} \quad (1.8)$$

From the preceding content, the RUL prediction method considered in this thesis contains the factors as follows [70]:

- an indicator describes health condition of the system
- a stochastic process describes the evolution of the health indicator
- a prediction considers the health condition

Now let's have a brief review about the RUL prediction for wind turbine components. A common way to estimate the RUL of wind turbine component (gearbox, bearing, etc.) is the load's calculation [25]. As the aforementioned method of RUL prediction lacks the consideration about the deterioration over time, the changeable environment and other uncertainties, this RUL is deterministic that is difficult to merge to the PHM system for a predictive maintenance decision. Several efforts about stochastic process based RUL prediction are mentioned in literature. In ref [71], a methodology to compute the RUL using the available observations is presented. In ref [72], a Wiener process is used to model the component deterioration and to estimate the RUL, the engaged data is from the PHM Data Challenge. And good result is obtained by the proposed approach. A real-time RUL prediction of wind turbine bearings based on stochastic process is proposed in ref [73]. By verifying on the temperature data of an actual 1.5 MW wind turbine, it proves that the proposed RUL prediction method is more effective than the traditional ones.

## 1.5.4 Maintenance and maintenance policies

### 1.5.4.1 Maintenance actions

Maintenance involves planned and unplanned actions carried out to retain a system or restore it to an acceptable condition [74]. The aim of studying maintenance policy is to minimize downtime, to provide the most effective use of system at the lowest possible costs. The general classes of maintenance types are corrective maintenance and preventive maintenance, shown in Figure 1.11.

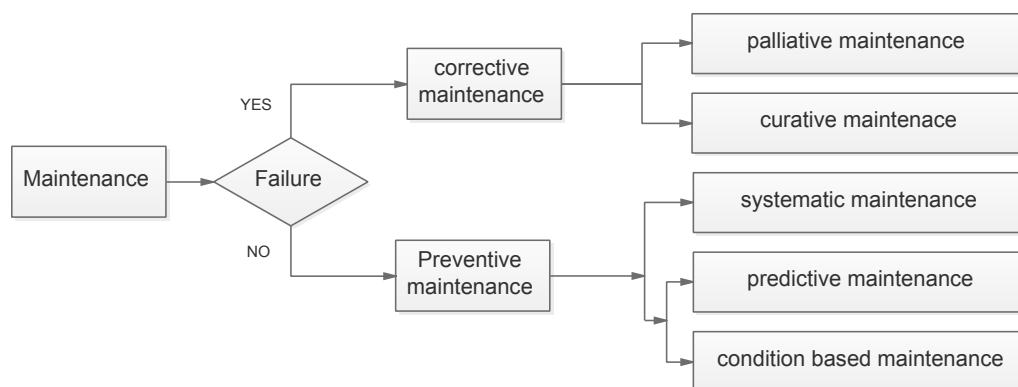


Figure 1.11: Maintenance types

The action of corrective maintenance is carried out after the detection of a system failure. The task of corrective maintenance is usually to make repairs as soon as possible. Corrective maintenance can be a palliative maintenance or curative maintenance.

**Palliative maintenance** comprises the activities that can maintain a part or all the functions of the system for a short period. It is commonly referred to as troubleshooting. Palliative maintenance can't totally correct the system, so it must be followed by curative maintenance.

**Curative maintenance**, the objective of curative maintenance is to avoid any further failure occurrences through identification failures' essential causes and repair of failed components. In the case of corrective maintenance implementation, the unavailability of the process is maximum and uncontrolled. The reduction of downtime due to failures then depends directly on the efficiency of the maintenance.

#### 1.5.4.2 Maintenance policies with corrective policy

Preventive maintenance aims to improve the availability and reliability of a system. Reducing the operation and maintenance cost is its another purpose. Preventive maintenance has three types: systematic maintenance, predictive maintenance and condition-based maintenance.

**Systematic maintenance** performs periodical replacements. However, the component may fail before the critical time predicted by its failure model, or the replaced component may live longer than the planned service time after the last replacement. Systematic maintenance applies to the system whose degradation evolution is generally continuous.

**Predictive maintenance**, its final aim is to perform maintenance at a scheduled time point when the maintenance activity is most cost-effective and before the system loses performance within a threshold.

**Condition based maintenance** can be considered as a practice within the pre-

dictive maintenance strategy. However, it is more down to earth. Condition based maintenance is based on the real-time continuous monitoring information provided by a monitoring system. It tries to maintain the correct component at the right time, i.e. maintain when it is actually necessary.

Since the predictive and condition based maintenance policies predict the evolution of system degradation by analysing the collected data, condition based maintenance policy is classified as a subject category of predictive maintenance policy. Therefore, the thesis will use these two terms without difference. Reliability criteria are necessary to make a maintenance decision with predictive maintenance policy. Such as failure rate, degradation level of system, or other information that can indicate the health condition of system.

Maintenance policy with periodical monitoring normally aims to finding optimal maintenance interval  $\Delta T$  with a minimum cost. For instance, Le Son et al. estimated three maintenance policies that based on the estimated RUL, reliability function and system condition, respectively [75]. Two types of inspection planning strategies for a two-unit system with independent stochastically deteriorating units are proposed in [76].

Bérenguer et al. [77] proposed a maintenance policy for a gradually and stochastically degraded system that is continuously monitored. An aging variable is inspected continuously. A breakdown occurs when the aging variable reaches a failure level  $L$ . Once the aging variable exceeds an alarm threshold  $A$  which is lower than  $L$ , maintenance is planned. The maintenance is carried out with a time delay, and its duration relates to the actual condition of the system when the maintenance begins. As a result of the existence of time delay of the maintenance operation, the system deteriorates during this period, the choice of  $A$  influences the performance of the maintenance. With this background, the authors proposed a mathematical model to evaluate the asymptotic unavailability of the system and to optimize the maintenance parameter i.e. the alarm threshold  $A$ . A maintenance policy that minimized the unavailability based on the previous work is proposed in [78].

Zhou et al. [79] tried to integrate sequential imperfect maintenance policy into a conditional based maintenance. The system is continuously monitored, and the hazard rate function is known. Both the scheduled and unscheduled (corrective) maintenance are considered. The first maintenance is operated whenever the system reliability reaches the threshold, while the latter one is performed when the system fails before the scheduled maintenance.

A maintenance policy that combines corrective, periodic and preventive maintenance for a continuously monitored multi-component system is proposed in [80]. Two thresholds about the degradation level are considered. When the degradation reaches a first ‘opportunistic’ threshold, the component is repaired as soon as maintenance operates on the other components; once it exceeds a second ‘intervention’ threshold, additional maintenance is planned to replace the component in order to avoid system failure.

## 1.6 Mathematical tools for wind speed and deterioration modelling: stochastic processes

According to [81], a stochastic process  $\{X_t, t \in T\}$  is a collection of random variables. For each  $t \in T$ ,  $X_t$  is a random variable. The index  $t$  is often interpreted as time, and  $X_t$  as the state of the process at time  $t$ . The set  $T$  is the index set of the process. When  $T$  is a countable set, the stochastic process is said to be a discrete-time process. If  $T$  is an interval of the real line, the stochastic process is a continuous-time process. The state space of a stochastic process is defined as the set of all possible values that the random variable  $X(t)$  can assume.

Therefore, a stochastic process is a family of random variables that could be used to describe the evolution through time of some process or physical process. Stochastic processes are able to model a random phenomena, such as the wind speed [82], system degradation [83], growth of population [84], cancer evolution [85] etc. This thesis mainly considered several stochastic processes that can be applied in the reliability engineering field and that can be used to model random environment phenomena. In this section, stochastic processes that are classically considered in the field of reliability are presented briefly. They will be used in the next chapters when developing the modeling framework for wind turbine pitch system degradation and lifetime modeling.

### 1.6.1 Markov chain

A Markov chain is a stochastic process without memory. Markov chain consists of discrete-time Markov chain and continuous-time Markov chain.

Defining that  $\mathbb{S}$  is a finite or has countable number state space,  $X_{t_i} = s_j$  represents that the system stays in state  $s_j \in \mathbb{S}$  at time  $t_i$ . For  $i \in \mathbb{N}$  and  $\forall s_{k_0}, s_{k_1}, \dots, s_{k_{i+1}} \in \mathbb{S}$ ,  $\{X_{t_i}\}_{i \in \mathbb{N}}$  is a Markov chain, if

$$\mathbb{P}(X_{t_{i+1}} = s_{k_{i+1}} | s_{k_0} = x_0, \dots, X_{t_i} = s_{k_i}) = \mathbb{P}(X_{t_{i+1}} = s_{k_{i+1}} | X_{t_i} = s_{k_i}) \quad (1.9)$$

If and only if the transition between  $X_{t_i}$  and  $X_{t_{i+1}}$  is independent of  $t_i$ , it is a homogeneous Markov chain.

$$\mathbb{P}(X_{t_{i+1}} = s_{k_{i+1}} | X_{t_i} = s_{k_i}) = \mathbb{P}(X_{t_1} = s_{k_{i+1}} | X_{t_0} = s_{k_i}) = P_X(k_i, k_{i+1}) \quad (1.10)$$

where function  $P_X : [\mathbb{S} \times \mathbb{S}] \rightarrow [0, 1]$  is the probability transition matrix of Markov chain, the distribution of  $X_{t_0}$  is denoted  $\lambda_X(0)$  and is called the initial distribution of Markov chain.

Hence, the probability distribution of the state at time  $t_i$  is:

$$\lambda_X(t_i) = \lambda_X(0) \times (P_X)^i \quad (1.11)$$

The mean sojourn time in each state  $s_m$  is noted as  $T_m$ . It can be calculated as

$$\mathbb{E}(T_m) = \frac{1}{\sum_{n \neq m} P_X(m, n)} \quad (1.12)$$

If and only if at least one of the power of the transition probability matrix  $P_X$  has the elements strictly positive, then the limited distribution  $\lambda_X(\infty)$  exists when  $t \rightarrow \infty$ . And it is independent of  $\lambda_X(0)$ .

If the stochastic process  $\{X_t\}$  takes the value from a finite or countable state space, and the time passed in each state is not negative and is exponential distributed, this stochastic process can be considered as a continuous-time Markov chain.

Markov chains have various applications, such as in the field of economics, the algorithms used in optimisation and simulation. As for the deterioration modelling, both discrete-time and continuous-time Markov chains are concerned. In some cases, a system is considered to operate under two or more situations where the deterioration rates are different, or the deterioration levels of system are different. The Markov chains model all the possibilities that the system deteriorates from a perfect condition to failure, and are applied to the preventive maintenance [86, 87, 88]. Markov chains are also used to model the stochastic phenomena, especially, the deterioration. Kharoufeh et al. studied a system whose deterioration rate depends on the environment, and the environment can be modelled by a continuous-time Markov chain [89].

## 1.6.2 Gamma process

### Homogenous gamma process

Recall that a gamma-distributed random variable  $x$  with shape parameter  $\alpha$  and scale parameter  $\beta$  is denoted  $x \sim \Gamma(\alpha, \beta)$ . The corresponding probability distribution function (pdf) is

$$\Gamma(x|\alpha, \beta) = \frac{\beta^\alpha}{\Gamma(\alpha)} x^{\beta-1} \exp(-\beta x) I(x) \quad (1.13)$$

where  $\Gamma(a) = \int_0^{+\infty} z^{a-1} e^{-z} dz$  is the Gamma function for  $a > 0$ , and  $I(x)$  is the indicator function.

A continuous stochastic process  $\{X_t, t \geq 0\}$  is a homogenous gamma process, if

- a.  $X_0 = 0$ ,
- b.  $X_t - X_s \sim \Gamma(\alpha(t-s), \beta), \forall t > s > 0$ ,
- c.  $X_t$  has independent non-overlapping increments.

Hence, homogenous gamma process is suitable to model gradual degradation phenomena, such as crack growth, wear, etc. Some homogenous gamma process properties make it become one of the most accepted degradation models in reliability engineering field. The trajectory of  $X_t$  is monotonic increasing, like most engineering degradation processes without maintenance.

- The expectation and variance of homogenous gamma process are linear functions.  $\mathbb{E}(X_t) = \frac{\alpha}{\beta}t$ ,  $\text{var}(X_t) = \frac{\alpha}{\beta^2}t$ . Hence, homogenous gamma process can be applied to the degradation process with linear tendency.
- $\frac{\mathbb{E}(X_t)}{\text{var}(X_t)}$  is a constant.
- Homogenous gamma process is a Markovian process that  $X_t$  only depends on the last one. This property simplify the situation when one wants to applied homogenous gamma process to engineering problems.

### Non-homogeneous gamma process

Introducing  $\alpha(t)$ , a non-decreasing, right continuous and real valued function for  $t \geq 0$ , with  $\alpha(0) = 0$ , definition of non-homogeneous gamma process is derived. In this case:

- a.  $X_t - X_s \sim \Gamma(\alpha(t) - \alpha(s), \beta)$ ,  $\forall t > s > 0$ ,
- b. The expectation and variance of non-homogenous gamma process are all adjustable functions. Hence, compared to homogeneous gamma process, non-homogenous gamma process is more flexible, it can model the degradation processes with nonlinear tendency.

M. Abdel-Hameed firstly proposed to model a wear deterioration by gamma processes [90] in 1975. Then gamma processes are widely applied in deterioration modelling, such as the deterioration of bearing [91], aging structure modelling [92], and a detail list of gamma process application for preventive maintenance is presented by Van Noortwijk in [93].

### 1.6.3 Wiener process

A stochastic process  $\{W_t, t \geq 0\}$  is denoted as a (standard) Wiener process, if

- a.  $W(0) = 0$ , with probability 1.
- b. For  $0 \leq t_i < t_{i+1} \leq T$ , the increment  $\Delta W_i = W(t_{i+1}) - W(t_i)$  is Gaussian distribution with zero mean and  $\sigma = t_{i+1} - t_i$ , namely,  $\Delta W_i \sim N(0, \sigma)$ .
- c. For  $0 \leq t_i < t_{i+1} < t_{i+2} \leq T$ , the non-overlapping increments  $\Delta W_i = W(t_{i+1}) - W(t_i)$  and  $\Delta W_{i+1} = W(t_{i+2}) - W(t_{i+1})$  are independent.

Some properties of Wiener process are listed,

- a. Wiener process has a zero mean and its variance is a linear function of time.
- b. It has independent non-overlapping increments.
- c. Its trajectories fluctuate.
- d. Different from gamma process, the trajectory of Wiener process is almost surely continuous without jumps.

A drifted Wiener process can be derived by adding drift term to the standard one, namely

$$X_t = x_0 + at + bW_t \quad (1.14)$$

where,  $x_0 \in \mathbb{R}$ ,  $a > 0$  and  $b > 0$  are the drift parameter and volatility parameter, respectively. Volatility can be considered as the degree of the process' fluctuation.

Similar to the standard Wiener process, when  $x_0 = 0$  a drifted Wiener process has independent increments that follow Gaussian distribution:

$$X_t - X_s \sim \mathcal{N}(a(t - s), b^2(t - s)), \quad \forall t \geq s \geq 0 \quad (1.15)$$

#### 1.6.4 Ornstein-Uhlenbeck process

The most famous mean reverting diffusion process is the Ornstein-Uhlenbeck (OU) process also called Vasicek model. Roughly speaking it describes the velocity of a massive Brownian particle under the influence of friction. To link with time series used in the literature for wind modeling, one can recall that the OU process can also be considered as the continuous-time analog of the discrete-time  $AR(1)$  process.

The OU process is initially proposed to model the velocity of a particle in liquid, viscous suspension. Presently, this process is widely used to model phenomenon in biology, medicine, finance, and economy. The OU process is a stochastic process that satisfies the following stochastic differential equation:

$$dX(t) = \alpha(\zeta - X(t))dt + \beta dW(t), \quad t \in [0, T], \quad X(0) = 0 \quad (1.16)$$

where  $W(t)$  is a Wiener process. The meanings of OU process parameters are listed below:

- $\alpha > 0$  is the rate of mean reversion, scaling the distance between  $X(t)$  and  $\zeta$  appropriately to match whatever is being modeled.
- $\zeta \in \mathbb{R}$  is the long-term mean of the process. If  $X(t) > \zeta$ , so  $(\zeta - X(t) < 0)$ , that means the drift of the process is negative and tends towards  $\zeta$ . The process will have positive drift when  $X(t)$  is smaller than  $\zeta$ .

- $\beta > 0$  is the volatility or average magnitude, per square-root time, of the random fluctuations that are modeled as Brownian motion. As it is representing the variance it must be strictly positive.

If we ignore the fluctuations due to  $W(t)$ , then  $X(t)$  has an overall drift towards a mean  $\zeta$ . The process  $X(t)$  reverts to this mean exponentially, at rate  $\alpha$ , with a magnitude proportional to the distance between the current value of  $X(t)$  and  $\zeta$ . The mean and the variance of  $X(t)$  are defined as follows [94]:

$$\begin{aligned}\mathbb{E}(X(t)|X(0) = x_0) &= e^{-\alpha t}x_0 + \zeta(1 - e^{-\alpha t}) \\ \text{var}(X(t)) &= \frac{\beta^2}{2\alpha}(1 - e^{-2\alpha t}).\end{aligned}\tag{1.17}$$

The first-passage time of the OU process to a given horizontal barrier,  $L$ , is a random variable which has tractable expressions for the PDF only in the special case  $L = \zeta$ , refer to [95]. Phillips in [96] proposed an approximation of the transition density for the OU process defined in equation (1.16) as follows:

$$X((i+1)h)|X(ih) \sim \mathcal{N}\left(\zeta(1 - e^{-\alpha h}) + e^{-\alpha h}X(ih), \frac{\beta^2}{2\alpha}(1 - e^{-2\alpha h})\right)\tag{1.18}$$

Y. Deng et al. used an OU process to model a deterioration process with fluctuations around its average behaviour [97]. Because the OU processes stabilises around some equilibrium point, O. Aalen et al. proposed a survival model based on OU processes [98].

### 1.6.5 Regenerative process

According to M. Ross [81], a regenerative process is a stochastic process  $\{X_t, t \geq 0\}$  with state space  $\mathbb{N}^+$ , having the property that there exist time points at which the process (probabilistically) restates itself. A repairable system starts to work at  $T_0$  and fails at time  $T_1$ . It is restored to an as-good-as-new condition with a maintenance action. Then it may fail again at  $T_1 + T_2$  and be restored as previous. Let the same procedure continue and record  $T_1, T_2, \dots$ . Without considering the time duration for the maintenance after failure, the basic concept of regenerative process is presented.

## 1.7 Conclusions

In this chapter, firstly, we reviewed the developments of wind turbine, the challenges for its safety and its life extension. As wind is the energy resource for wind

turbine, then we introduced the existing wind speed models. The work of this thesis is a part of wind turbine's Prognostics and health management, which contains condition monitoring, deterioration model, remaining useful life and maintenance policies. Therefore, we illustrated them respectively. In the domains of the wind speed model and deterioration model, stochastic processes are widely used, hence, several stochastic processes are illustrated.

The state-of-the-art provides initial ideas and elements for the work of the thesis. Since the wind turbine is our object of study, the work in the thesis have some novelties compared with the state-of-the-art. Firstly, we propose a more flexible wind speed model which meets the requirement of long-term high-frequency wind speed. Secondly, RUL estimation methods are studied for the system like a wind turbine that operates under various environment. Thirdly, an unavailability model caused by random maintenance delays are proposed for wind turbine. A wind turbine simulator with deteriorating hydraulic pitch system is established to provide the deterioration data for the study. Next chapter will focus on the wind turbine simulator.

# Chapter 2

## Wind turbine simulator

### 2.1 Introduction

The aim of the thesis is to propose a modelling framework composed of (1) a model of pitch system deterioration (2) an indicator which allows to estimate the deterioration level from monitoring data (3) a numerical simulator which allows to simulate the estimated deterioration behavior and to characterize the remaining useful lifetime. Therefore, to provide simulation data for the research and to evaluate the research result, a wind turbine simulator related to our research issue is required.

This chapter is devoted to the realisation of a wind turbine simulator combined with a deteriorating hydraulic pitch system. The 5-MW baseline wind turbine developed by the National Renewable Energy Laboratory (NREL) is the base of the work. First, an introduction about it will be given. Afterward the pitch control system (control strategy and pitch actuator) will be introduced. Then the hydraulic system deterioration modelling is addressed. Finally, this chapter ends with the wind turbine simulator realization method in the environment of Matlab/simulink<sup>®</sup>.

### 2.2 NREL 5-MW baseline wind turbine and its pitch control system

#### 2.2.1 NREL 5-MW baseline wind turbine properties

NREL 5-MW baseline wind turbine is developed for conceptual studies aimed at assessing offshore wind technology for the U.S supported by the National Wind Technology Centre. For the development of the NREL 5-MW baseline wind turbine, the researchers gathered a large deal of available information on wind turbines, such as:

- the wind turbine project of the Dutch Offshore Wind Energy Converter (DOWEC) [99, 100, 101],
- the project of the Recommendations for Design of Offshore Wind Turbine (RECOFF), the series studies of the land-based Wind Partnerships for Advanced Component Technology (WindPACT) [102, 103],
- the REpower 5M prototype wind turbine [104],
- the Multibrid M5000 prototype wind turbine [105].

Hence, the NREL 5-MW baseline wind turbine can be considered as a numerical large wind turbine that is representative of typical utility-scale-land and sea-based multi-megawatt turbines. This section gives a brief introduction about the NREL 5-MW baseline wind turbine abstracted from its technical report [106]. Its general properties are shown in Table 2.1.

Table 2.1: General properties of the NREL 5-MW baseline wind turbine

Rotor Orientation, Configuration	Upwind, 3 blades
Control	Variable Speed, Collective Pitch
Rotor Diameter	126m
Hub Height	90 m
Cut-In, Rated, Cut-Out Wind Speed	3 m/s, 11.4 m/s, 25m/s
Rated Tip Speed	80 m/s
Rating Power	5 MW

### Blade structural and aerodynamic properties

The blade structure design of 5-MW baseline wind turbine is based on the glasfiber blade applied to the DOWEC study. The blade root is located 1.5m along the pitch axis from the rotor center, namely, half the hub diameter. The researchers set the blade aerodynamic properties based on the DOWEC blades but made some corrections according to their results. Table 2.2 shows the properties of the blade.

Table 2.2: Blade structural properties

Length	61.5 m
Mass scaling factor	4.536%
Overall mass	17,740 kg
First mass moment of inertia with respect to the blade root	363,231 kg · m <sup>2</sup>
Second mass moment of inertia with respect to the blade root	11,776,047 kg · m
Structural damping ratio	0.4775 %

### Hub and nacelle properties

Table 2.3: Hub and nacelle properties

Hub Mass	56,780 <i>kg</i>
Hub inertia about low-speed shaft	115,926 <i>kg · m<sup>2</sup></i>
Nacelle mass	240,000 <i>kg</i>
Elevation of yaw bearing above ground	87.6 <i>m</i>
Nominal nacelle-yaw rate	0.3°/ <i>s</i>

This part of work merged the properties of DOWEC and REpower 5M turbines. Table 2.3 shows the main properties.

### Drivetrain properties

The NREL 5-MW baseline wind turbine has the same rated generator speed, rated rotor speed and gearbox ratio as the REpower 5M wind turbine. The natural frequency of the driveshaft is the same as the RECOFF turbine model. The high-speed shaft took the same properties of the DOWEC's. Table 2.4 shows the drivetrain properties.

Table 2.4: Drivetrain properties

Rated rotor speed	12.1 <i>rpm</i>
Rated generator speed	1173.7 <i>rpm</i>
Gearbox ratio	97:1
Electrical generator efficiency	94.4%

### Tower properties

The properties of tower for a wind turbine depend on the type support structure used to carry the rotor and the nacelle. However, the type support structure depends on the wind farm site (onshore, offshore, soil type, water depth etc). The NREL 5-MW baseline wind turbine tower is based on the tower used in DOWEC study. Table 2.5 shows the properties of the tower.

Table 2.5: Drivetrain properties

Height above ground	87.6 <i>m</i>
Overall mass	347,460 <i>kg</i>

With the above content, we have a general idea about the NREL 5-MW baseline wind turbine. Based on its representative information of real large wind turbines, even though it is a numerical simulator, it provides credible simulation data for our study.

## 2.2.2 Pitch control system

To capture as much as possible wind energy, the variable speed wind turbine is developed. The application of pitch system to the wind turbine makes the rotor rotate with a variable speed and makes the wind turbine be able to generate energy for a large scale of wind speed. Figure 2.1 shows a typical power control principle of variable speed wind turbine with respect to the wind speed. And from a point of view of the wind turbine's power control aim, Table 2.6 gives the definitions of Region 1, Region 2, Region 3 and Region 4, respectively.

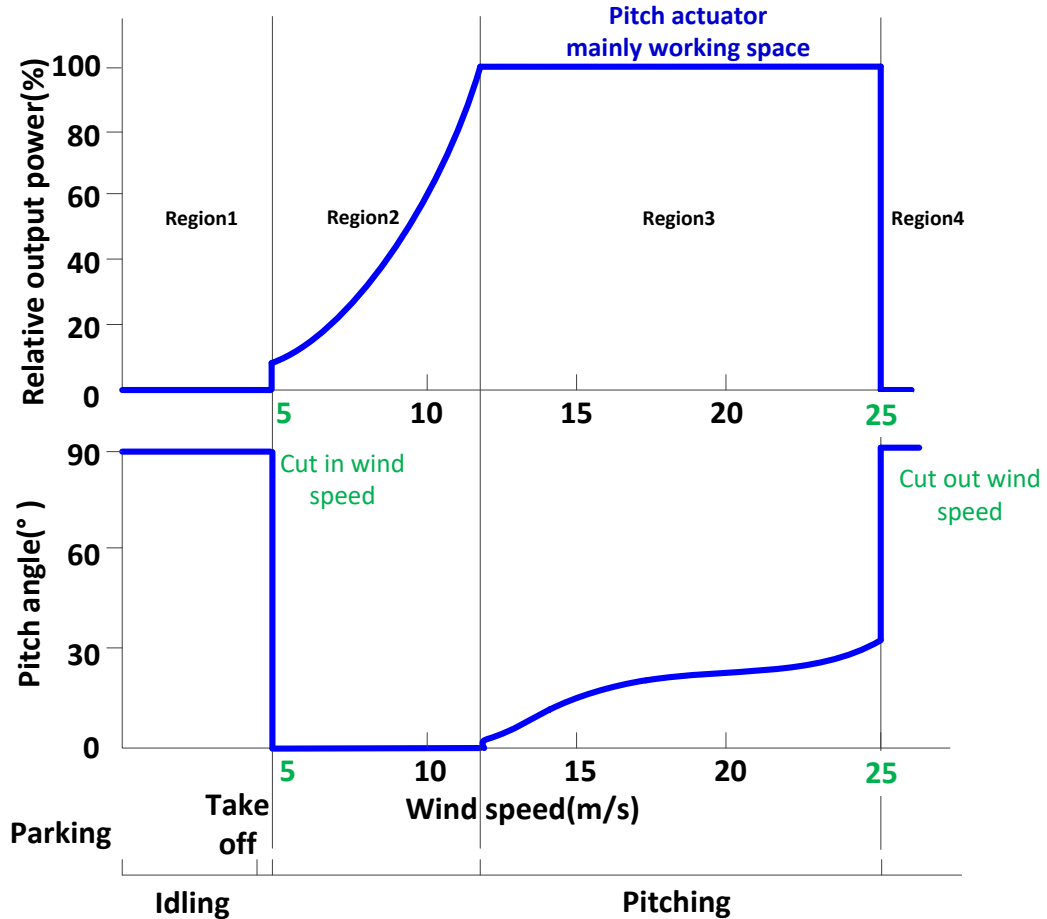


Figure 2.1: Operation ranges and control of a variable speed wind turbine with a power control by pitch system

From the control point of view, variable speed wind turbine operates in two regions: partial load region (from cut-in wind speed to rated wind speed, i.e., Region 2 shown in Figure 2.1) and full load region (wind speed varies from rated speed to cut-out speed, i.e., Region 3 shown in Figure 2.1). In partial load region, control aims to catch as much wind energy as possible. And the one in full load region is to reduce load and to limit the output power of wind turbine by regulating the rotor's rotational speed around the rated rotational speed of a wind turbine.

The system used to implement rotor's regulation is the pitch control system which works during the full load region. This latter also performs the aerodynamic brake

Table 2.6: Wind turbine control aims with respect to wind speed

Region	Wind Speed Range ( $m/s$ )	Control Aims and Actions
Region 1	0 ~ cut-in	A control region before cut-in wind speed. Rotor is idling and no power is captured from wind. The pitch angle keeps at 90 °.
Region 2	cut-in ~ rated	A control region for optimizing wind energy. The pitch angle is set to the optimization angle, no pitch action, rotor's speed varies over the wind speed.
Region 3	rated ~ cut-out	Pitch is active to limit input wind energy and output power of generator, which is regulated around rated power.
Region 4	> cut-out	Wind turbine shuts down, shafts are braked, in order to protect the wind turbine against the heavy load caused by strong wind.

in an urgent situation and regulates blades to the optimal position in the partial load region. During the period that the wind speed is between the rated wind speed and the cut-out wind speed, the pitch system operates continuously according to the wind speed.

Beside the adjustment of power, the other contributions of pitch control are expressed as follows [107]:

- Above the rated wind speed, pitching the blade provides an effective method of regulating the aerodynamic power and loads produced by rotor, hence, prevents the mechanical power to go beyond the design limit.
- Minimizing fatigue loads of the turbine components.

In engineering reality, pitch control is a part of the power control applied to rotor, another part is the torque control for generator (the thesis just mentions this point without further discussion).

A pitch system consists of a control strategy, controller for the control strategy realization and actuators for the implementation of control command. Basically, a Proportional and Integral (PI) pitch controller is enough, and it is widely applied in engineering field of wind energy.

### 2.2.2.1 Pitch control strategy

A baseline control pitch system is proposed by engineers, shown in Figure 2.2. In Region 3, pitch angle commands are computed using PI control on the speed error between the rated generator speed and the filtered generator speed.

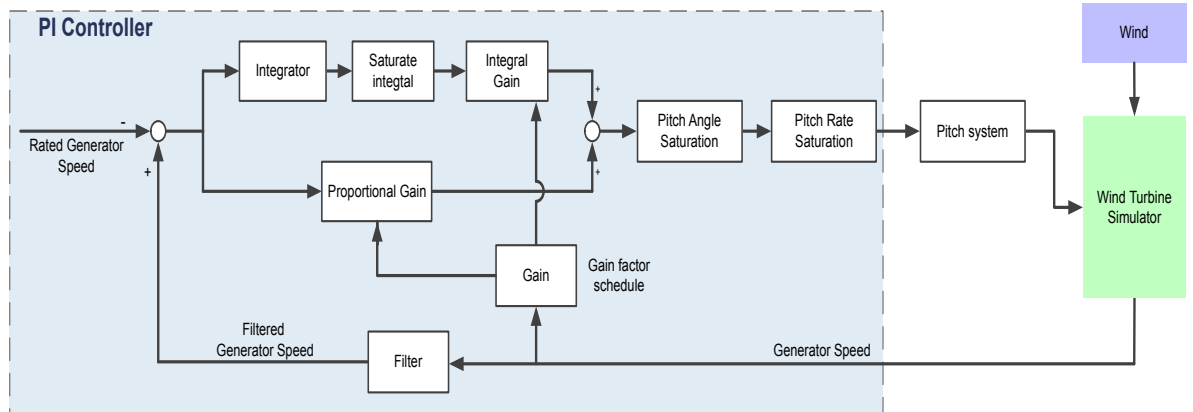


Figure 2.2: Flowchart of the baseline control pitch system for NREL 5-MW wind turbine

## 2.3 Hydraulic pitch system: principle and failures

### 2.3.1 Principle of hydraulic pitch system

The hydraulic and electric pitch system share the commercial wind power market. Both of them have advantages and disadvantages so that it is difficult to say which one is the best. With the development of multi-megawatt wind turbines, choosing hydraulic pitch system is a tendency, even though one can encounter the failure of leaking hydraulic fluid and oil contamination problems. The advantages of the hydraulic pitch system are as follows:

- quick response, higher power density and reliable,
- no electrical power (batteries) is required for emergence stop and when wind turbine is cut-off,
- simple structure requires less space inside the hub than the electric pitch actuator,
- easy diagnostic and maintenance.

Figure 2.3 shows a schematic diagram of the hydraulic pitch system. Briefly, the mechanism of a hydraulic pitch system is rotating the blade root by adjusting the piston's displacement inside the hydraulic cylinder. The displacement is proportional to the change of pitch angle.

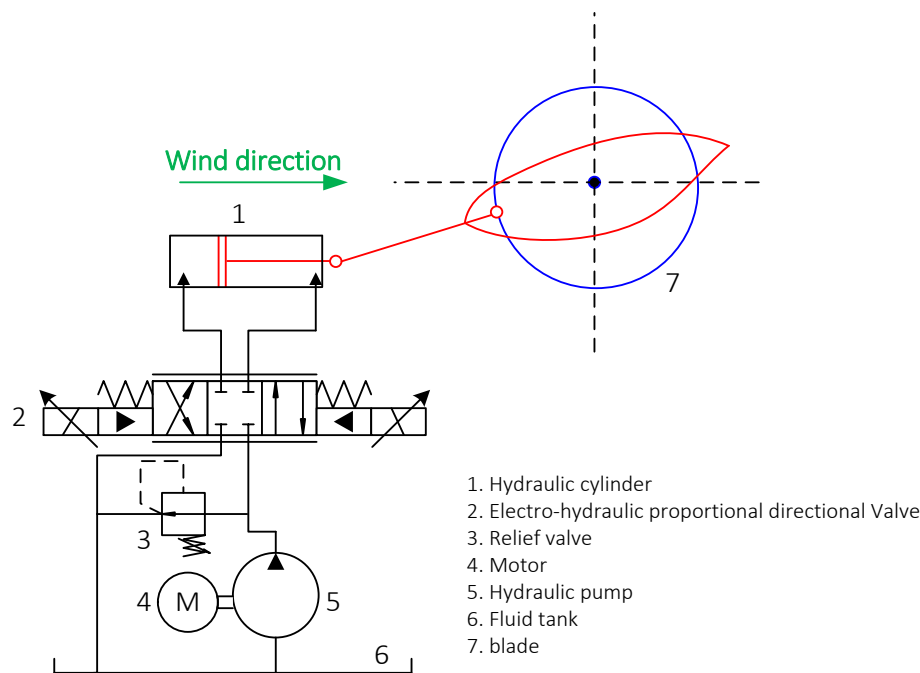


Figure 2.3: Diagram for a hydraulic pitch actuator

### 2.3.2 Failures of hydraulic pitch system

Failures of hydraulic pitch system may damage the wind turbine. Incorrect pitch angle of a single blade causes an imbalance to rotor that leads to high periodical loads to drive-train. Inefficient performance of pitch system will cause undesirable downtime of wind turbine. The common hydraulic pitch system failures are leakage, wear and excessive high air/oil ratio.

#### 1 Leakage:

A hydraulic system suffers two kinds of leakage: internal leakage (appearing at the piston inside the cylinder) and external leakage (appearing at the shaft seal for pipe connection). Leakage will cause inefficient operation of a hydraulic system. With leakage, the system will eventually break down. Even worse, a sudden leakage can trigger serious consequences when the wind turbine is working with load. Leakage is always one of the major threats to wind turbine's hydraulic system.

The internal leakage, difficult to measure directly, is a typical failure of hydraulic system. It decreases the loop gain and increases the effective damping, leading to the degradation of performance. The effect of internal leakage is to increase the damping characteristic of the actuator.

#### 2 Wear:

Wear between a piston and the cylinder may be divided into two parts: abrasive wear caused by hard pollutants in hydraulic oil; adhesive wear inside

the piston. Wear of the seals used for the separation of actuator rod from the cylinder results in a hydraulic fluid leakage to the environment, and it leads to a sluggish response of hydraulic system. Wear occurring to pump leads low pump pressure. Besides, wear leads to a contamination of hydraulic oil.

### 3 Excessive air/oil ratio:

There will always be some air in the hydraulic oil, and the content of air is hard to control. For the hydraulic system in service, air/oil ratio has an increasing tendency. Excessive air/oil ratio which leads to bulk modulus reduction, spongy operation and poor control system response is a typical deterioration of the hydraulic system. As air is much more compressible than oil, it changes the dynamics of the hydraulic system causing slow movement of hydraulic actuator.

The three main failures of hydraulic pitch system are related to sudden or gradual deteriorations with effects on the dynamic of actuator. More details are explained in the following section, and a deterioration model is proposed to model the phenomena.

## 2.4 Deteriorating hydraulic pitch system modelling

### 2.4.1 Fault-free hydraulic pitch system model

In principle, the fault-free hydraulic pitch system is a piston servo system which can be modeled by a second-order dynamic equation [108] as follows:

$$\ddot{\beta} + 2\zeta\omega_n\dot{\beta} + \omega_n^2\beta = \omega_n^2\beta_r \quad (2.1)$$

where  $\beta$  is the blade-pitch angle measurement,  $\beta_r$  is the reference blade-pitch angle from pitch control system,  $\omega_n$  is the natural frequency, and  $\zeta$  is the damping ratio. In the case of no failure, the following parameters are used:  $\zeta = 0.6$ ,  $\omega_n = 11.11$  rad/s [109].

### 2.4.2 Parameters for deteriorated hydraulic pitch system

In order to model the failures mentioned in Section 2.3 with equation (2.1), parameters for the pitch system under different conditions are defined as below:

#### 1 Leakage

Hydraulic leakage failure leading to low pressure can induce an abrupt change in the pitch system model parameters  $\omega_n$  and  $\zeta$  [110].

## 2 Wear

Wear failure causes the increase of the damping ratio, at the same time the natural frequency decreases.

## 3 Excessive air/oil ratio

This failure will manifests itself with slower actuator response over time, this failure is modeled as a slow, time varying change in system parameters  $\zeta$  and  $\omega_n$ . It can reduce the natural frequency  $\omega_n$  [108][111]. Besides, this deterioration process doesn't noticeably affect the damping ratio [111]. In the literature, when  $\omega_n$  decreases to  $3.42 \text{ rad/s}$ , they consider the pitch system is failed, and at this moment, the failure can be detected.

From now on, the thesis mainly considers the excessive air/oil ratio failure.

### 2.4.3 Response of deteriorated hydraulic pitch system

Step response with different  $\omega_n$  for equation (2.1) is given in Fig 2.4. A simulation of wind turbine simulator's reaction with different  $\omega_n$  is shown in Fig 2.5. Compared with the healthy system ( $\omega_n = 11.11 \text{ rad/s}$ ), the deteriorated pitch system leads to unsatisfied control results.

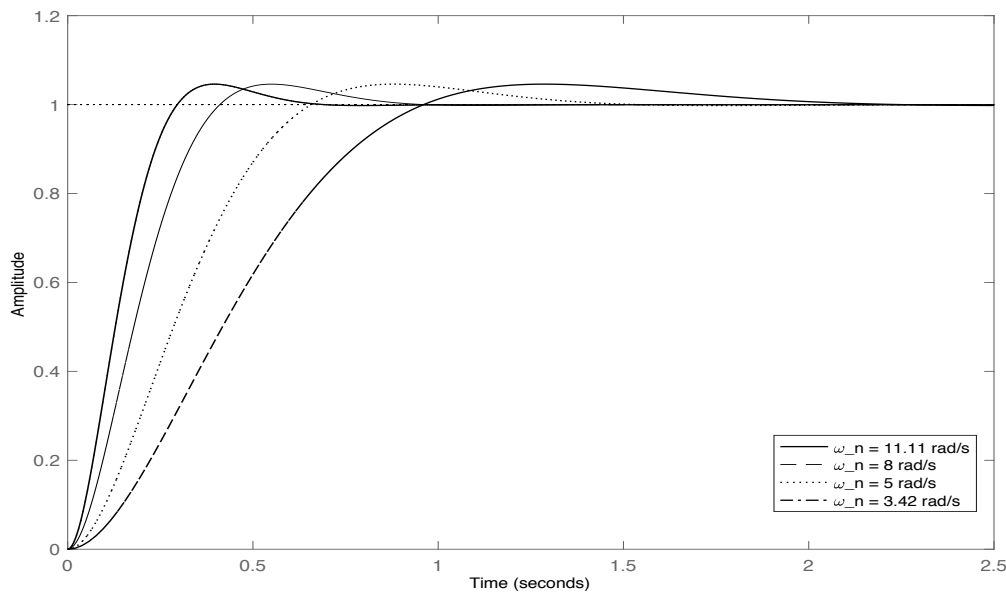


Figure 2.4: Wind turbine behavior according to the wind speed

Technically, reaching the failure level of excessive air/oil ratio in the hydraulic system is not an abrupt change, but a gradual process. This process is considered as the deterioration of pitch system in the thesis. It relates to the pitch system operation/usage driven by the wind speed variation. Quickly and stochastically wind speed changing are the main difficulty associated with hydraulic pitch system deterioration study. This phenomenon leads to random pitch operations, causing a random deterioration process.

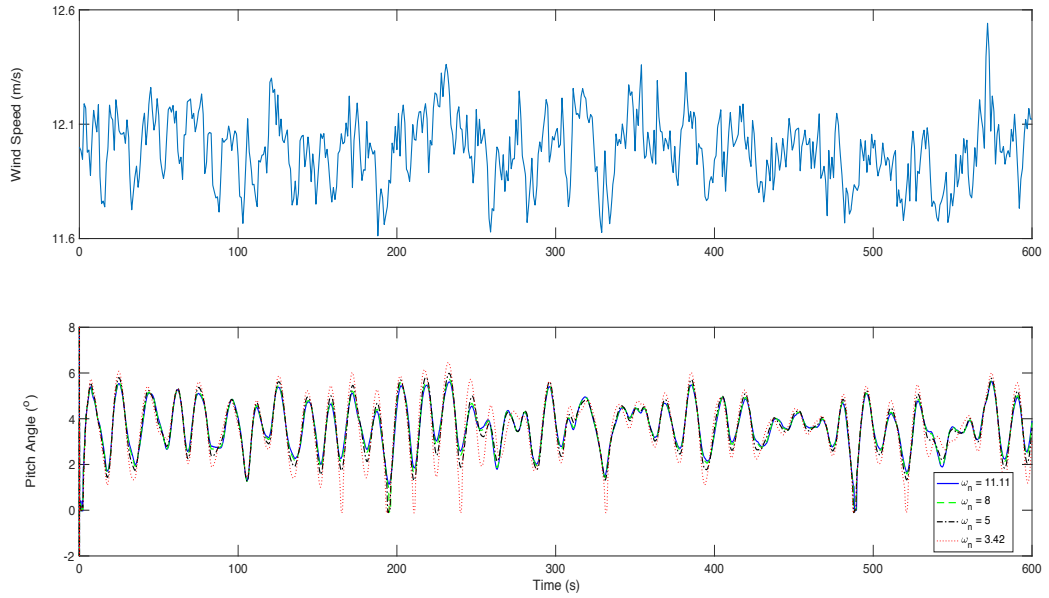


Figure 2.5: Transition among the operational states of variable-speed wind turbine

#### 2.4.4 Deteriorated hydraulic pitch system model considering wind speed influence

The available operation data from SCADA relating to pitch system are pitch angle and pitch rate. To quickly adjust the generator rotational speed and the rotor's rotational speed over the variable wind speed, current pitch rate can reflect the current wind speed turbulence. In order to model the actuator deterioration over time, we consider that the deterioration rate depends on its usage, which is directly related to wind speed fluctuations. Hence, the Accumulate Pitch Rate (APR) is introduced as a parameter used to represent the wind influence. Let  $APR(t, s)$  denote the accumulate pitch rate from time  $t$  to time  $s$  with  $s > t \geq 0$ . It is defined as

$$APR(t, s) = \int_t^s B_u du \quad (2.2)$$

where,  $B_t$  is the pitch rate at time  $t$  and is expressed in  $rad/s$ . Due to the intrinsic randomness of wind, the operation of pitch system is stochastic. Hence, for a given time period  $\delta t$ ,  $APR(t, t + \delta t)$  is a random positive real value. An example is shown in Figure 2.6. It shows the evolution of  $APR(t_i, t_{i+1})$  with  $t_i = 60$  i.e. a timescale of one minute.

The usage of pitch system, which is quantified as  $APR_i$ , slowly increases the air/oil ratio of hydraulic pitch system. The latter is assumed as monotonous increasing in the absence of maintenance. The air content at time  $t_i + s$  only depends on the one at time  $t_i$ .

The increment of deterioration during a time interval  $\delta t$  is modelled as a random variable which depends on  $\delta t$  and on the usage. It is proposed as an example

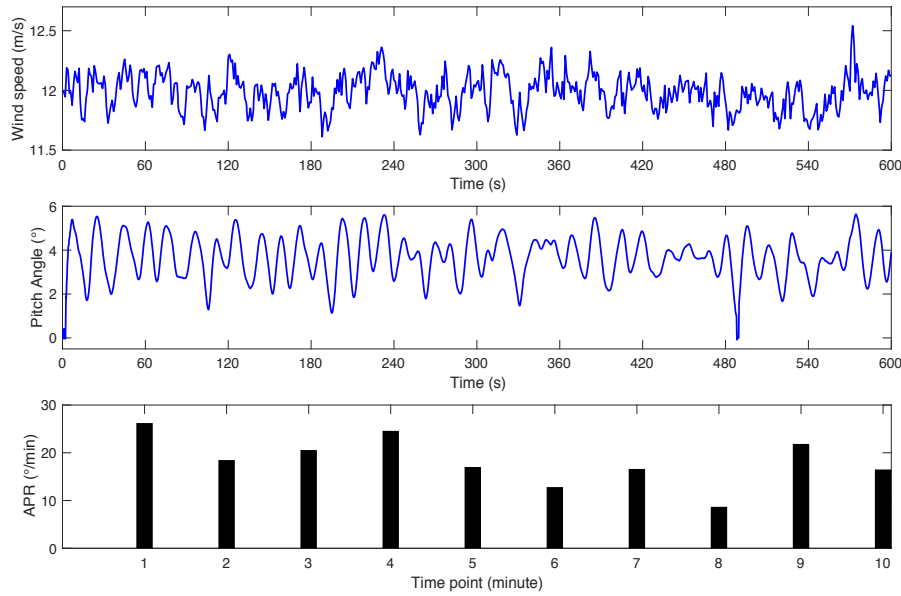


Figure 2.6: A sample for APR value

to consider gamma distributed random variables with deterioration increments every minute. A different random variable could be considered but such a choice requires an in-depth analysis of deterioration phenomenon from data and it is not the objective of this work.

Therefore, we consider that the shape parameter of gamma distribution is a linear product of APR and time, the deterioration increment distribution at time  $t$  could be defined as follows:

$$f(x|g(\text{APR})t, b) = \frac{1}{b^{g(\text{APR})t}\Gamma(g(\text{APR})t)} x^{g(\text{APR})t-1} e^{-\frac{1}{b}x} \quad (2.3)$$

where  $g(\text{APR})$  is a function related to APR,  $b$  is constant.

$x(t)$  is the deterioration increment at time  $t$ , therefore the value of degraded natural frequency of hydraulic pitch system  $\omega_{n_D}$  at time  $t$  is

$$\omega_{n_D}(t) = 11.11 - \sum_{i=0}^t x(i) \quad (2.4)$$

Substituting  $\omega_{n_D}(t)$  for  $\omega_n$  in equation (2.1), the deteriorated hydraulic pitch system is modelled. It is used to simulate the deteriorating hydraulic pitch system hereafter, as the input data for pitch system RUL and maintenance.

## 2.5 Realization with Matlab/simulink

Figure 2.7 shows how the different parts of the model are put together in the overall integrated wind turbine simulator with a deteriorated hydraulic pitch sys-

tem. The Fatigue, Aerodynamics, Structures and Turbulence (FAST) software is a wind turbine simulator designed by the US National Renewable Energy Laboratory (NREL). Several real and composite wind turbine models are available in FAST software, including the NREL-5MW baseline wind turbine [106]. FAST provides interfaces for the customized pitch system and wind speed sequence, and it can be embedded in the Simulink environment. In this thesis, the wind speed sequence is simulated by Matlab. While the PI controller and deteriorating actuator are implemented and are connected with FAST in the Simulink environment, as well as the wind speed data. The input wind speed sequence is used to drive the FAST wind simulator.

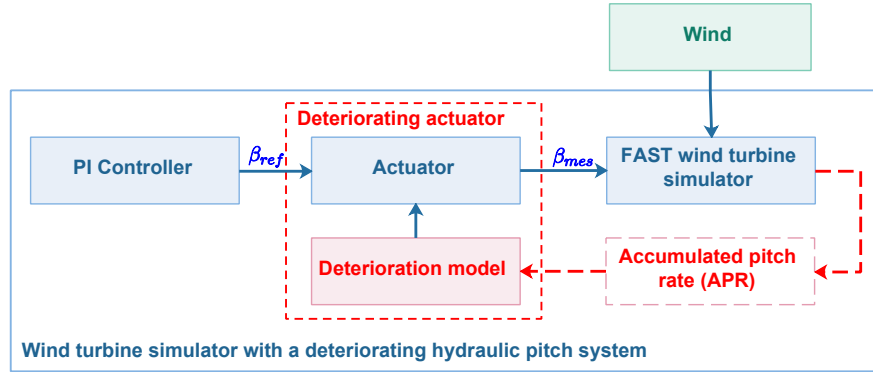


Figure 2.7: Wind turbine simulator with a deteriorating hydraulic pitch system

## 2.6 Deterioration indicator for hydraulic pitch system

The global model has been described previously and it includes pitch actuator deterioration. It can be considered as a digital twin of a real deteriorating wind turbine. But from a practical point of view the deterioration level cannot be measured easily. Then a process is proposed to estimate the degradation indicator from the data available from SCADA without any additional sensor or device.

Since reference pitch angle ( $\beta_{ref}$ ) and measured pitch angle ( $\beta_{mes}$ ) can be easily achieved from SCADA, they are used to estimate the parameters of transfer function, the estimated value of natural frequency ( $\hat{\omega}_n$ ) is the indicator for the hydraulic pitch system deterioration.

Taking into account of the SCADA data acquisition frequency and the actual long-term deterioration process,  $\hat{\omega}_n$  is estimated for every ten minutes using the **tfest** Matlab function. Hence, the estimated natural frequencies constitute a time series  $\hat{\omega}_n\{T_i\}$  ( $i = 1, 2, \dots, n$ ). Compared with its service time and, the pitch system can be considered as continuously monitored. If  $\hat{\omega}_n$  is smaller than  $3.42 \text{ rad/s}$ , the hydraulic pitch system is considered as failed.

## 2.7 Conclusion

The contribution of this chapter is the proposition of a wind turbine simulator incorporating with a deteriorating hydraulic pitch system. A method is proposed where the deterioration of hydraulic pitch system is related to wind speed which is a random phenomenon. The deterioration directly affects the natural frequency of the pitch system actuator. This parameter is then gradually decreasing with time and usage. Hence, the deterioration process is stochastic.

A wind turbine is driven by wind, similarly, to run the numerical wind turbine simulator, it needs wind data (wind speed and wind direction). The thesis assumes that due to the yaw system, the nacelle always faces the inflows of wind. Therefore, for the simulator, it only needs the wind speed with a high stamping frequency when compared to the slow deterioration phenomenon. The next chapter will focus on wind speed modelling.

# Chapter 3

## Wind speed model

### Problem statement

For degradation analysis, precise numerical results are necessary only when the wind speed is in full load region. Short-term continuous sequences of wind speed are required to characterize the degradation increments in different configurations. Furthermore, the dynamics of deterioration are very slow and require long-term trend analysis and simulation capabilities to know how the degradation leads to failure. Hence, for the study relating to a pitch system deterioration, a long-term wind speed model with embedded continuous parts is necessary.

### 3.1 Introduction

In order to take into account the possible non-linearity in wind speed data and to take advantage of the wind speed randomness, a general and flexible modeling framework is required. Since future wind speed trend does not depend on its past, Markov Chain is a good candidate to model mean wind speed data behaviour. Despite the simplicity of first-order Markov chain, it can reproduce an artificial wind speed series with faithful statistical characteristics to the measured data [112, 113, 114, 115]. However, as the autocorrelation of generated data is dropping off faster than the one of real data, Markov chain is not suitable for small timescale wind speed generation. The research done by [116] shows the unsuitability of Markov chain for time step smaller than fifteen minutes. Authors in [117] put emphasis on second-order Markov chain and semi-Markov chain and applied them for wind speed modelling in order to improve the accuracy of more sophisticated calculation demanding cases.

Another common stochastic modelling framework is derived from Stochastic Differential Equations (SDEs), refer to [118]. Differential Equations are standard models for deterministic dynamics. However, natural phenomena are exposed to factors that are neither entirely known nor easy to model explicitly. Hence, extended models considering more complicated changes in the dynamics are required.

SDEs can be considered as extensions of deterministic differential equations, where parameters are evolving randomly or where stochastic processes are added to the main dynamics. SDEs are especially suitable for modeling wind speed fluctuation and can be used to simulate wind speed at any timescales. However, considering e.g., diurnal and seasonal influences, the wind speed generation length of SDEs with constant parameters is limited to a few hours.

The existing wind speed models focus on either short-term modeling or long-term modeling with a large timescale. Therefore, the analysis of the wind turbine performance and operation relating to wind speed is limited. Short-term modeling results limit the analysis to a current short period; long-term modeling results can not provide sufficient and qualitative data for analysis. Especially consider the situation where continuous closed-loop control interacts with a long-term actuator degradation as described in previous chapter. The actuator degradation is affected by its usage, hence, closely connected to wind speed characteristics. This issue is related to problems of RUL assessment and to output power estimation of wind turbine. It falls into the field of prognosis and health management (PHM) and is a key input for condition-based maintenance. Both RUL and output power are affected by wind turbulence intensity which is defined as variance divided by mean wind speed. Researchers figure out that turbulence intensity is one of the critical influences on wind turbine lifetime [28]. Some studies indicate that wind speed has a significant impact on degradation of wind turbine components. For instance, the rapid variation of wind speed leads to frequent and sudden actions of the blade-pitch system, which has a high failure rate compared to other components. Moreover, it has been indicated that turbulence intensity affects the turbines power production [119, 120, 121, 122, 123, 124]. For RUL estimation, hourly average wind speed data is less satisfactory. They reflect the general trend of wind speed at the cost of loss of detailed information, namely the turbulence of wind speed. Besides, degradation occurring to wind turbine components is a long-term process, and the RUL of wind turbine component changes dynamically according to its working condition.

A method proposing continuous wind speed generation during long time horizon seems missing in the literature. In the meantime, wind speed at different timescales are applied in different ways. For example, long-term wind speed data is used to estimate wind energy for a future wind farm; various wind speed sequences are used to test a new control strategy; annual wind sequences with detailed information are considered in reliability study of wind turbine. The importance of a fulsome wind speed model in reliability, production and prognosis and the shortfall in the literature encourage us to propose a wind speed model which satisfies the requirements as follows:

- can reflect the trend of wind in long-term
- can contain turbulence information at small timescale
- can fit the real wind speed data's probability distribution
- can quickly generate data

In other words, this chapter proposes a mathematical model which permits to generate satisfiable wind speed sequences for wind turbine components RUL study and for accurate output power estimation.

The main contribution of this chapter could be summarized as follows:

- A new wind speed generation model benefiting the advantages of Markov chain and SDEs is proposed.
- Two kinds of SDEs are applied to different wind profiles generation.
- An application related to the operation of wind turbine is presented.

## 3.2 Wind Model description

### 3.2.1 General description

In wind power industry, the Reynolds decomposition needs to be considered for analyzing turbulence effects [125]. As shown in Figure 3.1, the wind speed time series  $U(t)$  can be decomposed into its mean value  $\bar{U}(t)$  and the fluctuation  $u(t)$ .

$$U(t) = \bar{U}(t) + u(t) \quad (3.1)$$

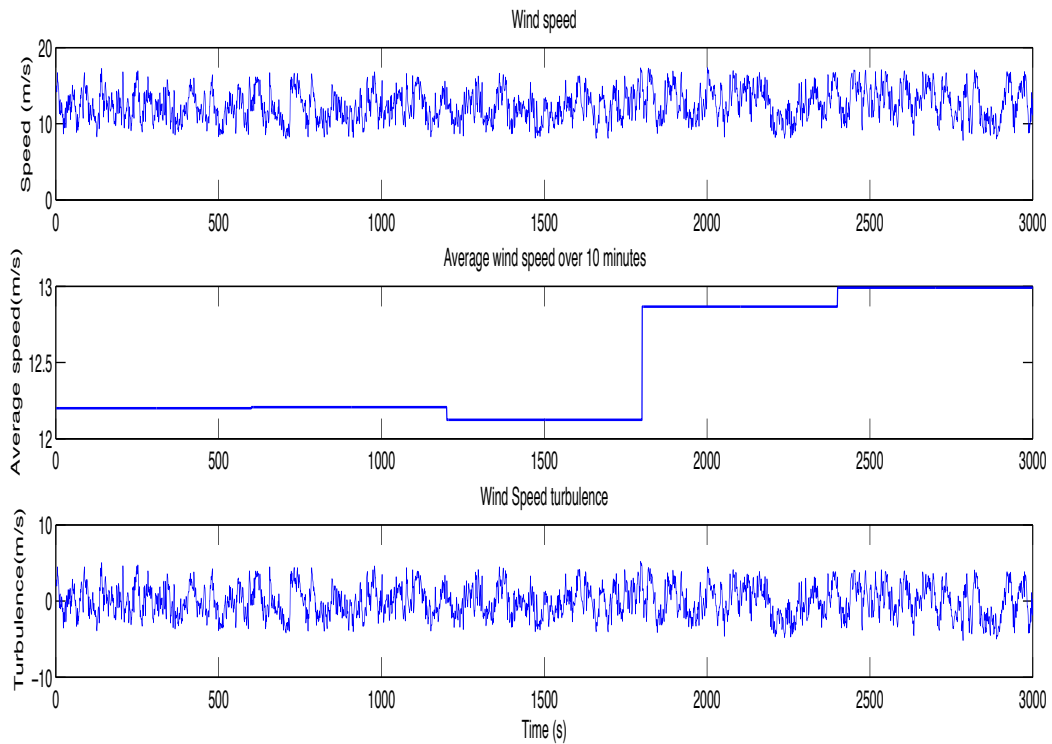


Figure 3.1: Wind speed series

This decomposition gives us an idea to model the mean wind speed and wind speed fluctuation separately. As it is mentioned in [10],  $\bar{U}(t)$  can be considered as a low-pass filter corresponding to the hourly, daily, monthly, seasonal or annual effects; turbulence  $u(t)$ , which has a zero mean value, can be seen as a high-pass filter corresponding to the turbulent impacts.

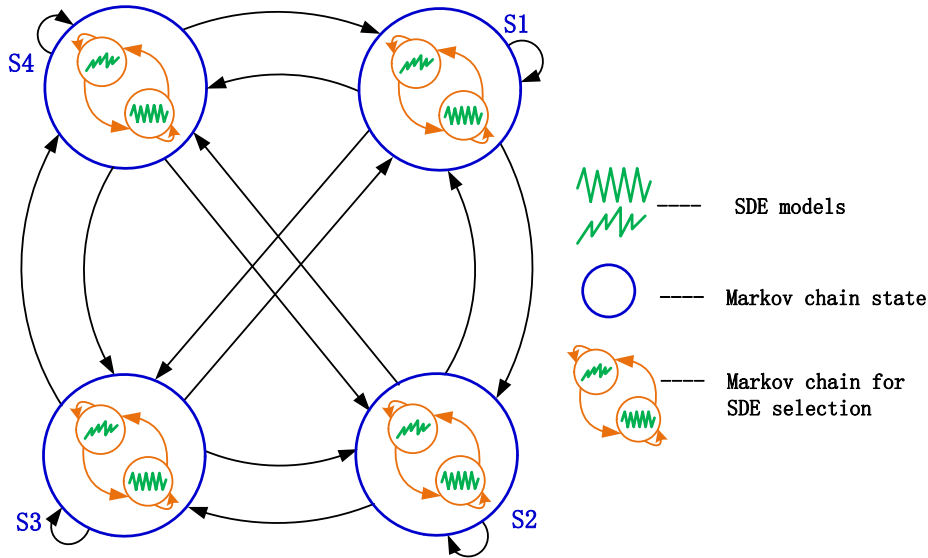


Figure 3.2: Wind speed generation model — 2-level Markov chain model embedded with SDE

Depending on research emphasis, wind speed can be modeled in different ways at different timescales. Since studies show that wind turbulence intensity has a significant impact on energy production and failures of wind turbine, continuous wind speed is more appropriate when one studies the operation of wind turbine. Hourly average wind speed is a good choice when one wants to estimate the wind resource of a site. And SCADA system records 10 minutes' average wind speed in wind turbine operation log file.

In this chapter, we propose a 2-level Markov chain model embedded with SDEs. Figure 3.2 shows the overall model with the Markov chain and the SDE model. This model is very flexible due to the following properties:

- Outer Markov chain (blue ones shown in Figure 3.2) is used to model macroscopical (general) wind speed trend. It can have several meanings, such as average wind speed for a specific timescale (hourly or daily average wind speed) or different wind speed classes (breeze, strong wind, storm, etc.).
- The embedded SDEs are mainly used to model continuous wind speed sequences depending on the states' environment which is set by the outer Markov chain. Different parameter settings and different SDEs give a large variety of continuous wind speed models.
- An inner Markov chain (Orange ones shown in Figure 3.2) is considered inside each state of the outer Markov chain to randomly toggle between the two classes.

- For different conditions of simulations such as gust or extreme weather, other SDEs can be supplemented. For these reasons, this model is easily modified according to the user's requirement.

Here two example of wind speed data that can be generated by this proposed model. They are given as follows,

- One day's (24 hours) wind speed generation

Each state of outer Markov chain represents hourly average wind speed. In this case, 23 transitions between states are generated to represent the average wind speed time series for one day. In each state, SDE is used to generate wind sequences data at small timescale like one second or continuous. The SDE considered for 10 minutes is driven by the inner Markov chain.

- Different wind class generation

Refer to IEC standards [126], wind condition contains normal, extreme and gust which could be generated by Markov chain. Inside the state of Markov chain, SDEs are used to simulate wind speed associated with considered wind condition.

### 3.2.2 Markov chain embedded with SDE

#### Markov chain as a macroscopic wind speed model

A Markov chain is uniquely defined by its state space, transition matrix and initial distribution. Markov chain wind speed modeling consists of four main steps: state definition, transition matrix estimation, state simulation and wind speed simulation. The state definition is related to a classification problem and depends on the purpose. It corresponds to the choice of interval over the wind speed range, which may depend on the occurrence frequency of speed values. Let  $S = [s_1, s_2, \dots, s_N]$  be the state space for the outer Markov chain corresponding to different possible states of the wind speed. Let  $\{X_t\}_{t \geq 0}$  represents the wind speed time series. The event " $X_0 = s_5$ " means that at time  $t = 0$ , the meanwind speed fluctuation wind speed is in state  $s_5$ . Table 3.1 shows an example of state assignment.

State	$s_1$	$s_2$	$s_3$	$s_4$
Wind speed (m/s)	[4,8]	(8,9.4]	(9.4,10.2]	(10.2,10.7]
State	$s_5$	$s_6$	$s_7$	$s_8$
Wind speed (m/s)	(10.7,11.2]	(11.2,12]	(12,12.8]	(12.8,25)

Table 3.1: Example for Markov chain state space

The initial distribution is estimated by dividing the dataset into bins according to the states. The obtained vectors of occurrences can then be normalized in each bin. Let  $p_i^0 = \mathbb{P}\{X_0 = s_i\}$  denote the probability that the first element of the wind time series is in the interval  $s_i$ . To estimate it, count the number of times that

there is a value belonging to the state  $s_i$  in the entire recorded time series and divide it by the total number of recorded values.

Let's denote the transition probability as follows:

$$p_{ij} = \mathbb{P}(X_{n+1} = s_j | X_n = s_i) \quad (3.2)$$

where  $s_i, s_j \in S$ . The probability  $p_{ij}$  can be estimated by counting the number of times a value in the state  $s_i$  followed by one in the state  $s_j$  in the wind time series, normalized by the total number of occurrences of values in state  $s_i$ . The transition matrix of the Markov chain is defined as follows:

$$\pi = \begin{bmatrix} p_{1,1} & p_{1,2} & \cdots & p_{1,n} \\ p_{2,1} & p_{2,2} & \cdots & p_{2,n} \\ \vdots & \vdots & \ddots & \vdots \\ p_{m,1} & p_{m,2} & \cdots & p_{m,n} \end{bmatrix}.$$

### SDEs for continuous short-term wind speed modeling

After studying 1 million wind speed fluctuation distributions, author of [10] concludes that broadly speaking there are three classes of wind speed fluctuation distributions. The analysis points out that 90% of wind speed fluctuation follows a kind of symmetrical mono-modal probability distribution function (PDF) which is well fitted by a Gaussian PDF (line with circle shown in Figure 3.3). 9% of wind speed fluctuation follows a kind of dissymmetrical mono-modal PDF which can be described by Gram-Charler series (dash line with square shown in Figure 3.3). And the rest 1% follows a kind of bimodal PDF which is fitted with a mixture of Gaussian PDF (dotted line with star shown in Figure 3.3). Figure 3.3 shows the mean PDF of wind speed fluctuation for each class.

Consider the first two classes pointed out by [10] which represent 99% of all the turbulence distributions. The aim is to associate an SDE with each class. In order to consider that wind speed dynamic is impacted by a Gaussian noise, one considers a diffusion process which is a particular stochastic differential equation whose general form is as follows:

$$dZ(t) = a(Z(t), t) dt + b(Z(t), t) dW(t), \quad t \in [0, T] \quad (3.3)$$

where  $Z(t)$  denotes here the wind speed at time  $t$ ,  $a(Z(t), t)$  and  $b(Z(t), t)$  are the drift and diffusion terms, respectively.  $W(t)$  is the standard Wiener process.

In other words, the Wiener process (or standard Brownian motion) is a continuous process whose increments are normally distributed. A large number of stochastic processes defined by equation (3.3) are available. Some of them are good candidates to fit the wind speed data.

Figure 3.4 to 3.6 show the histograms of real wind speed fluctuation. Three sequences of real wind speed that resemble the PDFs shown in Figure 3.3 are de-

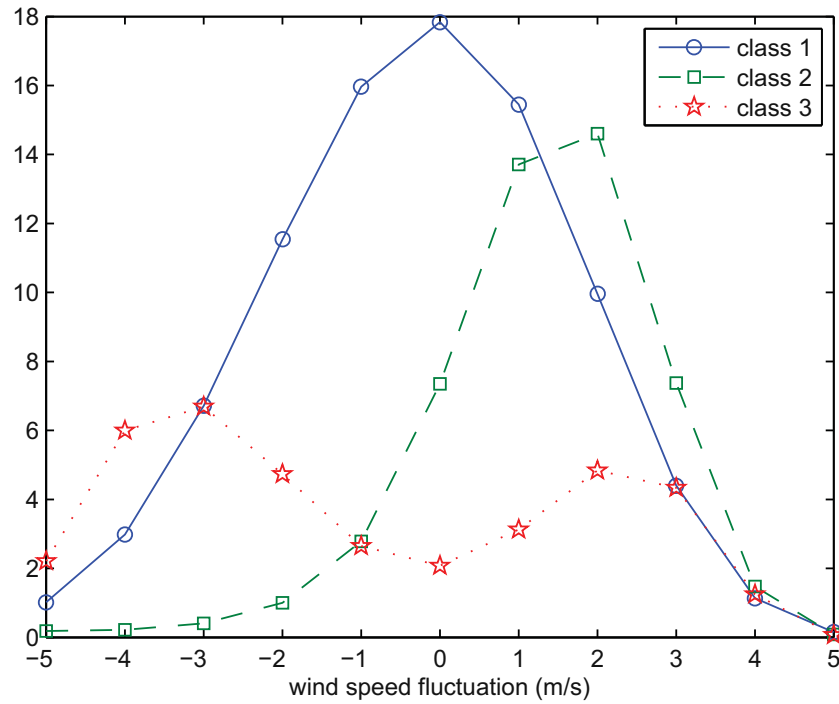


Figure 3.3: Three classes of wind speed fluctuation PDF (Source: [10] )

picted. These data record the wind speed during one hour at the site San Gorgonio, USA, downloaded from the website [www.winddata.com](http://www.winddata.com).

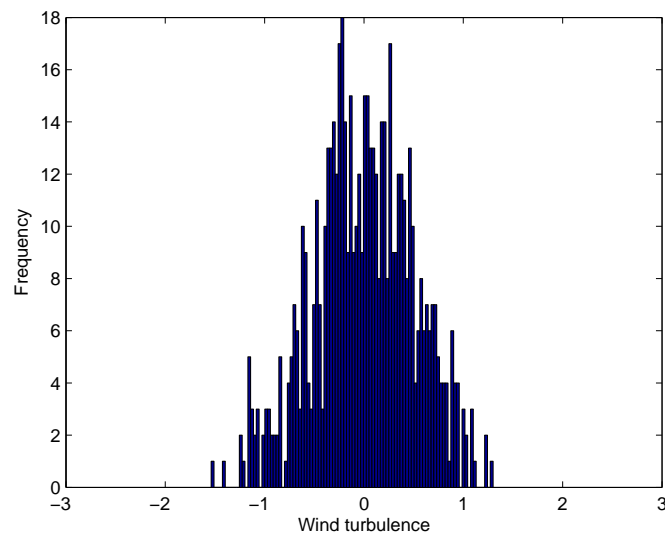


Figure 3.4: symmetrical PDF

The common scenario is that wind speed fluctuation  $u(t)$  follows a symmetrical mono-modal PDF. From equation (3.1) the mean value is always around zero (Figure 3.4). Combining with the research results of [10], a mean-reverting diffusion process seems to be a suitable candidate. For such diffusion processes, fluctuations in degradation records from an overall degrading trend are auto-correlated

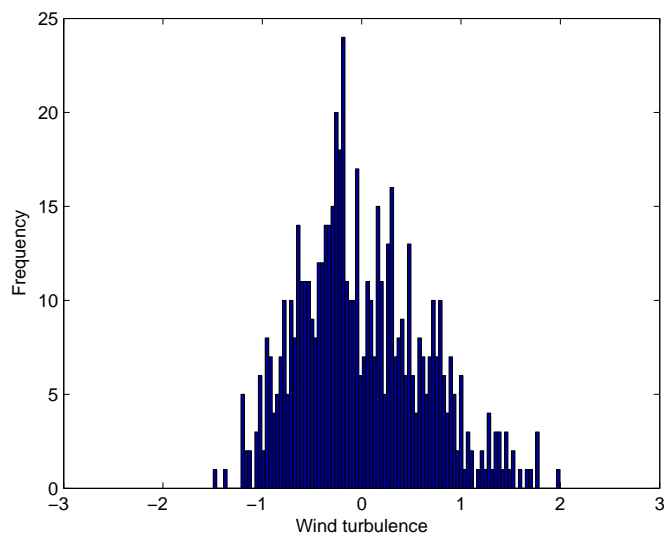


Figure 3.5: dissymmetrical PDF

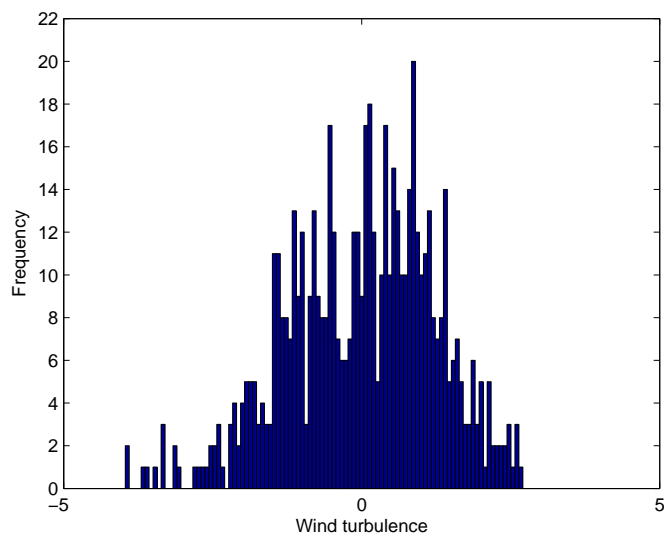


Figure 3.6: bimodal PDF

and the expectation of  $Z(t)$  tends to drift toward its long-term mean over time. The mean-reverting property ensures that volatility is not “exploding”. The class of “Ornstein Uhlenbeck” processes is particularly suitable to fulfil the previous requirements. It is presented more precisely in the next section.

### 3.2.3 OU process for wind generation

OU processes are used to model the first two classes about wind speed fluctuation presented by [10]. In other words, for each short-term wind speed class, an OU process is used. This model enables generation of continuous wind speed during a short period, such as several seconds or 10 minutes in our case.

General OU process has been present in section 1.6.4 of Chapter 1. Now two specific cases of OU process are presented for modeling the class 1 and class two wind speed fluctuations, and their parameters estimation methods are also given.

### 3.2.3.1 OU process for class 1

For equation (1.17), let  $\zeta = 0, a = -\alpha, b = \beta$ . In order to avoid confusion with the general case (equation (3.3)),  $Y(t)$  is used instead of  $Z(t)$ . The OU process chosen to describe the increment of wind speed sequence when turbulence is well fitted by Gaussian PDF is as follows:

$$dY(t) = aY(t)dt + b dW(t), \quad t \in [0, T], \quad Y(0) = 0 \quad (3.4)$$

where  $a$  is a strictly negative constant for all  $Y(t)$  and  $b$  is constant.  $Y(t)$  is the wind speed fluctuation at time  $t$  and it is a stationary autocorrelated diffusion process.  $W(t)$  is a standard Brownian motion.

According to equation (1.18) the log-likelihood approximation based on transition probability is defined as follows:

$$\begin{aligned} \log L(a, b) &= \log \prod_{i=1}^N \mathbb{P}(Y(t_{i+1})|Y(t_i), t_I, a, b) \\ &= -\frac{n}{2}(\log(b^2) + \log(v(a))) + \frac{1}{2b^2v(a)} \sum_{i=0}^{n-1} (Y_{t_{i+1}} - \exp(a\Delta)Y_{t_i})^2 \end{aligned} \quad (3.5)$$

where,  $\mathbb{P}$  is the conditional pdf of  $Y(t_{i+1})$  to  $Y(t_i)$ ,  $t_i$ ,  $a$ ,  $b$ ,  $\Delta = t_{i+1} - t_i, t_i = i\Delta$ , ( $i = 1, \dots, n$ ) and  $v(a) = \frac{\exp(2a\Delta)-1}{2a}$ .

Hence, the parameter estimators of  $a$  and  $b$  are as follows:

$$\hat{a} = \frac{1}{\Delta} \log\left(\frac{\sum_{i=1}^n Y_{t_{i-1}} Y_{t_i}}{\sum_{i=1}^n Y_{t_{i-1}}^2}\right) \quad (3.6)$$

$$\hat{b}^2 = \frac{1}{nv(\hat{a})} \sum_{i=1}^n (Y_{t_i} - \exp(\hat{a}\Delta)Y_{t_{i-1}})^2 \quad (3.7)$$

### 3.2.3.2 OU process for class 2

For class 2, wind speed fluctuation has the form of dissymmetrical mono-modal PDF. The OU process chosen to describe wind speed is as follows:

$$dY(t) = -(Y(t) - \mu)dt + \sigma dW(t), \quad Y(0) = 0 \quad (3.8)$$

where  $Y(t)$  is the wind speed at time  $t$ ,  $\mu$  and  $\sigma$  are constant parameters and  $W(t)$  is the standard Brownian motion. With  $\Delta t = t_i - t_{i-1}$ , according to equation (1.18) and [97] the density function is as follows:

$$\begin{aligned} & \mathbb{P}(Y(t_i)|Y(t_{i-1}), t_{i-1}, \mu, \sigma) \\ &= \frac{e^{\Delta t}}{\sqrt{\pi \cdot \sigma^2 (e^{2\Delta t} - 1)}} \exp\left(-\frac{(Y(t_i) \cdot e^{\Delta t} + \mu(1 - e^{\Delta t}) - Y(t_{i-1}))^2}{\sigma^2 (e^{2\Delta t} - 1)}\right) \end{aligned} \quad (3.9)$$

Hence, by numerically minimizing the following log-likelihood function, the estimated values of  $\hat{\mu}$  and  $\hat{\sigma}$  can be obtained.

$$\log L(\mu, \sigma) = \log \prod_{i=1}^N P(Y(t_i)|Y(t_{i-1}), t_{i-1}, \mu, \sigma) \quad (3.10)$$

### 3.2.3.3 Markov chain model for two switching wind class

The inner Markov chain is designated as an SDE-Selection model (SSM). According to the statistics given by [10] and with respectively 90% and 10% of wind speed fluctuation for class 1 and 2, the transition probability shown in Table 3.2 is assigned to SSM.

class	<i>Class</i> <sub>1</sub>	<i>Class</i> <sub>2</sub>
<i>Class</i> <sub>1</sub>	0.9	0.1
<i>Class</i> <sub>2</sub>	0.9	0.1

Table 3.2: Transition probability for SSM

## 3.3 Wind speed generation procedure

### 3.3.1 Experimental dataset

Long-term (one year sequences) hourly average wind speed data can be easily accessed. For instance, websites like [www.ncdc.noaa.gov/cdo-web](http://www.ncdc.noaa.gov/cdo-web) and [www.winddata.com](http://www.winddata.com) provide free time series of wind characteristics measured under different conditions during 10 minutes or 1 hour. The real data used in this chapter is downloaded from the two websites.

### 3.3.2 Wind speed generation

There are two difficulties to estimate the transition probability matrix of the Markov chain model from real wind speed data:

- Markov chain with plenty of states could be constructed resulting in a huge transition matrix that might cause additional difficulties in estimation;
- The number of data in certain states could be much smaller than others, resulting in a lot of probabilities close to 0 in the transition probability matrix.

In order to avoid the above phenomena, the number of states should be determined relatively small. It could be determined by users or based on some criterion. Authors in [127] recommend determining the interval with the empirical quantiles. Supposing that the wind speed time series is stationary and ergodic. Hence, the empirical cumulative distribution function is a consistent estimator of the cumulative distribution of the invariant measure of this time series. The boundaries are taken to be  $\hat{F}_N^{-1}(j/k)$ ,  $j = 1, 2, \dots, k$ , where  $k \in N$  is the number of state,  $N$  is the number of outer Markov chain state, and  $\hat{F}_N$  is the empirical cumulative distribution function.

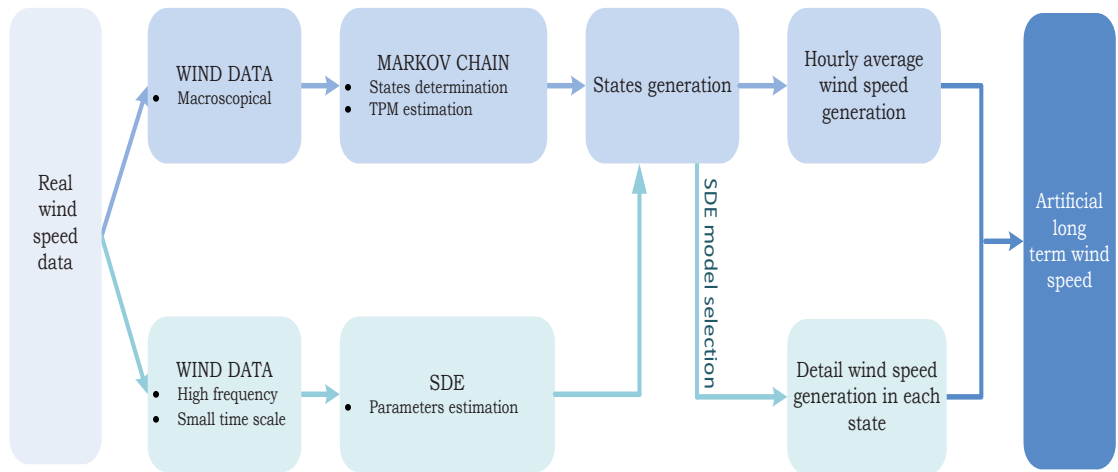


Figure 3.7: Steps for wind speed generation

The principal artificial wind speed data generation steps (shown in Figure 3.7) are as follows:

Step 1 Choose wind speed data for Markov chain and SDEs estimation separately

- Step 2
- Determine the outer Markov chain states
  - Estimate the transition probability matrix of Markov chain from real wind speed data
  - Estimate the parameters of SDEs from real wind speed data

Step 3 Generate hourly average wind speed

Step 4 Use SSM to select SDE and generate continuous wind speed data with respect to the condition of outer Markov chain state. If the outer state is not the last one, go back to Step 3, otherwise, finish.

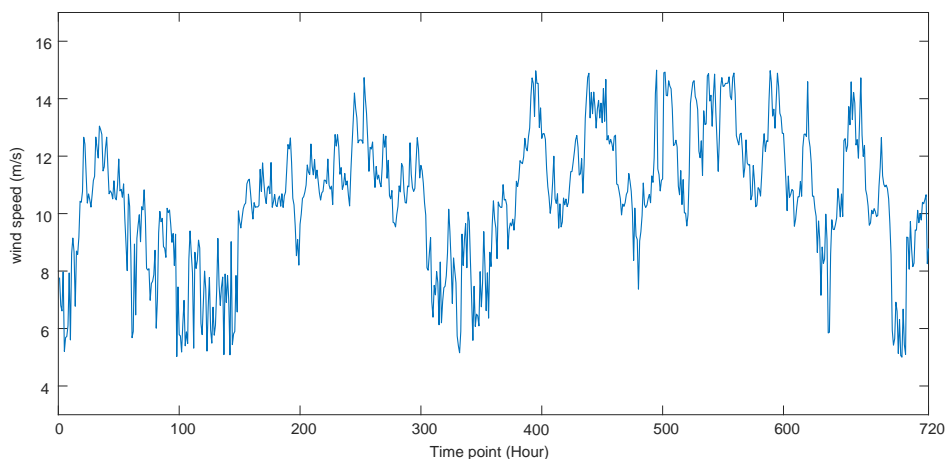


Figure 3.8: Hourly average wind speed generation (m/s)

We would like to give an example of one month's wind speed data at secondly timescale generation. Hence, the states of outer Markov chain represent the hourly average wind speed.

### 3.3.2.1 Generation of macroscopic wind speed using Markov chain model

The macroscopic wind speed represents hourly average wind speed in this thesis. A sequence of hourly average wind speed during one year is used to estimate the transition probability matrix of the Markov chain model. As a result of data acquisition reason, the available number of data is 6180 instead of 8760 ( $24 \text{ hours/day} \times 365 \text{ days}$ ). The number of states is determined as 8, according to the states shown in Table 3.1. We can obtain the transition probability matrix of Markov chain shown in Table 3.3. A sample of hourly average wind speed generation during one month is shown in Figure 3.8.

State Num	$s_1$	$s_2$	$s_3$	$s_4$	$s_5$	$s_6$	$s_7$	$s_8$
$s_1$	0.81383	0.179521	0.006649	0	0	0	0	0
$s_2$	0.200573	0.530086	0.219198	0.035817	0.014327	0	0	0
$s_3$	0	0.211043	0.541104	0.141104	0.045399	0.051534	0.008589	0.001227
$s_4$	0	0.026250	0.197500	0.450000	0.255000	0.063750	0.007500	0
$s_5$	0	0	0.068273	0.269076	0.398929	0.195448	0.068273	0
$s_6$	0	0	0.009576	0.135431	0.228454	0.385773	0.184679	0.056088
$s_7$	0	0	0	0	0.037783	0.248111	0.578086	0.13602
$s_8$	0	0	0	0	0	0.015421	0.161329	0.82325

Table 3.3: Estimation of Transition Probability Matrix

### 3.3.2.2 Continuous generation of wind speed using SDE

The aim of using SDE is to generate continuous wind speed data whose mean value is in accord with the hourly average wind speed set by the outer Markov chain state. Taking into account the common data collection frequency of SCADA

(an average wind speed value noted down per 10 minutes), an outer Markov chain state contains six successive sequences of 10 minutes. Each sequence is generated with one SDE model which represents the continuous wind speed for 10 minutes. The five switches from one SDE to the other during one hour depend on the state background set by Markov chain and are driven by SSM. Real wind speed sequences are classified according to their average value which refers to the states determined in Table 3.1. The estimated values are shown in Table 3.4.

State	$\hat{a}$	$\hat{b}$	$\hat{\mu}$	$\hat{\sigma}$
$s_1$	-0.1619	0.2878	7.5988	0.4337
$s_2$	-0.0855	0.1700	8.0542	0.4310
$s_3$	-0.0314	0.2573	10.0245	0.6459
$s_4$	-0.1049	0.3137	10.2984	0.6373
$s_5$	-0.0459	0.5118	10.6661	1.2831
$s_6$	-0.0196	0.2901	11.2078	0.8246
$s_7$	-0.0683	0.4051	12.4011	0.9461
$s_8$	-0.0957	0.3008	12.9833	0.5577

Table 3.4: Estimated value for SDE

To illustrate the performance of SDE wind speed model, the parameters of  $s_3$  are chosen to build the two OU processes. Class 1 model is expressed by equation (3.11); class 2 model is expressed by equation (3.12).

$$dy(t) = -0.0314 * y(t)dt + 0.2517 * dW(t) \quad (3.11)$$

$$dy(t) = -(y(t) - 10.0245)dt + 0.6459 * dW(t) \quad (3.12)$$

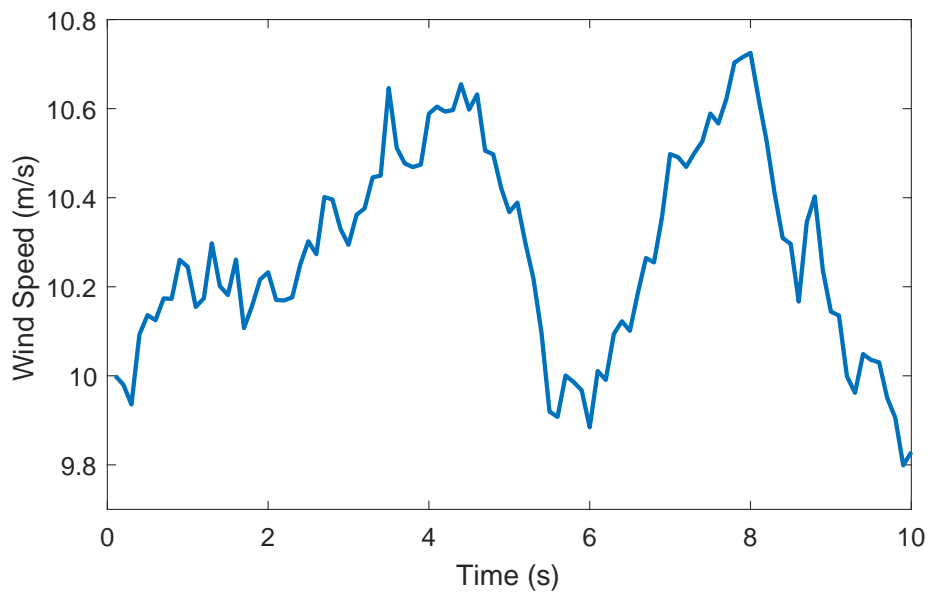


Figure 3.9: 10 sec. wind speed generation of class 1

SDEs have the ability to generate continuous wind speed, Figure 3.9 and Figure 3.11 show examples of wind speed simulation results for two different SDE classes

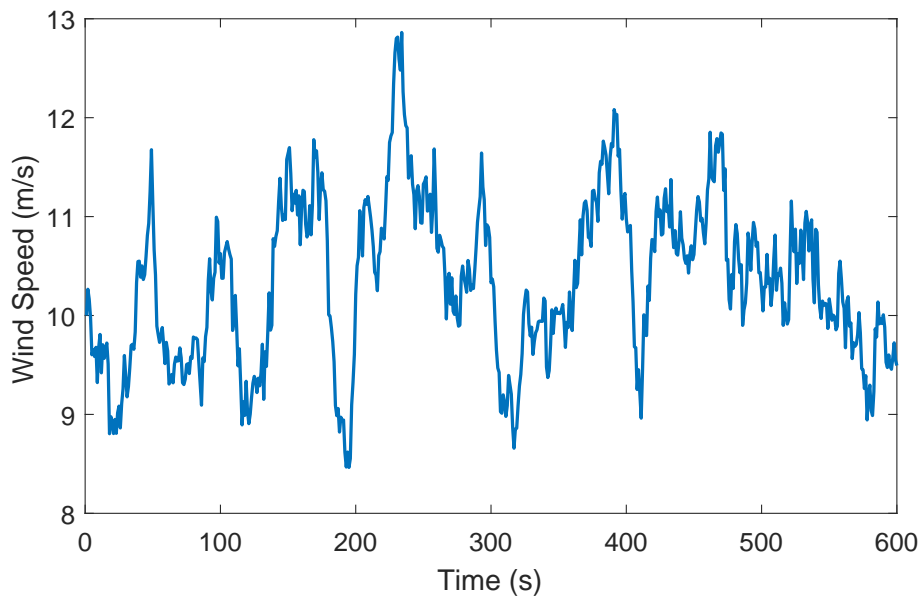


Figure 3.10: 10 minutes speed generation of class 1

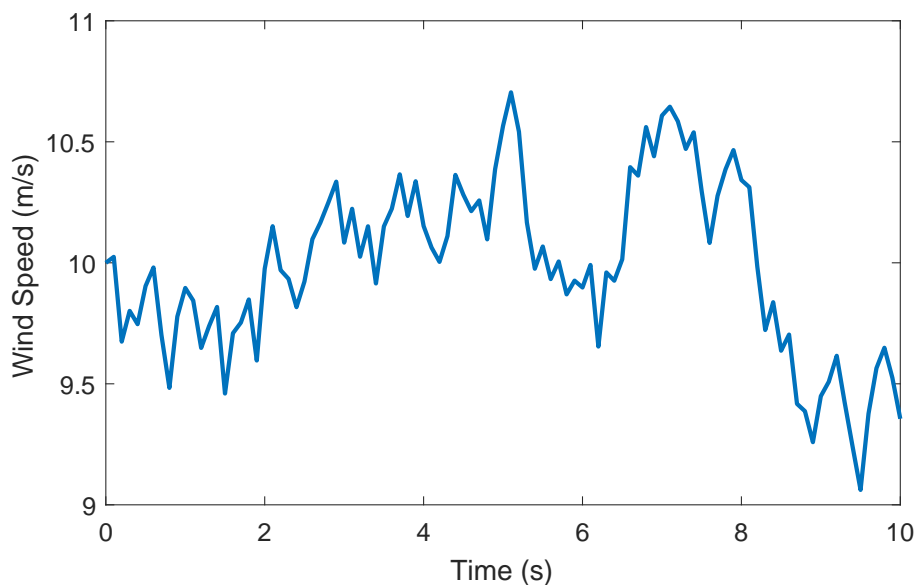


Figure 3.11: 10 sec. wind speed generation of class 2

and with two different timescales. Figure ?? shows a wind speed evolution during 10 sec, while Figure 3.11 shows a wind speed evolution during 10 minutes.

Figure 3.10 and Figure 3.12 show examples of wind speed simulation results by solving equation (3.11) and equation (3.12), respectively. They correspond to two different patterns of wind speed sequence both with 10 minutes average speeds belonging to the range  $(9.4, 10.2]$ . With different SDEs, various wind profiles can be generated. This latter helps us to simulate different wind conditions such as stable wind speed or wind speed with high turbulence intensity. This achievement is significant for wind turbine reliability engineering. Steady wind speed is good for the operation of wind turbine as it causes less vibration compared to the case with

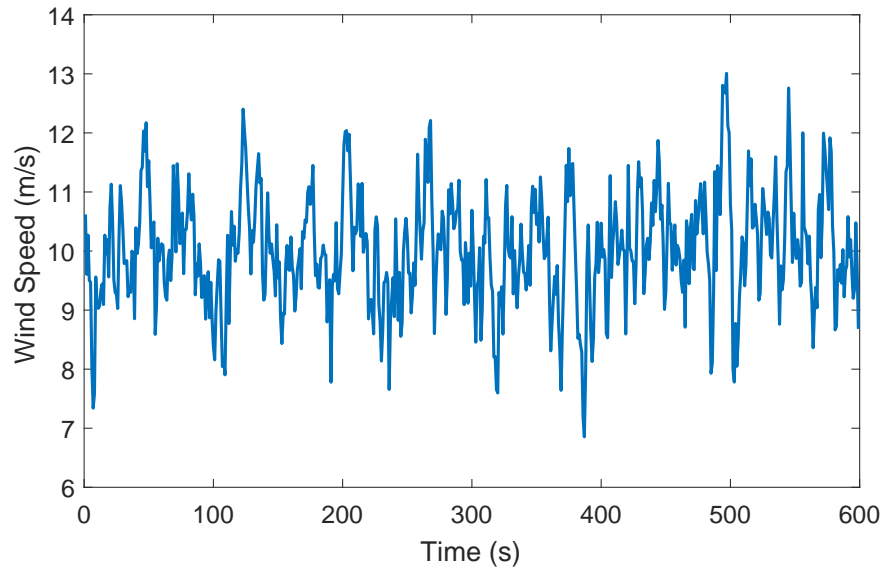


Figure 3.12: 10 minutes speed generation of class 2

the same average but high turbulence intensity wind speed. The latter may cause sudden overloads to wind turbine leading to its degradation. The real effect on the degradation may also depend on the wind turbine automatic control system.

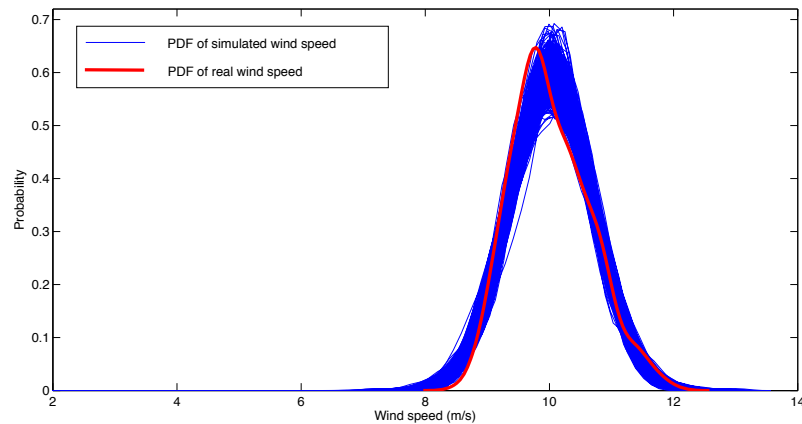


Figure 3.13: Probability density function of real data and simulated data

In Figure 3.13, the bold red line shows the probability density of a real wind speed sequence, the thin blue lines show the probability density of 500 samples of simulated data which are generated by solving Equation (3.12). The PDFs of the simulated wind speed fit to real data. But there still is a slight difference in the average values. Due to the limitation of available free real wind data, the model parameters are estimated from a reduce number of wind sequences which have similar statistical characteristics. Hence, with limited amount of real wind speed samples, the accuracy of estimated parameters may be weak leading to a bias between the real data and the simulated data.

Figure 3.14 shows an example of 30 days wind speed generation with Markov chain embedded with diffusion processes at secondly scale. The 10 minutes average

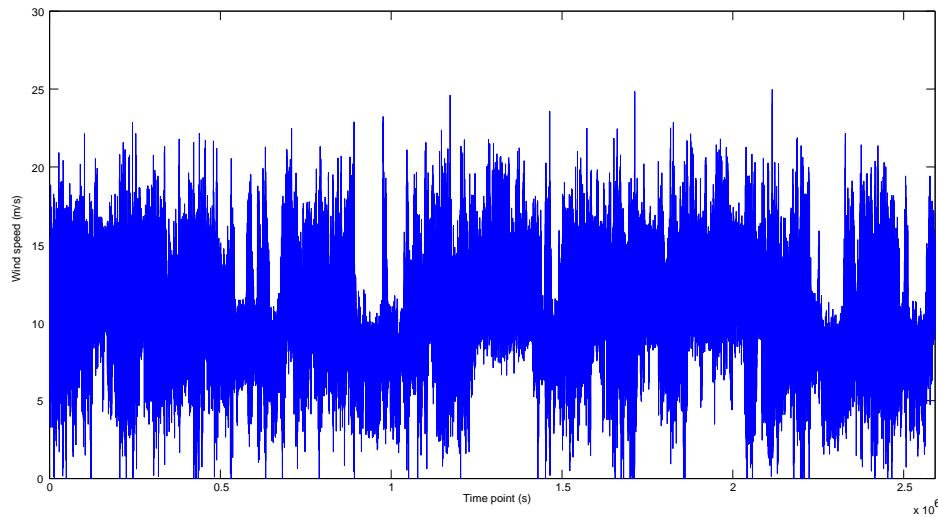


Figure 3.14: Wind speed simulation with Markov chain embedded with diffusion processes

wind speed of this sequence is calculated and plotted in Figure 3.15, to illustrate the graphical representation of a SCADA record. Comparing Figure 3.14 and Figure 3.15, it is not difficult to figure out that continuous wind speed data has higher fluctuation than 10 minutes average wind speed data. Moreover, in daily scale, the speed variation is much smaller as shown in Figure 3.15. It is the same in reality. However, once the wind condition is suitable, wind turbine operates continuously and rapidly adjust itself to the variation of wind speed. Therefore, if one wants to study the wind turbine operation, component degradation process and control strategy closely related to wind speed, the data provided by SCADA cannot meet the requirements. An application is considered in next section for further discussion.

## 3.4 Application and comparison

As mentioned in the motivation, the proposed wind speed generation model is able to generate long-term wind speed with continuous sequences when necessary. Hence, in this section, an application about the pitch angle evolution corresponding to wind speed is presented to illustrate this priority.

### 3.4.1 Wind turbine simulator

To illustrate the pitch system behavior, a wind speed sequence of 10-minutes is generated; the time step is set to 1 sec. The results of the pitch angle and the output power relating to this wind speed data are simulated by the health wind turbine simulator model is shown in Figure 3.16.

The simulation result (Figure 3.17) shows the phenomena as follows:

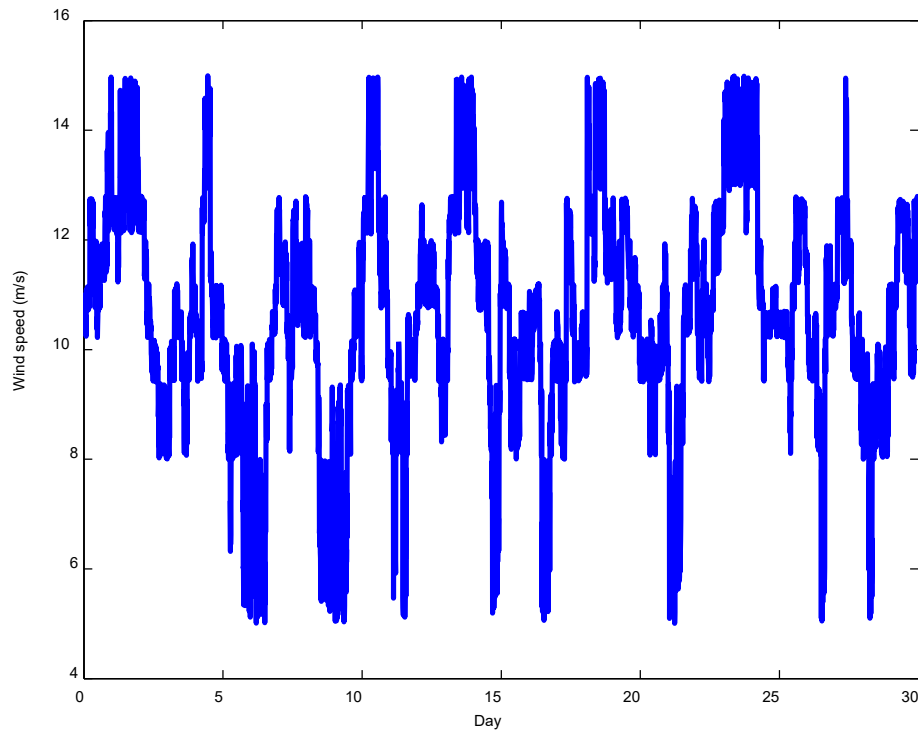


Figure 3.15: 10 minutes average wind speed data during 30 days

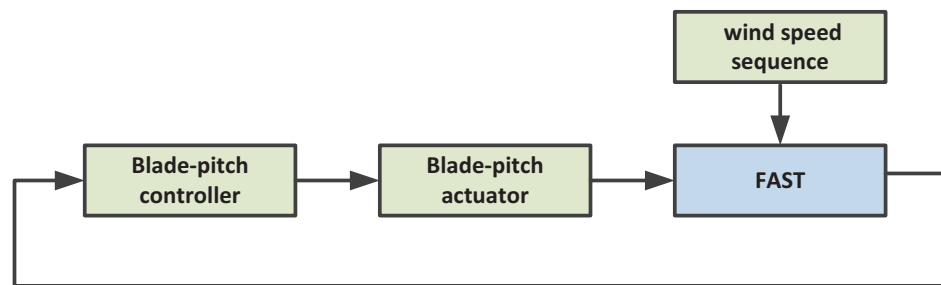


Figure 3.16: wind turbine simulator model

- The pitch system operates when wind speed is higher than the rated wind speed aiming to limit the output power of generator around the rated power. For the NREL 5 MW wind turbine, 11.4  $m/s$  is its rated wind speed.
- Wind turbulence influences the output power and the pitch angle, even though wind speed variation is not significant. It is apparent that small variations in wind speed can cause significant changes in pitch angle.
- Wind speed fluctuations around the rated wind speed and fluctuations above rated wind speed lead to frequent and random pitch actions.

Hence, the pitch system operation and output power are closely connected with the wind speed, whose turbulence can't be neglected. However, the deterioration of pitch system is a long-term process. From this point of view, wind speed estimation for several hours even several days is required at the same time.

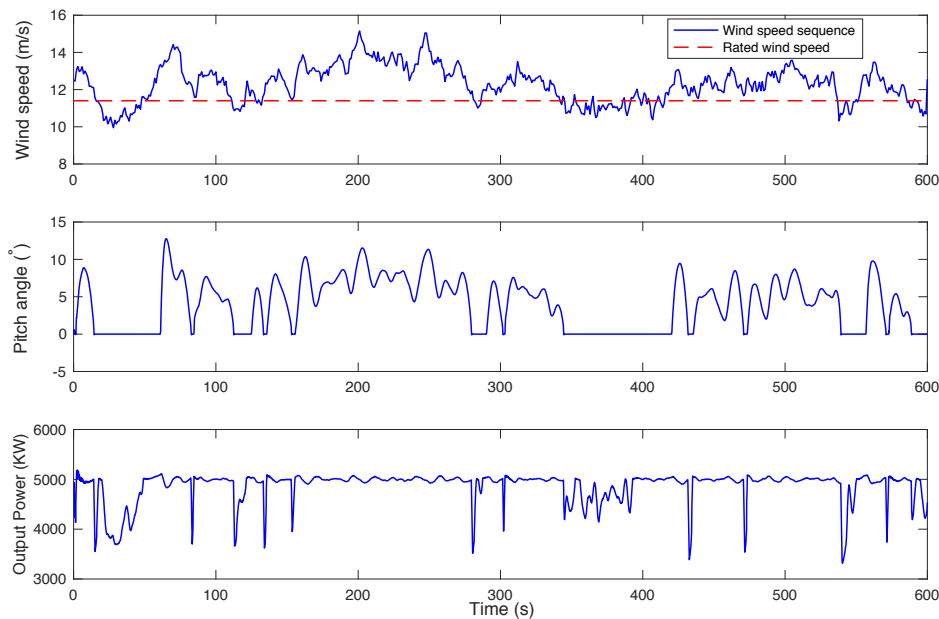


Figure 3.17: Output power and pitch angle of NREL 5MW wind turbine

### 3.4.2 Comparative Discussion

The key contribution of this chapter is the idea of global continuous wind speed generation, which is required by the RUL study of wind turbine. A flexible wind speed generation model is compatible with other proposed short-term wind speed models. To meet different demands, the SDE models can be replaced by different short-term wind speed models, for instance, the wind speed models based on Kaimal spectrum of IEC 61400-1 standard [126, 128].

Kaimal spectrum represents a relationship between three parameters relevant to the wind (the mean wind speed  $U$ , the friction velocity  $u_*$  and the height above ground  $z$ ) and the spectrum amplitude [128]. Its form is as follow:

$$S_{uu}(f) = u_*^2 \frac{52.5z/U}{(1 + 33n)^{5/3}} \quad \text{with } n = fz/U \quad (3.13)$$

If one has wind speed probability distributions of a specific site, and wants to generate wind speed following the statistical characteristics, a short-term model based on the probability distribution is suitable [118, 129].

Figure 3.18 shows the wind speed generation results of the proposed wind speed generation model, a long-term Markov chain wind speed generation model, a continuous wind speed model based on Gaussian PDF and a continuous wind speed model based on the Kaimal spectrum, respectively.

- Figure 3.18 - (a) shows a 24-hours continuous wind speed sequence, which is generated by the proposed model. Benefiting from the flexibility of the model, several wind profiles are presented in this picture. For instance, in the

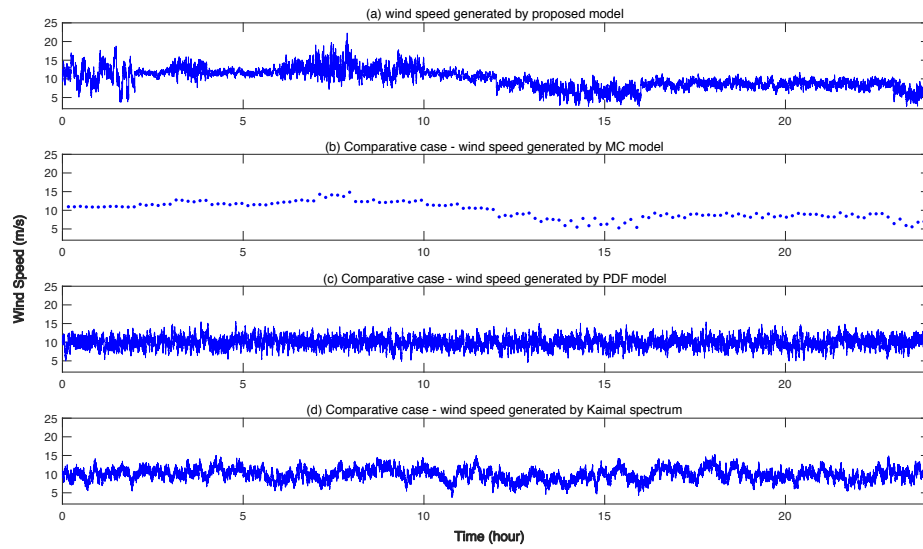


Figure 3.18: Comparison example

beginning, wind speed varies quickly. And some part shows a relatively stable wind, like the values between 4th and 6th hours. Besides, this wind sequence covers the operation wind speed range of wind turbine; it can provide a “vivid scene” for wind turbine simulator.

- According to reference [115], Markov chain model is used to generate long-term average wind speed. A 10-minutes average wind speed sequence over 24 hours which is generated by the Markov chain model is presented in Figure 3.18 - (b). Even though this sequence covers the wind turbine operation wind speed range, with a 10-minutes average value, it is very difficult to know the exact operation of the pitch system during this 10 minutes. That’s why the discrete long-term wind speed sequences with average value are not suitable for the deterioration and RUL study considered in this thesis.
- Figure 3.18 - (c) shows a 24-hours continuous wind speed sequences generated by equation (1), and the fluctuation  $u(t)$  is generated by a Gaussian PDF model proposed in [10].

The fluctuation model is as follow:

$$du(t) = -(u/\Lambda) * dt + (2\sigma^2/\Lambda)^{1/2} * dW \quad (3.14)$$

where  $u$  is wind speed fluctuation,  $\sigma$  is the standard deviation,  $\Lambda$  is an integral time scale equals 12s and  $dW$  is a normally distributed random increment. For the simulation,  $\sigma = 0.7$  and  $\bar{U} = 10m/s$ .

- Figure 3.18 - (d) shows a 24-hours continuous wind speed sequence generated by the Kaimal spectrum. The parameters for the simulation are  $z = 70m$ ,  $U = 15m/s$  and  $u_* = 1m/s$ .

Theoretically, there is no timescale limitation to generate wind speed sequence with the Gaussian PDF based model and the Kaimal spectrum. But the disadvantage

is obvious that it can not present the diurnal and seasonal influences with fixed parameters. Since outer Markov chain can provide different parameters settings, these model can replace the OU processes.

As this work requires the ability to predict the wind speed evolution on a long-term timescale and to be able to associate the wind characteristics to the degradation behavior by analyzing and simulating the response of the system on a short-term basis, a modular wind speed generation process has to be available. It is the one proposed in the chapter.

In next chapter, we will study the RUL estimation of the pitch control system taking account of wind speed fluctuation. It is then necessary to focus more precisely on the deterioration of the pitch angle control system over time. The degradation depends on the usage which is strongly related to the actual wind speed. In order to model the long-term deterioration process, the degradation characteristics associated with each outer Markov chain state have to be determined. The failure time probability law will be obtained directly from the stationary behavior of the outer Markov chain. For each outer state, the distribution of short time tiny degradation increments need to be characterized. In order to perform the characterization, the pitch angle evolution needs to be simulated from continuous short-term wind speed generation, i.e., using related SDE.

## 3.5 Conclusion

In this chapter, a continuous wind speed generation method based on a 2-level Markov chain and SDE is proposed. Two SDEs are discussed in this model framework and other could be added in the future. This model is capable of generating wind speed with different time scales. For example, a one-second step wind speed generation can be performed during 10 minutes or for a few hours based on SDE. In line with the short time generation, a long-term generation for a few months or years can be based on the outer Markov chain. The developed model is particularly suitable to be merged with the deterioration model of wind turbine's key component, like blade-pitch system. Furthermore, this model could be applied for studies of wind turbine's power system like the dynamic behavior of generator. This chapter is a part of a global modeling framework which allows jointly short-term wind speed generation for closed-loop control of wind turbine and long-term wind speed prognosis for remaining useful lifetime estimation in the case of degradation analysis.

Now we can input the wind speed to the wind turbine simulator proposed, and it give us information about wind turbine operation. We will have an idea about the behavior of wind turbine pitch system deterioration. Next chapter we will discuss the estimation of the hydraulic pitch system remaining useful life based on the operation information.

# Chapter 4

## Hydraulic pitch system remaining useful life estimation

### Problem statement

As mentioned in the previous chapters, the deteriorations of wind turbine's components are affected not only by their intrinsic deteriorations but also by the operational environment where the wind turbine operates. Due to the higher and higher electricity market share occupied by wind turbine, its priceless cost of manufacture, its remote and not easily accessible installation location, and the constraints for carrying out maintenance actions, wind turbines are required to run safely and efficiently for their design lifetime. Since wind turbines have to operate under harsh environment and age over time, the deteriorations of wind turbine are inevitable. The deterioration leads to undesired failure and downtime leading to lost of revenues for wind farm owners. In order to keep the wind turbines in good conditions and to schedule the efficient maintenance, the PHM is becoming important and it has a tendency to be an essential module for the wind turbine monitoring system. The RUL prediction of wind turbine is a way to avoid catastrophic failures and decide efficiently on the maintenance. The

A typical operational range and blade-pitch power control with respect to the wind speed is recalled in Figure 4.1. Due to the inherent random characteristic of wind speed, wind turbine operates randomly among these regions. During a period of time, the mean wind speed can be continuously increasing. An example of three possible real cases concerning wind turbine operation related to wind speed evolution are shown as follows:

- Since the mean wind speed continuously increases, the operational case is:

If the wind speed allows the idling wind turbine to start, and the wind speed is gradually increasing, the wind turbine will operate in Region 2, Region 3 and Region 4, consecutively, with respect to the gradually increasing wind speed.

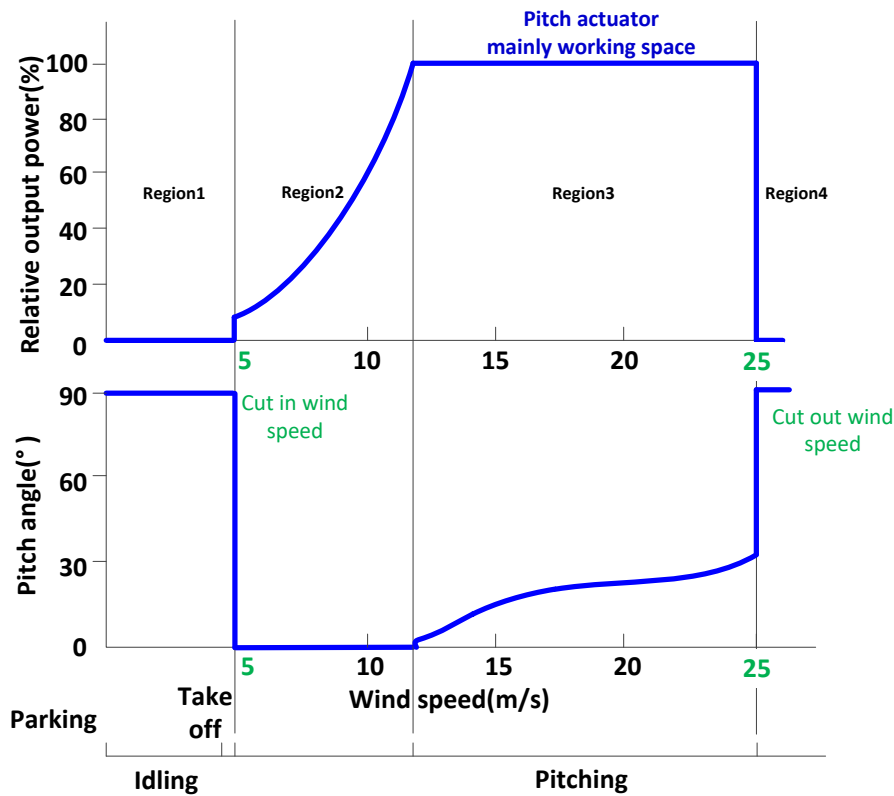


Figure 4.1: Operation ranges and control of a variable speed wind turbine with a power control by pitch system

- Since the wind speed is unstable and fluctuating in nature, an operational case is as follows.

As a consequence of unstable wind speed that oscillates around rated wind speed, to adjust the wind turbine itself according to the actual wind speed, a working wind turbine may oscillate between the operational Region 2 and Region 3.

- Since emergent environment events appear randomly, a possible operational case is as follows.

In the case of anti-typhoon, a wind turbine that operates in Region 3 may directly turn to idling when typhoon arrives.

For the RUL estimation of wind turbine, the following facts should be highlighted:

- the operational environment of wind turbine is harsh and various;
- maintenance preparation for wind turbine takes time;
- instead of immediately carrying out the maintenance, sometime the repair technicians need to wait a suitable time window for the implementation of maintenance.

Hence, when addressing the RUL prediction for wind turbine, two points should be considered. They are listed as follow:

- influence of various operational environment

Obviously, deterioration varies over different environments, it is appropriate to take into account the influence of environment for RUL estimation.

- timescale of prediction

As the various environment brings time constraints for carrying out maintenance, a long-term RUL prediction is more useful than a short-term prediction (for instance, one-hour ahead prediction). However, there is no clear definition about the limit between short and long-term prediction. To choose a reasonable timescale of RUL prediction is one of the research interests.

In this thesis, we define the environment of wind turbine as the wind speed evolution which has been modeled in Chapter 3. A finite number of wind speed classes will be considered and referred as “operational environment” which will be defined more precisely later.

## Notation and abbreviation

$E$	the set of operational environment states
$e_i$	the $i_{\text{th}}$ operational environment state, $e_i \in E$ ( $i \in \mathbb{N}^*$ )
OE	the abbreviation of Operational Environment in formula
$\text{OE}_i$ ( $i \in \mathbb{N}$ )	random variable that takes value in $E$
$D(t)$	deterioration level at time $t$
$\Delta D_{(t,\tau)}$	deterioration increment between time point $t$ and $t + \tau$ , $\tau > 0$
$\Gamma(\alpha, \beta)$	gamma distribution with shape parameter $\alpha$ and scale parameter $\beta$
$\Delta D_{i(t,\tau)}$	deterioration increment between time $t$ and $t + \tau$ in state $e_i$ .
$\alpha_i, \beta_i$	shape and scale parameter for gamma process with respect to the operational environment $e_i$

## 4.1 Introduction

As mentioned before, the wind turbine suffers harsh and random various environment. Wind turbine continuously adjusts itself according to this latter, meaning that the operation of wind turbine is stochastic and is related to the environment under which wind turbine operates. In wind power industry, according to the environment, wind turbine has five operational status which consists of idling, start, operation in Region 2, operation in Region3 and stop. On the basis of real wind turbine operation, Table 4.1 summarizes the possible switches among different operational status for a wind turbine.

Table 4.1: Switches among different operational status for a wind turbine ( $\checkmark$  means that the switch between the two status is possible, while  $\times$  means not possible )

From To	Idling	Start	Region 2	Region 3	Stop
Idling	$\checkmark$	$\checkmark$	$\times$	$\times$	$\checkmark$
Start	$\checkmark$	$\checkmark$	$\checkmark$	$\times$	$\checkmark$
Region 2	$\times$	$\times$	$\checkmark$	$\checkmark$	$\checkmark$
Region 3	$\checkmark$	$\times$	$\checkmark$	$\checkmark$	$\checkmark$
Stop	$\checkmark$	$\checkmark$	$\times$	$\times$	$\checkmark$

According to the research done by A.R. Nejad et al. [25], wind turbine withstands different loads associated to wind speed. In fact, higher loads usually generate higher vibrations for the drive-train of wind turbine. Excessive high vibration is a known cause that leads to deterioration for rotational components. Moreover, vibration can transmit to other components via the connection structure, hence, excessive high vibration makes other components' condition deteriorate. It also mentions in [24] that in windy season, pitch systems have higher rate of failure. Therefore, what can be concluded is listed as follows:

- (1) operational environment of wind turbine changes randomly;
- (2) operational environment affects the health condition of wind turbine and induces deterioration;
- (3) the deterioration rate varies with the operational environments.

An appropriate deterioration model is essential for RUL prediction. In literature, lots of deterioration models assume that operational environments are temporally invariant, or they don't affect the deterioration process of systems. However, referring the previous content of this thesis, it is more appropriate to take the influences from operational environment into account for deterioration modelling, especially for wind turbines. There are examples [130, 131] in real engineering fields that the deterioration of system can be affected by the operational environment of the system.

This chapter focuses on the deterioration modelling and RUL prediction for wind turbine subject to various operational conditions. This topic can be also extended to any dynamic system that operates under a dynamic operational environment, such as aero-engine and vehicle motor. This work will focus on the case where the environment can be described through a finite number of classes and the effect of environment is constant in each class. RUL prediction about hydraulic pitch system will be considered as a case used to analyse the method proposed in this chapter.

Compared with the whole wind turbine, hydraulic pitch system only operates in Region 3. Hence, it only deteriorates in this region. Therefore, the deterioration rates of pitch system are 0 in other regions. However, the Region 3 where the

wind speed randomly varies from the rated wind speed to the cut-out wind speed contains a large wind speed range. It means in this region that hydraulic pitch systems suffer various loads from wind leading to various deterioration rates correspond to the wind speed. Although wind speed appears inscrutably, the measured wind speed for a specific site follows frequency distributions, see [10]. From the statistical point of view, wind speed can be characterized by mean speed value and turbulence intensity. Assuming that the deterioration of hydraulic pitch system is only related to the wind speed, the regulations about the deterioration caused by environment for the hydraulic pitch system exist. And these regulations can be decided by different parameters of the deterioration models.

We consider that the inspection data which are relevant to describe the deterioration process can be frequently collected from the SCADA system. These data will be used to estimate the indicator of the wind turbine's deterioration and the parameters of deterioration models.

Compared with wind turbine operation timescale and the time for maintenance preparation, the inspection interval is short. Therefore, the timescale limitation of prediction is worth to be discussed. We provide two RUL prediction methods: one mainly considers the long-run average deterioration, another one estimates the RUL from the current operational states, and deduces an N-step forward RUL prediction formula. A discussion about these two methods timescale limitation will be given.

The contributions of this chapter are summarized as follows:

- A model is proposed to describe the deterioration phenomenon related to various operational environment,
- RUL prediction methods for a deteriorating system which operates under various operational environment are proposed,
- According to the numerical results applied on the wind turbine simulator, the limitations of prediction timescale are discussed.

## 4.2 Simplification and model description for the deteriorating system

The deteriorating system concerned in this chapter is the hydraulic pitch system. However, the proposed modelling method and RUL estimation can be applied to the dynamic systems similar to the hydraulic pitch system. Mainly this case study is an example of closed-loop controlled system with possible compensation of degradation effects by the control system. The deterioration caused by the operational environment concerns physical component as actuators. It influences the control system leading to low control efficiency. The condition monitoring system provides data that can be used to describe the deterioration process. In

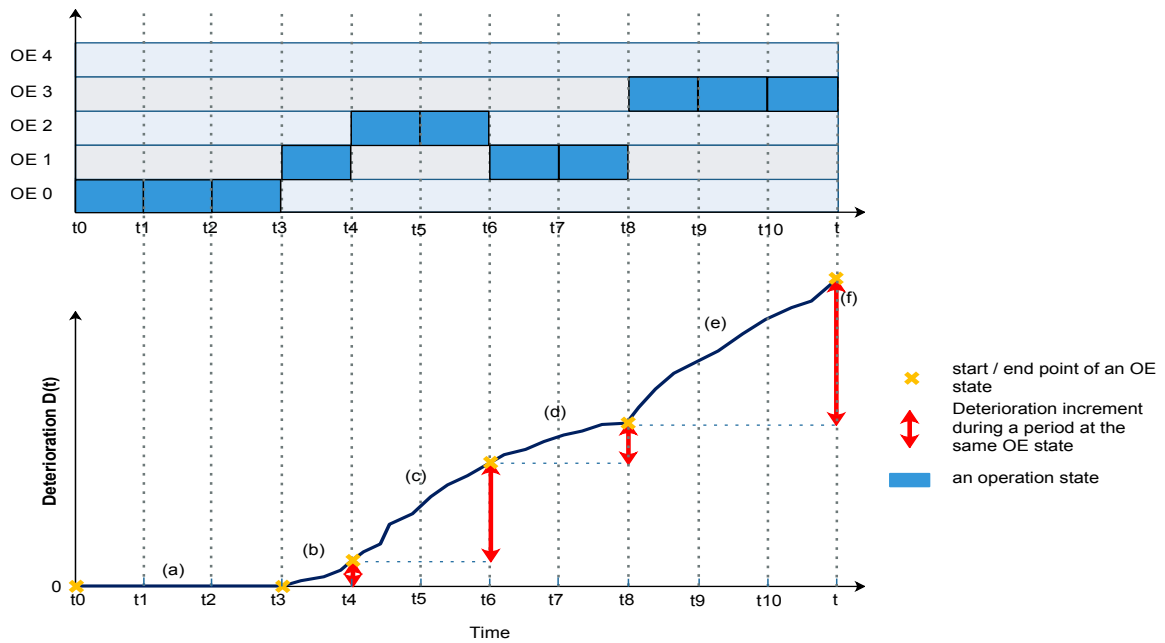


Figure 4.2: Diagram for the explanation about a deteriorating system operating under various operational environment

harsh operational environment, the system is much more seriously deteriorating than in a mild operational environment.

Figure 4.2 shows an explanation about a deteriorating system operating under various operational environment. The figure at the top represents a trajectory of the random switch between different operational environments over time. Higher value of operational environment means harsher operation condition. The figure at the bottom shows a trajectory of system deterioration corresponding to the operational environments. The deterioration process (a) - (f) can be modeled by a stochastic processes with different parameters related to the different deterioration rates.

In order to simplify the real engineering problem and to propose mathematical models, make the following assumptions:

- (1) The operational environment is classifiable according to a parameter, and it can be classified into a finite number of different operational states. Namely the operational environment of wind turbine can be classified based on wind speed characteristics, or the operational environment of vehicles can be classified by the rotational speed of motor.
- (2) The change to next operational environment state depends only on the present operational environment state.

- (3) Assume that only the operational environment affects the deterioration, excluding the inherent deterioration phenomenon. It is true that a dynamic system degrades more severely in harsh operational environments compared with the one in stable operational environments. Hence, the deterioration rate is correlated to the operational environment. Therefore, the deterioration of the system can be considered as a stochastic process whose parameters are piecewise constant.
- (4) The deterioration indicator is an information which can be estimated from the monitoring system.

### 4.2.1 Model for operational environment states

Markov chains usually describe the movements of a system among various states [132]. A discrete-time Markov chain is very suitable for the modelling of operational environment considered in this chapter. At each step the operational environment can either stay in the state where it is or change to another operational environment state.

Let  $E = \{e_1, e_2, \dots, e_n\}$ ,  $n \in \mathbb{N}$  be the set of operational environment states. Define  $P = [p_{ij}]$  ( $1 \leq i \leq n$ ,  $1 \leq j \leq n$ ) as the transition probability matrix, i.e.,  $p_{ij}$  is the probability of moving from  $e_i$  to  $e_j$  during a time interval  $\delta t$ . This time interval can be related to the sampling frequency of SCADA. For sake of simplicity, it will be hereafter considered as a unit of time ( $\delta t = 1$ ). Random variables  $\text{OE}_n$  of the sequence  $(\text{OE}_n)_{n \in \mathbb{N}}$  represent the value of operational environment at time  $t_n = n \cdot \delta t = n$  and take values in  $E$ .

$(\text{OE}_n)_{0 \leq n \leq N}$  is a discrete time discrete state Markov chain if and only if:

- $\mathbb{P}(\text{OE}_0 = e_{i_0}) = \lambda_{i_0}$
- $\mathbb{P}(\text{OE}_{n+1} = e_{i_{n+1}} \mid \text{OE}_0 = e_{i_0}, \dots, \text{OE}_n = e_{i_n}) = \mathbb{P}(\text{OE}_{n+1} = e_{i_{n+1}} \mid \text{OE}_n = e_{i_n}) = p_{i_n i_{n+1}}$

where  $\lambda_{i_0}$ ,  $i_0 \in \mathbb{N}^+$  describes the probability distribution of initial state (at time 0).

### 4.2.2 Model for the deterioration indicator under various operational environment state

Let  $\{D(t); t \geq 0\}$  be a continuous-time, monotonic increasing, stochastic process that represents the deterioration process of a dynamic system. If the process is Markovian then the deterioration increment  $\Delta D_{(t, \delta_t)}$  between time point  $t$  and  $t + \delta_t$ ,

$$\Delta D_{(t, \delta_t)} = D(t + \delta_t) - D(t) \quad (t > 0, \delta_t > 0)$$

depends only on the present and not on the past. Especially,  $\Delta D_{(t,\delta_t)}$  depends on the current time  $t$  and on  $\delta_t$ .

Gamma process is an example of Markovian process. Non-homogenous gamma process is a stochastic process whose increments are independent, non-negative and following a gamma distribution. It is suitable to model the gradual monotonically accumulating deterioration over time, such as fatigue, wear, corrosion, crack growing, etc..

To model different deterioration rates according to the various operational environment, the deterioration of system can be considered as a gamma process whose parameters are piecewise constant and related to the operational environments, see Table 4.2.

Table 4.2: Parameters of gamma process that are piecewise constant and related to the operational environments

Operational environment	$e_1$	$e_2$	$\cdots$	$e_i$	$\cdots$	$e_n$
Parameters of gamma process	$\alpha_1, \beta_1$	$\alpha_2, \beta_2$	$\cdots$	$\alpha_i, \beta_i$	$\cdots$	$\alpha_n, \beta_n$

### 4.3 Remaining useful life prediction

The deterioration value  $D(t+\tau)$  at time  $t+\tau$  is the sum of the known deterioration value  $D(t)$  at time  $t$  and the deterioration increment  $\Delta D_{(t,\tau)}$  between time  $t$  and  $t+\tau$ :

$$D(t+\tau) = D(t) + \Delta D_{(t,\tau)}$$

RUL prediction requires estimating the deterioration value  $D(t+\tau)$  at time  $t+\tau$ , with the known deterioration value (or its estimated value from the monitoring data) at time  $t$ . Therefore, the solution is to estimate the increment of deterioration between time  $t$  and  $t+\tau$ . Considering the uncertainties, it turns to an issue about the probability distribution of the increment  $\Delta D_{(t,\tau)}$ .

The calculation of  $\Delta D_{(t,\tau)}$  is concerned with timescale, i.e. the length of  $\tau$ . A RUL estimation focuses on the influence caused by the current condition to the nearly future. On a long period  $\tau$ , the influence of the current state vanishes and can be neglected. Therefore, two different calculation methods are developed for the RUL estimation hereafter.

#### 4.3.1 Case 1: RUL estimation for a long period $\tau$

If  $\tau$  is enough long, the wind turbine experiences all the operational environment during  $\tau$ . Equivalently, the model of operational environment is based on an ergodic Markov chain, which means that every environment can be reached from

every one according to the transition matrix. For such a Markov chain, there exists a unique steady state distribution (so-called stationary distribution)  $\pi^\infty = \{\pi_1, \pi_2, \dots, \pi_n\}$  (where  $n$  is the number of states) which is independent of the initial state, and satisfies:

$$\pi^\infty P = \pi^\infty, \quad \sum \pi_i^\infty = 1.$$

For a finite state Markov chain, the stationary distribution can be considered as the proportion of time spent in each state in long-run case [133]. Studying the Markov chains model along with the analysis of its stationary distribution have been proved to be useful in applications such as the analysis about queuing networks [134], the study about compartmental ecological models [135] or research about least-squares adjustment of geodetic networks [136].

If  $\tau$  is enough long, it can include all of the operational environment states different times. In this case, the RUL estimation is based on the expected average value of deterioration in long period. Hence, according to the stationary distribution, an average sojourn time in each operational environment state can be estimated.

The average sojourn time  $\bar{\tau}_i$  spent in state  $e_i$  over time duration  $\tau$  is:

$$\bar{\tau}_i = \pi_i \times \tau \quad (4.1)$$

For a given value of  $i$ , the distribution of the accumulated deterioration increment in state  $e_i$  between  $t$  and  $t + \tau$  is:

$$\Delta D_{i(t,\tau)} \sim \Gamma(\alpha_i \cdot \bar{\tau}_i, \beta_i) \quad (4.2)$$

Therefore, the asymptotic expectation of deterioration increment of state  $e_i$  between  $t$  and  $t + \tau$  is:

$$\mathbb{E}(\Delta D_{i(t,\tau)}) = \alpha_i \cdot \bar{\tau}_i \beta_i \quad (4.3)$$

The total mean deterioration increment of the dynamic system between time  $t$  and  $t + \tau$  is:

$$\mathbb{E}(\Delta D_{(t,\tau)}) \simeq \sum_i^n \mathbb{E}(\Delta D_{i(t,\tau)}) \quad (4.4)$$

From the prediction point of view, the PDF/CDF of deterioration increment  $\Delta D_{(t,\tau)}$  is also interesting and gives more information than the mean value. With the properties of gamma process [137, 138], we can obtain the probability distribution of the average deterioration increment  $\Delta \bar{D}_{(t,\tau)}$  for a dynamic system. Denote  $\bar{\alpha}$  the average shape parameter of gamma process, defined with formula:

$$\bar{\alpha} = \frac{\sum_i^n \alpha_i \cdot \bar{\tau}_i}{\tau} \quad (4.5)$$

As a consequence, when  $\tau \rightarrow \infty$ , it is possible to have tractable analytical calculations with the additional hypothesis “ $\beta_i = \beta, \forall i \in \{1, \dots, n\}$ ”. Under this hypothesis, the probability law of  $\Delta \bar{D}_{(t,\tau)}$  and the approximation of RUL cumula-

tive distribution function are as follow:

$$\Delta \bar{D}_{(t,\tau)} \sim \Gamma(\bar{\alpha}.\tau, \beta) \quad (4.6)$$

$$F_{RUL(t)}(\tau) \simeq \frac{\Gamma(\bar{\alpha}.\tau, (d - D(t))\beta)}{\Gamma(\bar{\alpha}.\tau)} \quad (4.7)$$

where  $\Gamma(m, n) = \int_{z=n}^{\infty} z^{m-1} e^{-z} dz$  is the incomplete gamma function and  $\bar{\alpha}$  is given by equation (4.5).

### 4.3.2 Case 2: RUL estimation considering the current operational environment state

This case is related to a short-term prediction. As a consequence of the limited time horizon, the RUL estimation closely depends on the last operational environment state and the prediction timescale. In this section, a one-step and two-step prediction are given firstly. Then the general expression about N-step prediction is derived and an approximation method is introduced.

At the beginning, let consider the notations as follows:

- $t$  is the present time when the prediction is calculated and the last information about degradation level is available;
- To simplify the notation,  $t+k$  stands for  $t+k\delta t$ . Hence  $t+1, t+2, \dots, t+N$  represents one-step, two-step,  $\dots$ , N-step forward from time  $t$ , respectively;
- between time  $t-1$  and  $t$ , the operational state doesn't change and is denoted by  $e_i$ .

In the case of an operational environment without degradation, the degradation increment during a time step is 0. In this section, to simplify the expressions it is considered that if the operational environment after time  $t$  is such that  $\alpha_{i_{t+1}} = 0$ , then:

$$\mathbb{P}(\Delta D_{(t,1)} < u \mid \text{OE}_{t+1} = e_{i_{t+1}}) = F_{\alpha_{i_{t+1}}, \beta}(u) = \int_0^u f_{\alpha_{i_{t+1}}, \beta}(x) dx = 1$$

### 4.3.2.1 One-step forward RUL prediction

Assuming the current time is  $t$ , let  $T$  be the time of next failure. The probability of the system surviving until  $t + 1$  given the information up to time  $t$  is

$$\begin{aligned}
 & \mathbb{P}(T > t + 1 | D(t) = d_t, \text{OE}_t = e_{i_t}) \\
 &= \mathbb{P}(D(t + 1) < d | D(t) = d_t, \text{OE}_t = e_{i_t}) \\
 &= \mathbb{P}(\Delta D_{(t,1)} < d - d_t | \text{OE}_t = e_{i_t}) \\
 &= \sum_{i_{t+1}=1}^n \mathbb{P}(\Delta D_{(t,1)} < d - d_t | \text{OE}_t = e_{i_t}, \text{OE}_{t+1} = e_{i_{t+1}}) \\
 & \qquad \qquad \qquad \mathbb{P}(\text{OE}_{t+1} = e_{i_{t+1}} | \text{OE}_t = e_{i_t}) \\
 &= \sum_{i_{t+1}=1}^n p_{i_t i_{t+1}} \int_0^{d-d_t} f_{\alpha_{i_{t+1}}, \beta}(x) dx
 \end{aligned} \tag{4.8}$$

where  $n$  is the total number of operational environment's states, and  $f_{\alpha_{i_{t+1}}, \beta}(x)$  is the PDF of a gamma distribution with shape parameter  $\alpha_{i_{t+1}}$  and scale parameter  $\beta$  given by:

$$f_{\alpha_{i_{t+1}}, \beta}(x) = \frac{(x/\beta)^{\alpha_{i_{t+1}} - 1}}{\beta \Gamma(\alpha_{i_{t+1}})} \exp^{-\frac{x}{\beta}}.$$

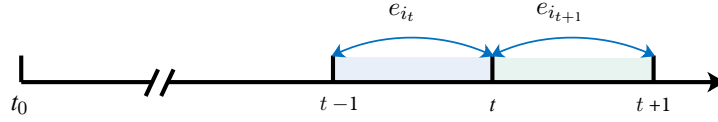


Figure 4.3: Illustration of one-step forward prediction

### 4.3.2.2 Two-step forward RUL prediction

Assuming the current time is  $t$ , the probability of the system surviving until  $t + 2$  given the information up to time  $t$  is developed hereafter. In these expressions, the notation  $\Delta D_{(u,1)}^{(e_j)}$  refers to an increment of degradation between time  $u$  and  $u + 1$  under the operational environment  $e_j$  i.e. which follows a gamma distribution with

parameters  $\alpha_j$  and  $\beta$ . It comes:

$$\begin{aligned}
& \mathbb{P}(T > t + 2 | D_t = d_t, \text{OE}_t = e_{i_t}) \tag{4.9} \\
&= \mathbb{P}(D(t+2) < d | D_t = d_t, \text{OE}_t = e_{i_t}) \\
&= \mathbb{P}(\Delta D_{(t,1)} + \Delta D_{(t+1,1)} < d - d_t | \text{OE}_t = e_{i_t}) \\
&= \int_0^{d-d_t} \sum_{i_{t+1}=1}^n \mathbb{P}(x + \Delta D_{(t+1,1)} < d - d_t | \text{OE}_{t+1} = e_{i_{t+1}}, \text{OE}_t = e_{i_t}, \Delta D_{(t,1)}^{(e_{i_{t+1}})} = x) \\
&\quad f_{\Delta D_{(t,1)}^{(e_{i_{t+1}})}}(x) dx \times \mathbb{P}(\text{OE}_{t+1} = e_{i_{t+1}} | \text{OE}_t = e_{i_t}) \\
&= \int_0^{d-d_t} \sum_{i_{t+1}=1}^n \mathbb{P}(\Delta D_{(t+1,1)} < d - d_t - x | \Delta D_{(t,1)}^{(e_{i_{t+1}})} = x, \text{OE}_t = e_{i_t}) p_{i_t i_{t+1}} f_{\Delta D_{(t,1)}^{(e_{i_{t+1}})}}(x) dx \\
&= \sum_{i_{t+1}=1}^n \sum_{i_{t+2}=1}^n p_{i_t i_{t+1}} p_{i_{t+1} i_{t+2}} \int_0^{d-d_t} F_{\alpha_{i_{t+2}}, \beta}(d - d_t - x) f_{\Delta D_{(t,1)}^{(e_{i_{t+1}})}}(x) dx
\end{aligned}$$

where  $n$  is the total number of operational environment's states.  $F_{\alpha_{i_{t+2}}, \beta}$  is the CDF of a gamma distribution with shape parameter  $\alpha_{i_{t+2}}$  and scale parameter  $\beta$ .  $f_{\Delta D_{(t,1)}^{(e_{i_{t+1}})}}$  is the PDF of a gamma distribution with shape parameter  $\alpha_{i_{t+1}}$  and scale parameter  $\beta$ .

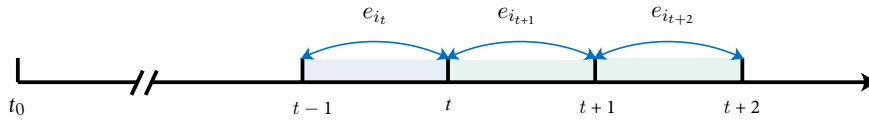


Figure 4.4: Illustration of two-step forward prediction

#### 4.3.2.3 Approximation of the N-step forward RUL prediction: algebraic expression

Let now consider the same process as described in sections 4.3.2.1 and 4.3.2.2. Assuming the current time is  $t$ , the probability of the system surviving until  $t + N$  is

$$\begin{aligned}
& \mathbb{P}(T > t + N | D_t = d_t, \text{OE}_t = e_{i_t}) \tag{4.10} \\
&= \mathbb{P}(D(t+N) < d | D_t = d_t, \text{OE}_t = e_{i_t}) \\
&= \mathbb{P}(\Delta D_{(t,1)} + \Delta D_{(t+1,1)} + \dots + \Delta D_{(t+(N-1),1)} < d - d_t | \text{OE}_t = e_{i_t}) \\
&= \underbrace{\sum_{i_{t+1}=1}^n \dots \sum_{i_{t+N}=1}^n p_{i_t i_{t+1}} \dots p_{i_{t+N-1} i_{t+N}}}_{N \text{ times}} \int_0^{d-d_t} \dots \int_0^{d-\sum_{i=0}^{N-1} d_{t+i}} F_{\Delta D_{(t,t+N-1)}}(d - \sum_{i=1}^{N-1} d_{t+i}) \\
&\quad \prod_{i=1}^{N-1} f_{\Delta D_{(t+i,1)}^{(e_{i_{t+i+1}})}}(d_{t+i}) d(d_{t+i})
\end{aligned}$$

Equation (4.10) is difficult to calculate while  $N$  increases. Successive convolutions lead to multiple sums and integrals. In this section we consider an approximation which allows to use matrix calculations and which is tractable even with high values of  $N$ . If the independent increments of deterioration follow gamma distributions with the same scale parameter  $\beta$  in all the operational environments, the sum of the increment follows a gamma distribution with a shape parameter that is the sum of the different shape parameters and the scale parameter, namely,

$$\sum_{m=1}^M \Delta X_m \sim \Gamma\left(\sum_{m=1}^M \alpha_m, \beta\right).$$

This property is very convenient for the computational purpose. Even if a single value of  $\beta$  for all the operational environments reduces the number of parameters and modeling capabilities, it allows to derive simpler expressions. Considering that the deterioration increment of each step is independent from each other, the  $N$ -step forward RUL prediction can be expressed as follow:

$$\begin{aligned} & \mathbb{P}(T > t + N | D_t = d_t, \text{OE}_t = e_{i_t}) \\ &= \mathbb{P}(D(t + N) < d | D_t = d_t, \text{OE}_t = e_{i_t}) \\ &\simeq \int_0^{d-d_t} f_{\alpha_s, \beta}(x | e_{i_t}) dx \end{aligned} \quad (4.11)$$

where  $f_{\alpha_s, \beta}(x | e_{i_t})$  is the pdf of a gamma distribution with shape parameter  $\alpha_s$  and scale parameter  $\beta$  given that the initial operational environment is  $e_{i_t}$ . As a consequence:

$$f_{\alpha_s, \beta}(x | e_{i_t}) = \frac{(x/\beta)^{\alpha_s-1}}{\beta \Gamma(\alpha_s)} \exp^{-\frac{x}{\beta}}$$

and  $\alpha_s$  has the following expression,

$$\alpha_s = (0 \cdots 1_t \cdots 0)_{1 \times n} \left( \sum_{m=1}^N P^m \right) A \mathbb{I}_{n \times 1} \quad (4.12)$$

where  $N$  is the prediction step;  $(0 \cdots 1_t \cdots 0)_{1 \times n}$  represents the initial state of operational environment at time  $t$ ;  $P$  is the probability transition matrix of operational environment;  $A$  is a diagonal matrix of shape parameter for the different operational environments as shown below,

$$A = \begin{bmatrix} \alpha_1 & 0 & \cdots & 0 \\ 0 & \alpha_2 & \cdots & 0 \\ \vdots & \vdots & \ddots & \vdots \\ 0 & 0 & \cdots & \alpha_n \end{bmatrix}$$

and  $\mathbb{I}_{n \times 1}$  with value 1. To illustrate the expression of  $\alpha_s$ , an example is given as follows.

**Example** Assuming that a dynamic system operates under an operational environment which has 4 states, i.e,  $n = 4$ ; the shape parameters of deterioration process for each state are  $\alpha_1, \alpha_2, \alpha_3$  and  $\alpha_4$ , respectively; at time  $t$ , the system

stays in the 3rd state, hence the initial state is the third; a 5-step forward RUL prediction is wanted. Therefore, the expression of  $\alpha_s$  is as follows:

$$\alpha_s = (0 \ 0 \ 1 \ 0) \left( \sum_{m=1}^5 P^m \right) A \mathbb{I}_{4 \times 1}$$

where

$$A = \begin{bmatrix} \alpha_1 & 0 & 0 & 0 \\ 0 & \alpha_2 & 0 & 0 \\ 0 & 0 & \alpha_3 & 0 \\ 0 & 0 & 0 & \alpha_4 \end{bmatrix}, \quad P = \begin{bmatrix} p_{11} & p_{12} & p_{13} & p_{14} \\ p_{21} & p_{22} & p_{23} & p_{24} \\ p_{31} & p_{32} & p_{33} & p_{34} \\ p_{41} & p_{42} & p_{43} & p_{44} \end{bmatrix}.$$

■

### Discussion:

Different from the ideas applied to calculate one-step and two-step forward RUL prediction (equation (4.8) and equation (4.9)), the method of the N-step forward RUL prediction can be considered as a stationary probabilities of deterioration.

For instance,  $N = 1$ , equation (4.11) is

$$\mathbb{P}(T > t + 1 | D_t = d_t, \text{OE}_t = e_{it}) = \int_0^{d-d_t} f_{\alpha_s, \beta}(x) dx \quad (4.13)$$

where,

$$\alpha_s = (0 \cdots 1 \cdots 0)_{1 \times n} P A \mathbb{I}_{n \times 1} = \sum_{i_{t+1}=1}^n p_{i_t i_{t+1}} \alpha_{i_{t+1}}$$

Comparing equation (4.13) with equation (4.8), they are not the same probability distribution. But the expected deterioration levels are the same for the two cases i.e.  $\mathbb{E}(D_{t+1}) = \sum_{i_{t+1}=1}^n p_{i_t i_{t+1}} \alpha_{i_{t+1}} \beta$ . The RUL prediction by the algebraic expression is based on an approximation of the probability law of future degradation levels. The mixture of probability laws in equation (4.8) is replaced by a single probability law with combined shape parameters. Hence it gives a tractable approximation of RUL's pdf which can be assessed numerically for the considered parameters.

Figure 4.5 shows the difference between the result of equation (4.8) and equation (4.13) known  $\text{OE}_t = 7$  and  $D_t = 0$ . The probability that  $\Delta D(t, 1) < x$  is plotted. The picture shows that the difference is small except for small values of  $x$ , because of the cases  $\alpha_i = 0$  which are not taken into account in the same way. But the approximation is overestimating the failure so it is better than underestimation.

## 4.4 Numerical results and analysis

In this section, we are going to apply the proposed RUL prediction method to the hydraulic pitch system. As the work is based on a numerical wind turbine

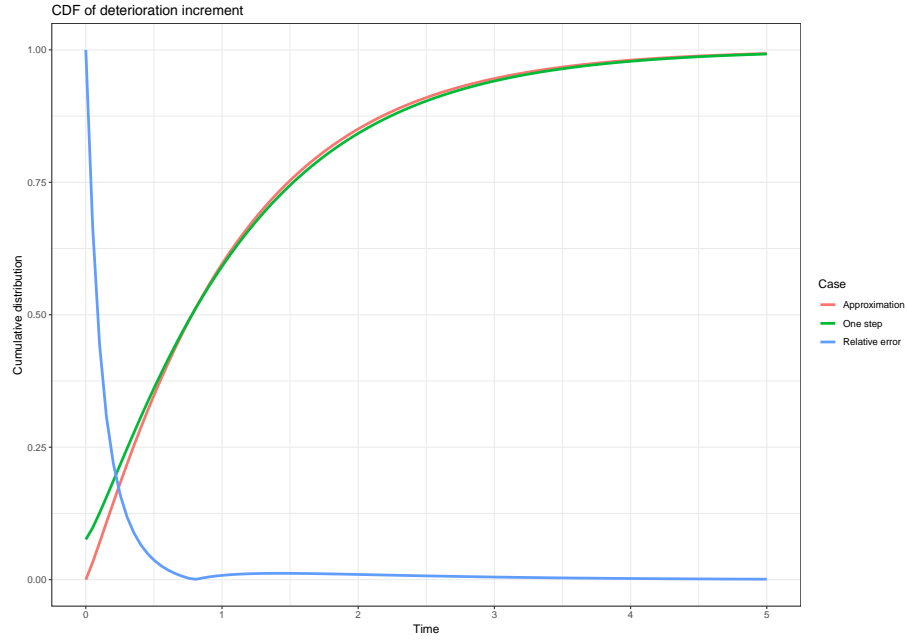


Figure 4.5: Comparison of the CDFs of deterioration increment

and data simulation, the data about the life of hydraulic pitch system is lacking. Therefore, it is necessary to add a subsection about the prediction of indicators to evaluate the proposed method before the numerical results of RUL. Parameters estimation is given at the beginning of the section followed by the numerical results of indicators prediction and RUL prediction.

#### 4.4.1 Parameters estimation

##### Parameter estimation when considering the influence .....

To avoid any confusions, recall the extraction of deterioration indicator for hydraulic pitch system is necessary. See Figure 2.7, the details are as follows:

- Step 1. Generate a wind speed sequence
- Step 2. Input the wind speed to the wind turbine simulator to get SCADA data
- Step 3. Save the data sequence of blade-pitch angle measurement  $\beta_{mes}$ , and the reference blade-pitch angle  $\beta_{ref}$  from SCADA
- Step 4. Calculate the APR, and the real-time  $\omega_{nD}(t)$ , simultaneously
- Step 5. Replace the  $\omega_{nD}(t)$  of the deteriorating pitch system

Estimate  $\hat{\omega}_n$  with the saved sequences of  $\beta_{mes}$ ,  $\beta_{ref}$  via an estimation of the system second order transfer function. Numerically, Matlab function **tfest**<sup>1</sup> is used.

<sup>1</sup>f= tfest( $\beta_r, \beta_m$ ) finds a transfer function estimate f, given an input signal  $\beta_r$ , and an output signal  $\beta_m$ .

Therefore,  $\hat{\omega}_n$  is the indicator for the deterioration process of pitch system. Figure 4.6 shows the difference between  $\omega_{nD}$  and  $\hat{\omega}_n$ . The trajectories of  $\omega_{nD}$  simulated in the 8th state of wind speed are shown in Figure 4.6 (a). While Figure 4.6 (b) shows the results of estimated  $\hat{\omega}_n$  according to the measurement blade-pitch angle  $\beta_{mes}$  and the reference blade-pitch angle  $\beta_{ref}$  provided by the output information of wind turbine simulator.

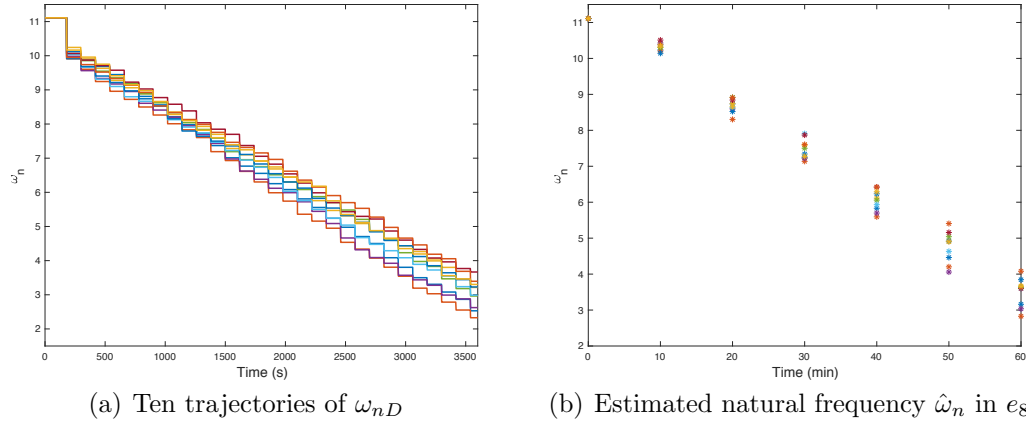


Figure 4.6: (a)Ten trajectories of the deterioration of  $\omega_{nD}$  (b)Estimated natural frequency  $\hat{\omega}_n$  in  $e_8$

Table 4.3: The states of operational environment

Operational environment	$e_1$	$e_2$	$e_3$	$e_4$
Wind speed ( $m/s$ )	[4,8]	(8,9.4]	(9.4,10.2]	(10.2,10.7]
Operational environment	$e_5$	$e_6$	$e_7$	$e_8$
Wind speed ( $m/s$ )	(10.7,11.2]	(11.2,12]	(12,12.8]	(12.8,25]

The data sequences of  $\hat{\omega}_n$  in different operational environment are used to estimate the parameters of deterioration model. The number of trajectories of  $\omega_{nD}$  in each state is 500. The operational environments have been determined as 8 states shown in Table 4.3. However, refer to the property of the NREL-5MW wind turbine, only the operational Region 3 is closely related to the deterioration of hydraulic pitch system. As the rated wind speed is  $11.4 m/s$ , the hydraulic pitch system mainly works in  $e_6$ ,  $e_7$  and  $e_8$ . It is not active in states  $e_1$  to  $e_5$ , which means that the pitch system doesn't deteriorate in these operational environments. Namely, the shape parameters  $\alpha_i$  ( $i = 1, \dots, 5$ ) are equal to zero. Therefore, parameters  $\alpha_6$ ,  $\alpha_7$ ,  $\alpha_8$  and  $\beta$  need to be estimated with the sequences of  $\hat{\omega}_n$ , and they are globally estimated by the maximum likelihood method in order to have the same  $\beta$ . Table 4.4 shows the estimation results of parameter estimation.

### Parameter estimation when

From Table 3.3 and section 4.3.1, the proportion of time spent in each operational state  $e_i$  can be calculated and they are shown in Table 4.5. Therefore, according to equation (4.5), the parameters for case 1 is obtained, as shown in Table 4.6.

Table 4.4: Parameters for deterioration model related to different operational environments

parameters	$\alpha_1 - \alpha_5$	$\alpha_6$	$\alpha_7$	$\alpha_8$	$\beta$
value	0	1.2019	1.2199	1.2897	0.0946

Table 4.5: Proportion time in each operational state

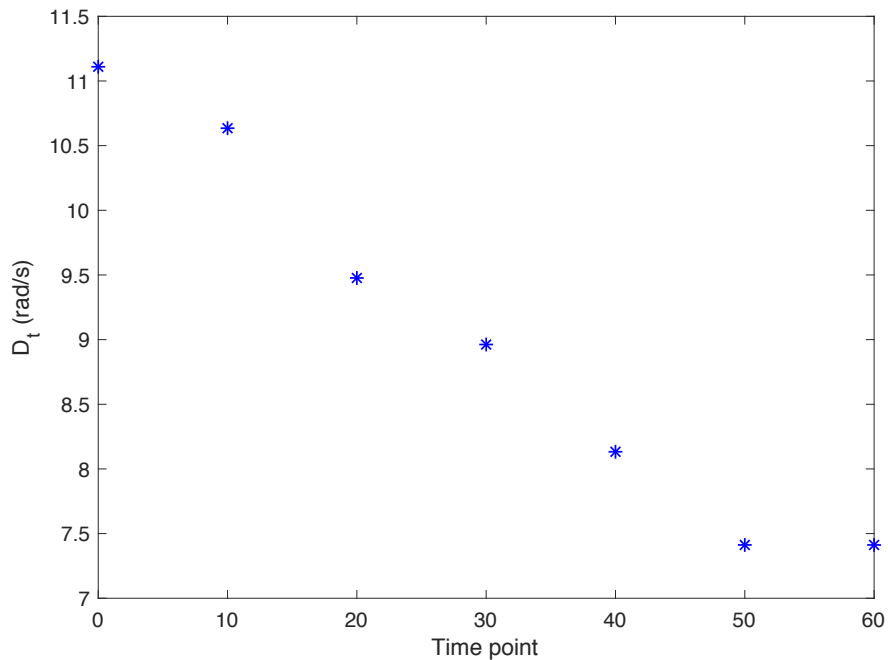
Operational environment	$e_1$	$e_2$	$e_3$	$e_4$	$e_5$	$e_6$	$e_7$	$e_8$
Time proportion	0.1213	0.1126	0.1315	0.1291	0.1205	0.1183	0.1289	0.1378

Table 4.6: Parameters for case 1

$\bar{\alpha}$	$\beta$
0.4771	0.0946

#### 4.4.2 Numerical results for indicators prediction

Hereafter, the estimated natural frequency at time  $t$  is defined as  $D_t$ , and the  $N$ -step forward prediction for  $D_t$  is defined as  $D(t+N)$ . Because of the computational limit set by the NREL-5MW wind turbine, the deterioration of hydraulic pitch system is accelerated in the thesis. Figure 4.7 shows a sequence of estimated deterioration indicator applied to the followed numerical experiments as well as the numerical experiments of RUL prediction.

Figure 4.7: Simulated deterioration indicator  $D_t$

#### 4.4.2.1 N-step prediction when N is small

Prediction is an issue about probability, and its result is a confidence interval. However, this point is difficult to accept by some engineers, in their opinion, the result should be an exact value. As a way to verify the method proposed in this chapter, we compare the actual value with the median value and the mean value from probability distribution of prediction, respectively.

Define  $\epsilon_{\text{Med}}$  as the relative error between the actual value of indicator  $D_t$  and the median from predicted distribution  $\text{Med}_{D_t}$ , denoted by

$$\epsilon_{\text{Med}} = \frac{|D_t - \text{Med}_{D_t}|}{D_t} \times 100\%.$$

Define  $\epsilon_M$  as the relative error between the actual value of indicator  $D_t$  and the mean from predicted distribution  $M_{D_t}$ , denoted by

$$\epsilon_M = \frac{|D_t - M_{D_t}|}{D_t} \times 100\%.$$

Considering the computational facility, we use the approximation of the N-step forward RUL prediction by the algebraic expression.

The subfigures of Figure 4.8 show the median, mean and the probability distribution of 1-step prediction for the  $D_0$ ,  $D_{10}$ ,  $D_{20}$ ,  $D_{30}$  and  $D_{40}$ , respectively. Table 4.7 summaries the results. And the subfigures of Figure 4.9 show the median, mean and the probability distribution of 1-step, 3-step and 5-step prediction results for the deterioration indicator  $D_0$ , given the current operational environment  $\text{OE} = 7$ .

Table 4.7: 1-step prediction results for  $D_t$ , ( $t=0,10,20,30,40,50$ )

Time $t$	Observed information	Median from predicted probability density distribution	$\epsilon_{\text{Med}}$	Mean	$\epsilon_M$
0	$D_0 = 11.11$ , $\text{OE}_0 = 7$	No data			
10	$D_{10} = 10.63$ , $\text{OE}_{10} = 7$	$\text{Med}_{D_{0+10}} = 10.0262$	5.72%	$M_{D_{0+10}} = 9.9948$	6.02%
20	$D_{20} = 9.477$ , $\text{OE}_{20} = 7$	$\text{Med}_{D_{10+10}} = 9.5510$	0.79%	$M_{D_{10+10}} = 9.5196$	0.45%
30	$D_{30} = 8.962$ , $\text{OE}_{30} = 8$	$\text{Med}_{D_{20+10}} = 8.2999$	7.39%	$M_{D_{20+10}} = 8.2685$	7.74%
40	$D_{40} = 8.133$ , $\text{OE}_{40} = 8$	$\text{Med}_{D_{30+10}} = 7.7854$	4.27%	$M_{D_{30+10}} = 7.7540$	4.66%
50	$D_{50} = 7.412$ , $\text{OE}_{50} = 6$	$\text{Med}_{D_{40+10}} = 7.4438$	0.43%	$M_{D_{40+10}} = 7.4125$	0.01%
60	$D_{60} = 7.412$ , $\text{OE}_{60} = 5$	$\text{Med}_{D_{50+10}} = 7.1420$	3.64%	$M_{D_{50+10}} = 7.1111$	4.06%

From Figure 4.8 and Table 4.7, we can find that the median value from probability distribution of predicted deterioration indicator and the mean are little smaller than the actual value. From Figure 4.9 and Table 4.8, as a consequence of lacking the update of present operational environment, when  $N > 1$ , the results of N-step turns to be not accurate over N. For instance, in the case of 5-step forward prediction for indicator  $D_0$ , the errors  $\epsilon_{Me}$  and  $\epsilon_M$  are 39.15% and 39.45%,

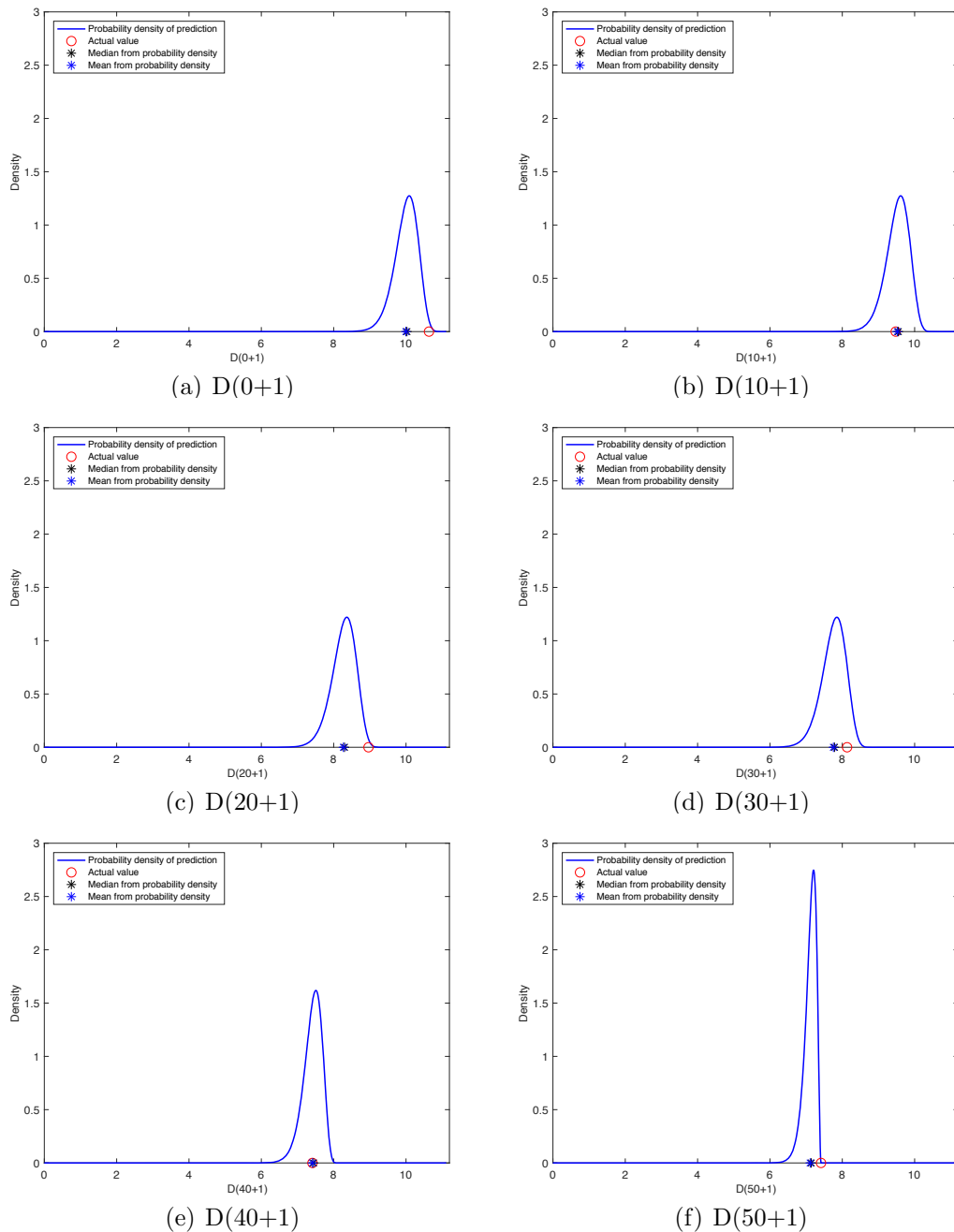
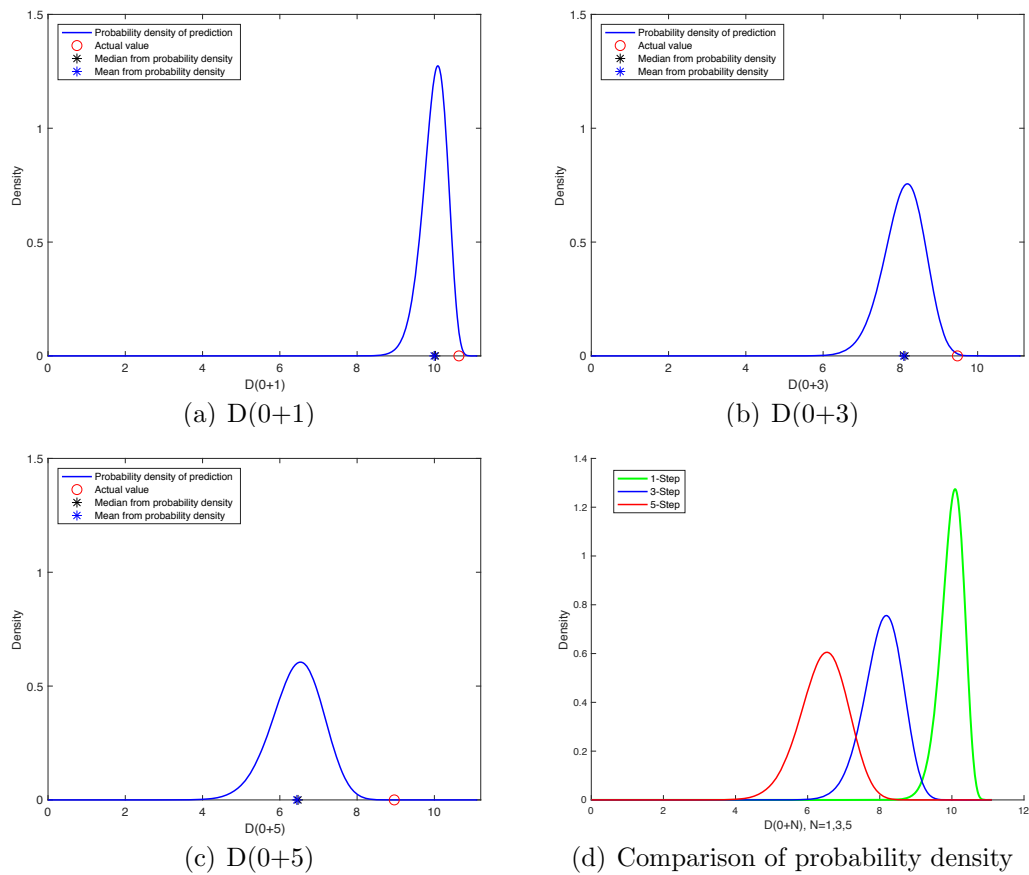


Figure 4.8: 1-step forward prediction for deterioration indicator Probability density of 1-step prediction for deterioration indicator  $D_0$ ,  $D_{10}$ ,  $D_{20}$ ,  $D_{30}$ ,  $D_{40}$  and  $D_{50}$ , respectively

respectively. Therefore, for system operating under various operational environment, the influence of environment should be taken into account for prediction. Moreover, 1-step forward prediction is recommended for the predictions requiring higher prices results. Since the prediction method of algebraic expression considers all the possible deterioration cases, most results overestimate the deterioration, which means that the predicted results are severe than actual ones. However, for 1-step prediction, the errors are within 10%, which is quite good and acceptable for engineering application.

Table 4.8: 1-step, 3-step and 5-step prediction results according to  $D_0$ 

Observed information	$D_0 = 11.11, OE_0 = 7$		
Actual value	$D_{10} = 10.63$	$D_{30} = 8.962$	$D_{50} = 7.412$
Median from predicted probability density distribution	$Med_{D_{0+10}} = 10.0262$	$Med_{D_{0+30}} = 8.1197$	$Med_{D_{0+50}} = 6.4709$
$\epsilon_{Med}$	5.73%	23.67%	39.15%
Mean	$M_{D_{0+10}} = 9.9948$	$M_{D_{0+30}} = 8.0864$	$M_{D_{0+50}} = 6.4393$
$\epsilon_M$	6.02%	23.96%	39.45%

Figure 4.9: 1-step, 3-step and 5-step prediction results for the deterioration indicator  $D_0$ 

### 4.4.3 Numerical results for remaining useful life prediction

The computable timescale of wind turbine simulator is a little bigger than one hour<sup>2</sup>. Hence, this section presents the results of RUL prediction with figures.

<sup>2</sup>The timescale here is different from the one of prediction. The timescale of wind turbine simulator depends on the length of wind speed. Time is an obligatory parameter for the wind

The resulting predicted probabilities of system surviving at time  $T$  according to indicators  $D_t$  are shown in Figure 4.10. The predicted cumulative probability of system surviving at time  $T$  according to indicators  $D_t$  are shown in Figure 4.11. In other words in these figures PDF and CDF of the RUL are depicted. The results prove that the RUL is a random variable depends on the current condition of system and the operational environment.

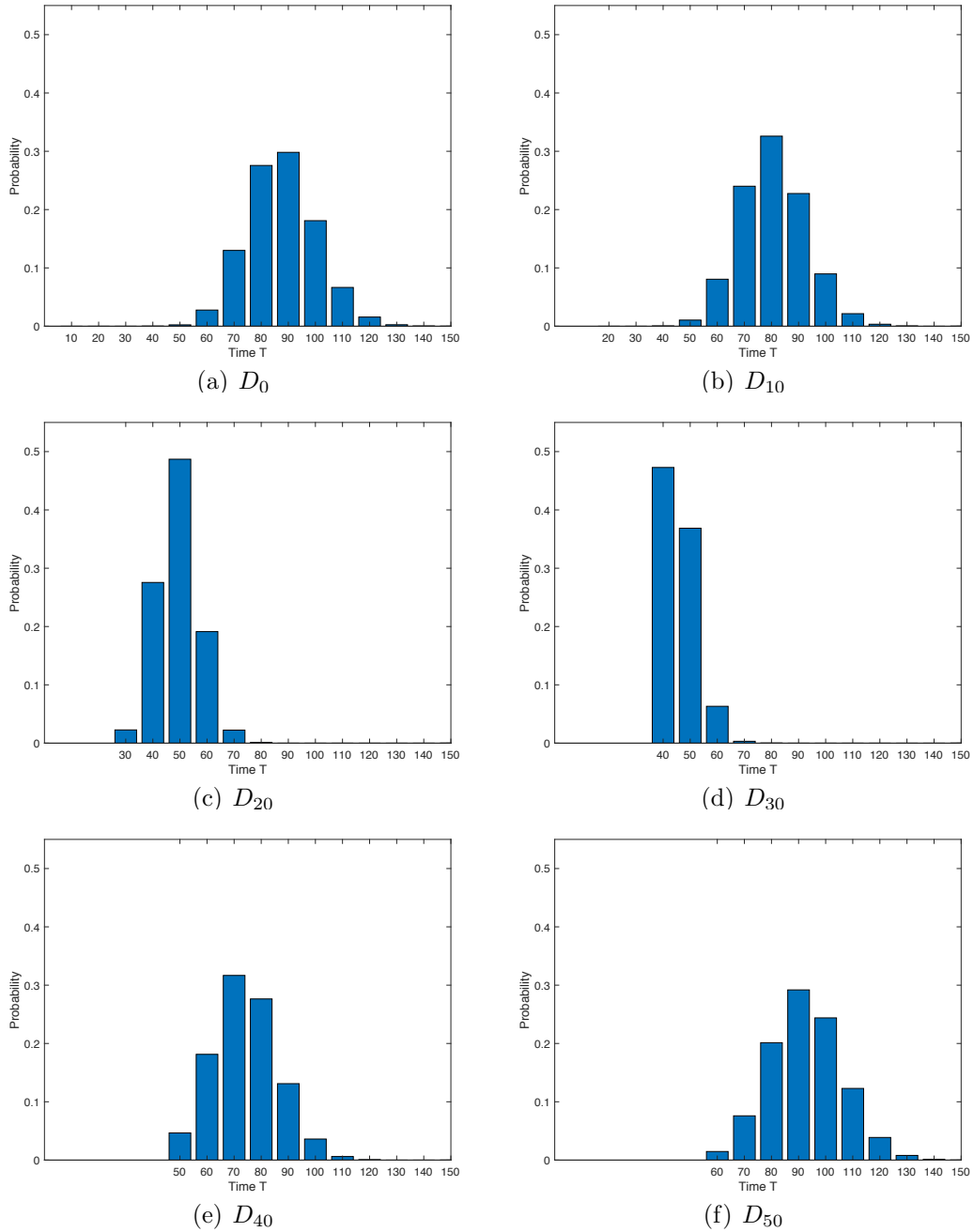


Figure 4.10: Predicted probability of system surviving at time  $T$   $\mathbb{P}(t = T)$  according to indicators  $D_0$ ,  $D_{10}$ ,  $D_{20}$ ,  $D_{30}$ ,  $D_{40}$  and  $D_{50}$ , respectively

sequence inputted into the wind turbine simulator. The wind turbine simulator can only give results when wind speed length is a little bigger than one hour.

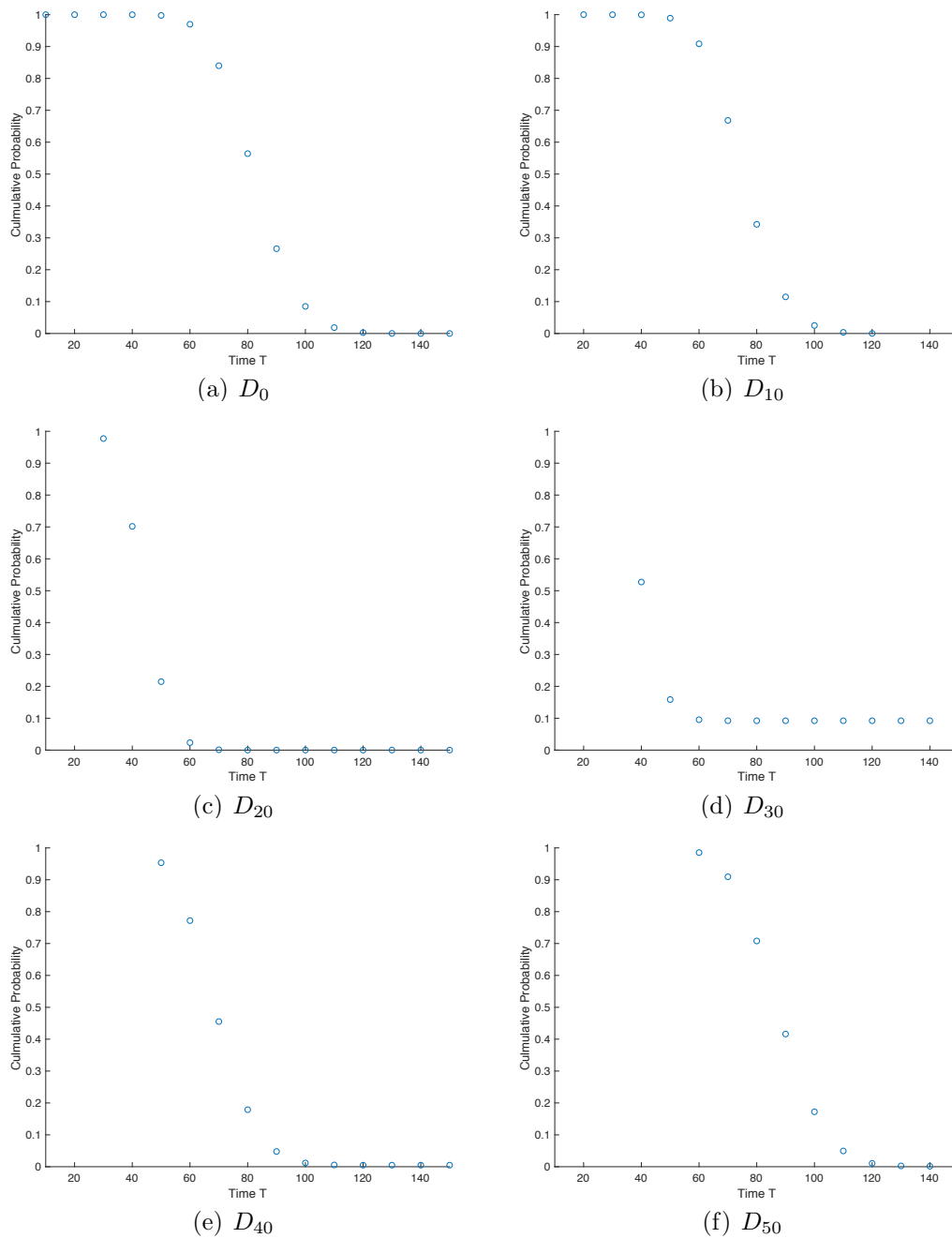


Figure 4.11: Predicted cumulative probability of system surviving at time  $T$   $\mathbb{P}(t = T)$  according to indicators  $D_0$ ,  $D_{10}$ ,  $D_{20}$ ,  $D_{30}$ ,  $D_{40}$  and  $D_{50}$ , respectively

#### 4.4.4 Discussions

- According to the results shown in Figure 4.8, Table 4.7, Figure 4.9 and Table 4.8, we can conclude as expected that the initial state i.e. the state of the system at prediction time has a significant impact on the future behaviour of the system. It has significant influence on the prediction results. Therefore, it is necessary to estimate accurately current environment information from the CMS.
- Comparing the results between Figure 4.8 and Figure 4.9, without surprise

1-step prediction result is more accurate. As the  $N$  of  $N$ -step becomes bigger, the uncertainty increases in the prediction results due to the variability of the environment. Hence, the prediction results are the less accurate.

- The  $N$ -step forward RUL prediction by means of matrix calculation is not suitable for long-term predictions, instead of it, the method of the RUL estimation for a long period  $\tau$  can be applied for long-term predictions when we know the minimum timescale for long-term prediction.

## 4.5 Conclusions

This chapter proposes RUL prediction methods for hydraulic pitch system which operates under multivariate environment, and the proposed method can be applied to other dynamic system operating under various environment. The research work also responses the question related to prediction timescale, i.e., how long is long-term prediction and how short is short-term prediction. According to the numerical results, 1-step forward prediction is more precise than  $N$ -step prediction when  $N > 1$ . The environment state where the prediction is carried out has a significant influence. Hence, in order to obtain convincing prediction result for the deterioration of dynamic system, it demands that the CMS provides accurate information about the current environment. The future research work will focus on the proposition of maintenance policies based on the prediction results.

The operational environment not only affects the deterioration of wind turbine, but also has influences on the maintenance decision-making. To ensure the maintenance can be implemented efficiently and safely, a safe and low-speed wind speed range is required for carrying out the maintenance action. Hence, next chapter will model the unavailability of wind turbine coming from random maintenance delay which is caused by the unfavourable operational environment.

# Chapter 5

## Unavailability model

### Notation and abbreviation

$E$	set of operational environments $E = \{e_1, e_2, e_3, e_4, e_5, e_6, e_7, e_8\}$
$E_M$	set of operational environments that allow to repair $E_M = \{e_1, e_2, e_3, e_4\}$
$\overline{E_M}$	set of operational environment that don't allow to repair $\overline{E_M} = \{e_5, e_6, e_7, e_8\}$
$D_t$	deterioration value of wind turbine at time $t$
$L_F$	threshold of failure
$L_A$	threshold of alarm
$\sigma_A$	the time when deterioration across the alarm threshold $L_A$
$\sigma_F$	the time when deterioration across the failure threshold $L_F$
$e_{i_t}$	the operational environment state at time $t$ ; $e_{i_t} \in E$
$\alpha, \beta$	shape and scale parameter of a gamma distribution, respectively
$\tau$	the delay for carrying out the maintenance
$\rho$	the duration of carrying out the maintenance
$U(t)$	unavailability of system
$\mathbb{I}_A$	identity function. It equals to 1 when $A$ is true, otherwise 0.
$\mathbf{1}_d$	a $d \times 1$ matrix valued 1.

### 5.1 Motivation

As mentioned previously, wind turbine automatically operates under various environment, then, it is meaningful to find a method to measure its reliability. Moreover, having information on its reliability is helpful for maintenance scheduling which plays an important role in assuring the operation and energy production. Considering the operational environment of wind turbine and carrying out maintenance actions, it is necessary to find an alarm threshold for the deterioration indicator to schedule the maintenances appropriately. This chapter focuses on the study of the unavailability of wind turbine. The definition of alarm threshold depends on the maintenance policy, the estimation of the unavailability caused by failures, maintenance is also studied in this chapter.

## 5.2 Simplifications, assumptions and maintenance policy

### 5.2.1 Operational environment simplification

The security average wind speed for maintenance is below 11  $m/s$ . And the operational environment is considered to evolve as a discrete state space and time Markov chain. Hence, to simplify the issue concerned in this chapter, we classify the operational environment set  $E$  into two subsets: a subset  $E_M$  in which the mean wind speed is less than 11  $m/s$ , another one  $\overline{E_M}$  in which the mean wind speed is higher than 11  $m/s$ . Denote them as  $E_M = \{e_1, e_2, e_3, e_4\}$ ,  $\overline{E_M} = \{e_5, e_6, e_7, e_8\}$ , respectively.

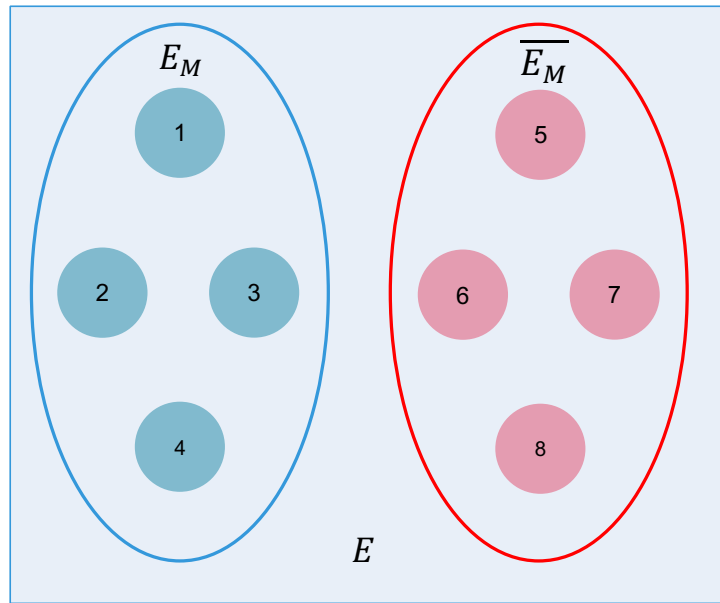


Figure 5.1: Two subsets of the operational environment

### 5.2.2 Maintenance policy

We consider the wind turbine as a repairable system, and the proposed maintenance action is according to the following scheme:

- If the deterioration indicator  $D_t$  is higher than the failure threshold  $L_F$ , the system fails. The time when the deterioration indicator arrives or crosses  $L_F$  is denoted by  $\sigma_F$ .

$$\sigma_F = \inf\{t > 0, D_t \geq L_F\} \quad (5.1)$$

- When the deterioration indicator  $D_t$  becomes bigger or equal to the alarm threshold  $L_A$ , a preventive maintenance is planned. The time when  $D(t)$

arrives or crosses  $L_A$  is denoted by  $\sigma_A$ .

$$\sigma_A = \inf\{t > 0, D_t \geq L_A\} \quad (5.2)$$

- Only the operational environments  $e_1, e_2, e_3, e_4$  allow to implement the maintenance. Hence, the maintenance operation has a random delay time  $\tau$  when the operational environment belongs to  $\overline{E_M}$ . The length of  $\tau$  depends on the time duration to reach a states of  $E_M$  from a state of  $\overline{E_M}$ .
- We assume that the maintenance can be carried out immediately when the environment allows. The maintenance operation has a fixed duration  $\rho$ , and the system is unavailable during this period.
- Between  $\sigma_A$  and  $\sigma_A + \tau$ , the wind turbine deteriorates and a failure may appear before the maintenance. Depending on the appearance of a failure, a preventive or a corrective maintenance action has to be performed.
  - a. If a failure does not occur in the time interval, namely,  $\sigma_F \geq \sigma_A + \tau$ , the wind turbine is unavailable from the time  $\sigma_A + \tau$  when the maintenance is carried out until the end of the maintenance operation  $\sigma_A + \tau + \rho$ , as shown in Figure 5.2.
  - b. If a failure occurs in the time interval, namely,  $\sigma_F \leq \sigma_A + \tau$ , the wind turbine is unavailable from the failure time until the time of the end of the maintenance operation  $\sigma_A + \tau + \rho$ , as shown in Figure 5.3.
- At the end of the maintenance, the wind turbine is assumed to be “as-good-as-new”.

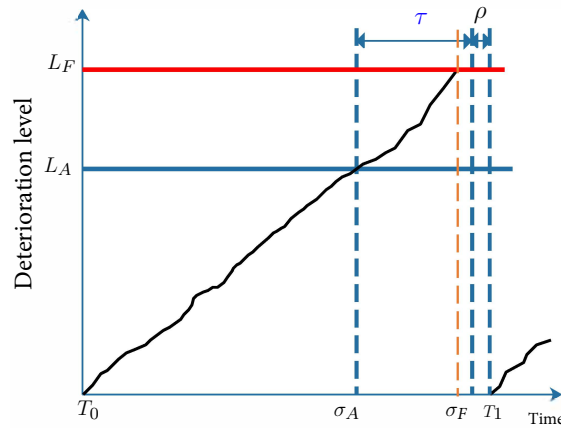
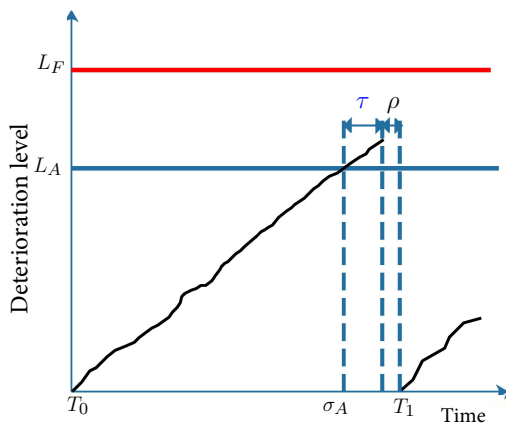


Figure 5.2: Description of the maintenance policy in case of  $\sigma_F \geq \sigma_A + \tau$       Figure 5.3: Description of the maintenance policy in case of  $\sigma_F \leq \sigma_A + \tau$

### 5.2.3 Stationary assumption

According to the above 2-subset operational environment assumption and the maintenance scheme, from a long-run point of view, the maintained deterioration process of wind turbine can be considered as a regenerative process. In other

words, the wind turbine is put into operation and is functioning at time  $T_0$ . When it fails, at time  $T_1$ , it will be restored to the "as-good-as-new" condition. When the wind turbine fails again at time  $T_1 + T_2$ , it is again restored, and so on. The restored time  $T_1, T_2, \dots$  are independent from each other. For simplification, the unavailability is considered in one life cycle, for instance, the life cycle from time  $T_0 = 0$  to time  $T_1$ . The asymptotic unavailability model for wind turbine is based on the stationary distribution of operational environment states.

### 5.3 Asymptotic unavailability model for wind turbine

There are two causes of unavailability: one is the unavailability caused by a deterioration or a failure leading to a downtime; another one is caused by improper wind speed, for instance, low speed wind can't drive the turbine to work. This chapter only treats in the unavailability caused by deteriorations and failures.

Denote  $T_1 = \sigma_A + \tau + \rho$  as the first renewal time (first time of repair). Let  $U_\infty$  be the asymptotic unavailability of the wind turbine,  $U(t)$  be the unavailability duration before time  $t$ . If a maintenance starting at the hitting time  $\sigma_A$  and not finished until time  $t$ , let it be  $t - \sigma_A$ . We have  $U_\infty, U(t)$  respectively as following,

$$U_\infty = \lim_{t \rightarrow \infty} \frac{U(t)}{t} = \frac{\mathbb{E}(U(T_1))}{\mathbb{E}(T_1)}.$$

For  $t \geq \sigma_A + \tau + \rho$ ,

$$U(t) = (t - \min(\sigma_A + \tau, \sigma_L))^+$$

where,  $(x)^+$  is the positive part of  $x$  (0 if  $x < 0$ ,  $x$  otherwise).

Hence, for the first life cycle, the unavailability duration  $U(T_1)$  of wind turbine is

$$U(T_1) = \rho \mathbb{I}_{\{\sigma_F \geq \sigma_A + \tau\}} + ((\sigma_A + \tau + \rho) - \sigma_F) \mathbb{I}_{\{\sigma_F \leq \sigma_A + \tau\}} \quad (5.3)$$

where,  $\mathbb{I}_{\{A\}} = 1$  if  $A$  is true and 0 otherwise.

Considering the average performance of wind turbine, we have

$$\begin{aligned} U_\infty &= \frac{\mathbb{E}(\rho \mathbb{I}_{\{\sigma_F \geq \sigma_A + \tau\}} + ((\sigma_A + \tau + \rho) - \sigma_F) \mathbb{I}_{\{\sigma_F \leq \sigma_A + \tau\}})}{\mathbb{E}(\sigma_A + \tau + \rho)} \\ &= \frac{\mathbb{E}(\rho) + \mathbb{E}((\sigma_A + \tau - \sigma_F) \mathbb{I}_{\{\sigma_F \leq \sigma_A + \tau\}})}{\mathbb{E}(\sigma_A) + \mathbb{E}(\tau) + \mathbb{E}(\rho)} \end{aligned} \quad (5.4)$$

As we assume that the maintenance duration is a constant  $\rho$ , there are three interest terms to derive in equation (5.4):

- the average maintenance delay time  $\mathbb{E}(\tau)$ ,

- the average time when deterioration level equals to (or is firstly higher than) the alarm threshold  $\mathbb{E}(\sigma_A)$ ,
- the unavailability period caused by failure or maintenance  $\mathbb{E}((\sigma_A + \tau - \sigma_F)\mathbb{I}_{\{\sigma_F \leq \sigma_A + \tau\}})$ .

Therefore, the unavailability model is,

$$U_\infty = \frac{\rho + \mathbb{E}((\sigma_A + \tau - \sigma_F)\mathbb{I}_{\{\sigma_F \leq \sigma_A + \tau\}})}{\mathbb{E}(\sigma_A) + \mathbb{E}(\tau) + \rho} \quad (5.5)$$

### 5.3.1 Hitting time in the alarm threshold $\mathbb{E}(\sigma_A)$

This term can be obtained from the deterioration model proposed in chapter 4. There are three ways to estimate the deterioration increment hitting the alarm threshold  $L_A$ .

1. Considering that the deterioration increment is the sum of the increments deteriorating in each operational state.

$$D_t = \sum_{i=1}^8 P_i D_{t,i}$$

where  $P_i = \mathbb{P}(\text{OE} = e_i)$

Therefore,

$$\begin{aligned} \mathbb{P}(\sigma_A < t) &= \mathbb{P}(D_t > L_A) \\ &= \sum_{i=1}^8 \mathbb{P}(D_t > L_A | \text{OE} = e_i) \mathbb{P}(\text{OE} = e_i) \\ &= \int_{L_A}^{+\infty} \sum_{i=1}^8 \mathbb{P}(\text{OE} = e_i) f_{\alpha_i t, \beta}(x) dx \end{aligned}$$

Hence,

$$\mathbb{E}(\sigma_A) = \int_0^\infty \left( \sum_{i=1}^8 \mathbb{P}(\text{OE}_i = e_i) \int_0^{L_A} f_{\alpha_i t, \beta}(x) dx \right) dt$$

Where  $f_{\alpha_i t, \beta}$  is a gamma pdf function, with shape parameter  $\alpha_i t$  and scale parameter  $\beta$ .

2. According to the assumption that  $\tau$  is enough long, consider the approximation  $\Delta \bar{D}_{(t, \tau)} \sim \Gamma(\bar{\alpha}, \tau, \beta)$  with  $\bar{\alpha} = \frac{\sum_i^n \alpha_i \cdot \bar{\tau}_i}{\tau}$ .
3. Via the N-step forward prediction (equation (4.10)). This method is difficult to deal with, hence, using way 2 to instead.

Hence, in this chapter, we calculate the expectation of the hitting time  $\sigma_A$  by the followed formula.

$$\begin{aligned}\mathbb{E}(\sigma_A) &= \int_0^\infty \left( \int_0^{L_A} f_{\bar{\alpha}t, \beta}(x) dx \right) dt \\ &= \int_0^\infty F_{\bar{\alpha}t, \beta}(L_A) dt\end{aligned}\quad (5.6)$$

### 5.3.2 Maintenance delay $\mathbb{E}(\tau)$

Maintenance delay occurs only when deterioration  $D(t)$  firstly arrives or exceeds the alarm threshold  $L_A$ , but the current operational environment is not favorable for carrying out the maintenance, i.e., it belongs to the subset  $\overline{E_M}$ . Therefore, the engineering meaning of  $\tau$  is a time delay from  $\sigma_A$  necessary to enter an operational environment favorable for maintenance. Namely, the time consecutively spent in the operational environment subset  $\overline{E_M}$  after  $\sigma_A$  until the operational environment is no longer unfavorable for a maintenance. Since the operational environment model is modelled as a discrete-time Markov chain, we assume the step length of the Markov chain is  $\delta t$ , we are looking for a  $k$ th operational environment state  $\text{OE}_k$  that firstly belongs to  $E_M$ .

For a discrete Markov chain, the maintenance delay  $\tau$  actually is the sojourn time spent in the operational environment  $\overline{E_M}$ , or the first hitting time of  $E_M$  from  $\overline{E_M}$ . Let  $T$  be the hitting time in an operational environment state of the subset  $E_M$ , when the operational environment state is initially in a state of  $\overline{E_M}$ . We have,

$$T = \inf\{k > 0; \text{OE}_k \in E_M | \text{OE}_0 \in \overline{E_M}\} \quad (5.7)$$

The only assumption is that the subset  $\overline{E_M}$  must be transient at all time  $t \geq \sigma_A$ . The subset  $E_M$  will be considered as the terminal class. This is not difficult to understand. Since the wind speed randomly changes and it can include all the wind speed ranges of the subset  $\overline{E_M}$ , realistically, the subset  $\overline{E_M}$  is transient. The maintenance will be carried out as soon as the operational environment state belongs to the subset  $E_M$ , and the wind turbine is restored to "as-good-as-new" condition after the maintenance. In this sense, the subset  $E_M$  is an absorbent state for a Markov chain, and it can be considered as terminal for a life cycle of the regenerative process.

Now, we are going to give the explicit expression about the expectation of maintenance delay  $\mathbb{E}(\tau)$ . The transition matrix  $P$  of the Markov chain representing the operational environment is partitioned as follows:

$$P = \begin{bmatrix} \mathbf{p}^{\overline{E_M}} & \mathbf{p}^{\overline{E_M}E_M} \\ \mathbf{p}^{E_M\overline{E_M}} & \mathbf{p}^{E_M} \end{bmatrix}$$

Where,  $\mathbf{p}^{\overline{E_M}}$  is the probability that operational environment stays in subset  $\overline{E_M}$  itself;  $\mathbf{p}^{\overline{E_M}E_M}$  is the probability from subset  $\overline{E_M}$  to  $E_M$ ;  $\mathbf{p}^{E_M\overline{E_M}}$  is the probability

from subset  $E_M$  to  $\overline{E_M}$ , and  $\mathbf{p}^{E_M}$  is the probability staying in  $E_M$  itself.

Define another Markov chain  $Y$  whose states space is  $E_Y = \overline{E_M} \cup E_{M_\Delta}$ , where  $E_{M_\Delta}$  contains the states of  $E_M$  that are directly reached by an operational state of  $\overline{E_M}$ , namely,  $E_{M_\Delta} \subset E_M$ . The illustrative figures are shown in Figure 5.4 and in Figure 5.5. The transition matrix of Markov chain  $Y$  is given by

$$\mathbf{Q} = \begin{bmatrix} \mathbf{p}^{\overline{E_M}} & \mathbf{p}^{\overline{E_M}E_{M_\Delta}} \\ \mathbf{0} & \mathbf{I} \end{bmatrix} \quad (5.8)$$

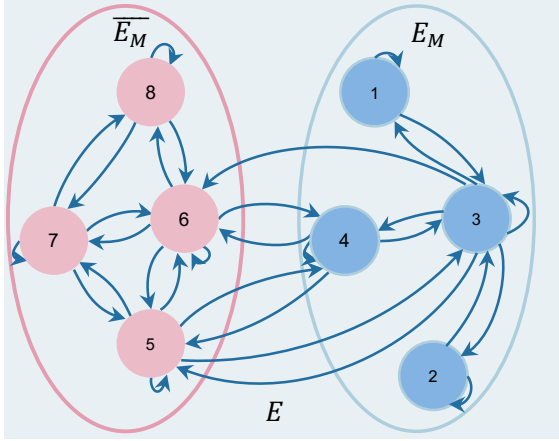
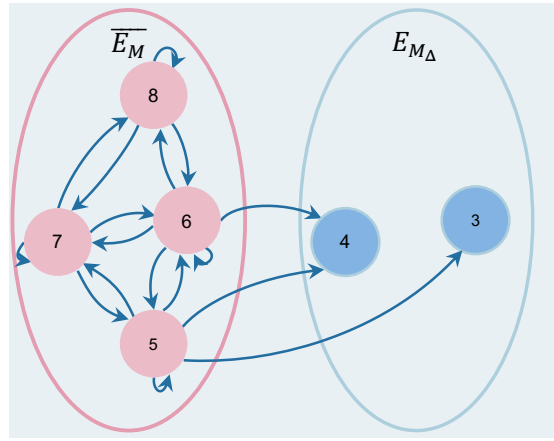


Figure 5.4: Original Markov chain

Figure 5.5: Markov chain  $Y$ 

Therefore, the hitting time in  $E_M$  of the original operational environment Markov chain is as same as the hitting time in  $E_{M_\Delta}$  of the Markov chain  $Y$ , by doing this, the computation is easier. According to the research done by A. Platis et al. [139], the distribution of the hitting time of the subset  $E_M$  at time  $k$  is

$$\mathbb{P}(T > k | OE_0 \in \overline{E_M}) = \mathbb{P}(\forall i, i \leq k, OE_i \in \overline{E_M}) = \alpha_{\overline{E_M}} (\mathbf{p}^{\overline{E_M}})^k \mathbf{1}_d \quad (5.9)$$

Where,  $\alpha_{\overline{E_M}}$  is the initial distribution given that the system starts with operational environment in  $\overline{E_M}$ , and the value of  $d$  equals the dimension of  $\overline{E_M}$ .

And the expected hitting time is given by

$$\begin{aligned} \mathbb{E}(T) &= \sum_{k \geq 0} k \times \mathbb{P}(T = k) = \sum_{k \geq 0} \mathbb{P}(T > k) \\ &= \alpha_{\overline{E_M}} (\mathbf{I} + \sum_{k \geq 1} (\mathbf{p}^{\overline{E_M}})^k) \mathbf{1}_d \end{aligned} \quad (5.10)$$

Hence, the expected maintenance delay  $\mathbb{E}(\tau)$  is

$$\begin{aligned} \mathbb{E}(\tau) &= \mathbb{E}(\tau | OE_{\sigma_A} \in \overline{E_M}) \mathbb{P}(OE_{\sigma_A} \in \overline{E_M}) + \mathbb{E}(\tau | OE_{\sigma_A} \in E_M) \mathbb{P}(OE_{\sigma_A} \in E_M) \\ &= \mathbb{E}(\tau | OE_{\sigma_A} \in \overline{E_M}) \mathbb{P}(OE_{\sigma_A} \in \overline{E_M}) \end{aligned} \quad (5.11)$$

Since  $\mathbb{P}(\text{OE}_{\sigma_A} \in \overline{E_M})$  is approximated by stationary distribution, i.e.  $\sum_{i=5}^8 \mathbb{P}(e_i \in \overline{E_M})$ , we have,

$$\mathbb{E}(\tau) \approx \alpha_{\overline{E_M}} (\mathbf{I} + \sum_{k \geq 1} (\mathbf{p}^{\overline{E_M}})^k) \mathbf{1}_d \left( \sum_{i=5}^8 \mathbb{P}(e_i \in \overline{E_M}) \right) \quad (5.12)$$

### 5.3.3 Unavailable period caused by maintenance or failure

$$\mathbb{E}((\sigma_A + \tau - \sigma_F) \mathbb{I}_{\{\sigma_F \leq \sigma_A + \tau\}})$$

The meaning of the term  $\mathbb{E}((\sigma_A + \tau - \sigma_F) \mathbb{I}_{\{\sigma_F \leq \sigma_A + \tau\}})$  is an average unavailable period in the case of failure coming earlier than maintenance. However, the parameters  $\sigma_A$ ,  $\sigma_F$  and  $\tau$  are random variables. In fact, the three random variables represent two independent stochastic phenomena but the unavailability of wind turbine is affected by them. In others words, the unavailable period is constrained by the deterioration process of system and the operational environment. Therefore, a new probability law should be produced aiming to express the probability distribution of the unavailable period with the two constraints.

Let's define the survival function  $\overline{G}(s)$  of  $\sigma_F - \sigma_A$ . The corresponding pdf is  $g_{\sigma_A - \sigma_F}$  and  $g_\tau$  is the pdf of hitting time in  $E_M$  from  $\overline{E_M}$ . Let random variable  $X = \tau - (\sigma_F - \sigma_A)$  represents the unavailable period,  $f_X$  is its pdf. Actually, the function  $f_X$  is the convolution of  $g_{\sigma_F - \sigma_A}$  and  $g_\tau$ .

$$f_X = g_{\sigma_F - \sigma_A} * g_\tau \quad (5.13)$$

The distribution of hitting time in  $E_M$  (equation (5.9)), we have

$$\begin{aligned} g_\tau(k) &= \mathbb{P}(T = k) = -\mathbb{P}(T > k) + \mathbb{P}(T > k - 1) \\ &= -\alpha_{\overline{E_M}} (\mathbf{p}^{\overline{E_M}})^k \mathbf{1}_d + \alpha_{\overline{E_M}} (\mathbf{p}^{\overline{E_M}})^{k-1} \mathbf{1}_d \end{aligned} \quad (5.14)$$

According to the work of C. Bérenguer et al. [77], the survival function  $\overline{G}(s)$  of  $\sigma_F - \sigma_A$  is,

$$\begin{aligned} \overline{G}(s) &= \mathbb{P}(\sigma_F - \sigma_A > s) \\ &= \iint_{\{L_A < x < L_F, 0 < x+y < L_F, 0 < y\}} \left( \sum_{i=5}^8 \mathbb{P}(\text{OE}_i = e_i) \int_0^\infty f_{\alpha_i, u, \beta}(x) du \right) \\ &\quad \left( \sum_{i=5}^8 \mathbb{P}(\text{OE}_i = e_i) \frac{\partial f_{\alpha_i, s, \beta}(y)}{\partial s} \right) dx dy \end{aligned} \quad (5.15)$$

Under regularity conditions,

$$\begin{aligned}
g_{\sigma_F - \sigma_A}(s) &= \frac{\partial}{\partial s} \overline{G}(s) & (5.16) \\
&= \iint_{\{L_A < x < L_F, 0 < x+y < L_F, 0 < y\}} \left( \sum_{i=5}^8 \mathbb{P}(\text{OE}_i = e_i) \int_0^\infty f_{\alpha_i u, \beta}(x) du \right) \\
&\quad \left( \sum_{i=5}^8 \mathbb{P}(\text{OE}_i = e_i) \frac{\partial^2 f_{\alpha_i s, \beta}(y)}{\partial s^2} \right) dx dy
\end{aligned}$$

We have  $g_{\sigma_A - \sigma_F}(x) = g_{\sigma_F - \sigma_A}(-x)$ , so,

$$\begin{aligned}
f_X(x) &= g_\tau * g_{\sigma_A - \sigma_F}(x) & (5.17) \\
&= \sum_{k \in \mathbb{N}} g_\tau(k) g_{\sigma_A - \sigma_F}(x - k) \\
&= \sum_{k \in \mathbb{N}} g_\tau(k) g_{\sigma_F - \sigma_A}(k - x)
\end{aligned}$$

According to the definition of expectation, the average unavailable period  $\mathbb{E}(X)$  is denoted

$$\begin{aligned}
\mathbb{E}(X) &= \int_0^\infty x f_X(x) dx & (5.18) \\
&= \int_0^\infty x \left( \sum_{k \in \mathbb{N}} g_\tau(k) g_{\sigma_F - \sigma_A}(k - x) \right) dx \\
&= \sum_{k \in \mathbb{N}} \left( \int_0^\infty x g_\tau(k) g_{\sigma_F - \sigma_A}(k - x) dx \right)
\end{aligned}$$

Finally, with equations (5.6), (5.11), (5.18) and equations (5.5), the expression of  $U_\infty$  is obtained.

## 5.4 Approximation of the asymptotic unavailability

For calculating the equation (5.18), there are two difficulties as follows.

- The deterioration process of hydraulic pitch system is modelled as a continuous-time gamma process, while the operational environment is modelled by a discrete-time Markov chain.
- It is not easy to calculate equation (5.16) directly. The asymptotic unavailability is calculated based on a heuristic approximation of the difference between the hitting times,  $\sigma_F - \sigma_A$ . If the trajectories of the deterioration

process  $(D_t)_{t \geq 0}$  were continuous, then  $\sigma_F - \sigma_A$  would have the same probability law as  $\sigma_{F-A}$  [77]. Therefore, we consider the  $\sigma_{F-A}$  as the approximation of  $\sigma_F - \sigma_A$ .

Hence,

$$\begin{aligned} \bar{G}_1(s) &= \mathbb{P}(\sigma_F - \sigma_A > s) \simeq \mathbb{P}(\sigma_{F-A} > s) \\ &= \mathbb{P}(D_s < L_F - L_A) \\ &= \int_0^{L_F - L_A} \sum_{i=1}^8 \mathbb{P}(\text{OE}_t = e_i) f_{\alpha_i, s, \beta}(x) dx \end{aligned} \quad (5.19)$$

$$\begin{aligned} g_{\sigma_{F-A}}(s) &\simeq \mathbb{P}(\sigma_{F-A} = s) \\ &\simeq -\mathbb{P}(\sigma_{F-A} > s) + \mathbb{P}(\sigma_{F-A} > s - 1) \end{aligned} \quad (5.20)$$

According to the deterioration model proposed in chapter 4, equation (5.20) turns to

$$g_{\sigma_{F-A}}(s) \simeq \int_0^{L_F - L_A} \left( -\sum_{i=1}^8 \mathbb{P}(\text{OE}_s = e_i) f_{\alpha_i(s), \beta}(x) + \sum_{i=1}^8 \mathbb{P}(\text{OE}_{s-1} = e_i) f_{\alpha_i(s-1), \beta}(x) \right) dx \quad (5.21)$$

The approximated expectation of  $X \simeq \tau - (\sigma_F - \sigma_A)$  is

$$\begin{aligned} \mathbb{E}_1(X) &= \sum_{x=0}^{\infty} x f_X(x) \\ &= \sum_{x=0}^{\infty} x \left( \sum_{k=0}^x g_{\tau}(k) g_{\sigma_{F-A}}(k-x) \right) \end{aligned} \quad (5.22)$$

The approximation of the asymptotic unavailability  $U_{\infty}^1$  is

$$U_{\infty}^1 = \frac{\rho + \sum_{x=0}^{\infty} x \left( \sum_{k=0}^x g_{\tau}(k) g_{\sigma_{F-A}}(k-x) \right)}{\rho + \mathbb{E}(\sigma_A) + \mathbb{E}(\tau)} \quad (5.23)$$

## 5.5 Numerical experiment

Recall the parameters of deterioration process estimated in Chapter 4 and the probability of system stays in each operational environment state, as shown in Table 5.1 and Table 5.2, respectively.

According to the transition probability of wind speed (Table 3.3), the transition

Table 5.1: Parameters for deterioration model related to different operational environments

parameters	$\alpha_1 - -\alpha_5$	$\alpha_6$	$\alpha_7$	$\alpha_8$	$\beta$
value	0	1.2019	1.2199	1.2897	0.0946

Table 5.2: Probability of system stays in each operational environment state

Operational environment	$\mathbb{P}(\text{OE}_i = e_1)$	$\mathbb{P}(\text{OE}_i = e_2)$	$\mathbb{P}(\text{OE}_i = e_3)$	$\mathbb{P}(\text{OE}_i = e_4)$
Probability	0.1213	0.1126	0.1315	0.1291
Operational environment	$\mathbb{P}(\text{OE}_i = e_5)$	$\mathbb{P}(\text{OE}_i = e_6)$	$\mathbb{P}(\text{OE}_i = e_7)$	$\mathbb{P}(\text{OE}_i = e_8)$
Probability	0.1205	0.1183	0.1289	0.1378

probability of operational states in  $\overline{E}_M$  is shown below,

$$\mathbf{p}^{\overline{E}_M} = \begin{bmatrix} 0.3989 & 0.1954 & 0.0683 & 0 \\ 0.2285 & 0.3858 & 0.1847 & 0.0561 \\ 0.0378 & 0.2481 & 0.5781 & 0.1360 \\ 0 & 0.0154 & 0.1613 & 0.8233 \end{bmatrix}$$

Recall that as mentioned in section 3.2.2, the initial distribution is estimated by dividing the dataset into bins according to the states. The obtained vectors of occurrences can then be normalized in each bin. Then, according to the real average wind speed data used to estimated the parameters of outer Markov chain of wind speed model, the initial distribution of  $\alpha_{\overline{E}_M}$  is shown as below.

$$\alpha_{\overline{E}_M} = [0.1209 \quad 0.1183 \quad 0.1285 \quad 0.1364]$$

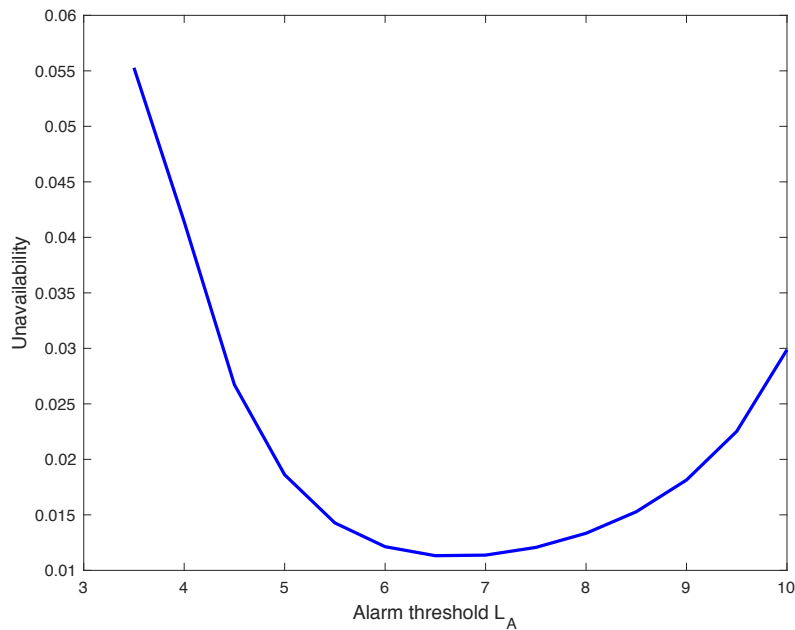
The initial value of deterioration is  $11.11 \text{ rad/s}$  and the failure threshold  $L_F$  of deterioration is  $3.42 \text{ rad/s}$ . Let  $\rho = 1$ , Table 5.3 shows the results of the approximation of the asymptotic unavailability of system  $U_\infty^1$ ,  $\mathbb{E}(\sigma_A)$  and  $\mathbb{E}_1(X)$  corresponding to different alarm threshold  $L_A$  calculated by the proposed approximation method. Figure 5.6 shows the relationship between alarm threshold  $L_A$  and unavailability of wind turbine.

Table 5.3: Unavailability of system corresponding to different alarm threshold  $L_A$ 

$L_A$	10	9.5	9	8.5	8	7.5	7
$U_\infty^1$	<b>0.0298774</b>	<b>0.0225259</b>	<b>0.0181417</b>	<b>0.0152803</b>	<b>0.0133429</b>	<b>0.0120678</b>	<b>0.0113739</b>
$\mathbb{E}_1(X)$	0.0032444	0.006064	0.011334	0.0211841	0.0395947	0.0740055	0.1383221
$\mathbb{E}(\sigma_A)$	25.154697	36.238533	47.322355	58.406163	69.489958	80.573739	91.657507
$\mathbb{E}(\tau)$	7.4240088						

---

$L_A$	6.5	6	5.5	5	4.5	4	3.5
$U_\infty^1$	<b>0.0113213</b>	<b>0.0121328</b>	<b>0.0142739</b>	<b>0.0186138</b>	<b>0.0267239</b>	<b>0.0414085</b>	<b>0.0552794</b>
$\mathbb{E}_1(X)$	0.258535	0.483227	0.9031838	1.688143	3.1555673	5.8979837	8.8213537
$\mathbb{E}(\sigma_A)$	102.74126	113.825	124.90873	135.99244	147.07614	158.15983	169.2435
$\mathbb{E}(\tau)$	7.4240088						

Figure 5.6: Numerical experiment results of the unavailability according to different alarm threshold  $L_A$ 

From Table 5.3 and Figure 5.6, we can find that the optimal alarm threshold is  $L_A = 6.5 \text{ rad/s}$  for the wind turbine considered in this chapter.

## 5.6 Conclusion

In this chapter, an unavailability model of wind turbine caused by random maintenance delay is proposed. Based on the work of C. Bérenguer et al. [77] approximations are proposed to assess numerically the system unavailability. The results of numerical experiment shows that an optimal alarm threshold  $L_A$  can be proposed for a deteriorating system operated under various operational environment. This chapter proposes an initial numerical experiment. Additional work still has to be

---

done especially to evaluate the effects of successive approximations. The first part will be to put efforts on a numerical algorithm to calculate exact formulas when available. The second part will be to compare with Monte Carlo simulation.

# Chapter 6

## Conclusion and perspective

### 6.1 Conclusions

Wind turbines extract energy from wind, at the same time, wind can cause deteriorations, failures to the wind turbines. Therefore, it is crucial to study the influences of operational environment (wind speed in this thesis) on the reliability of wind turbine.

In this thesis, we have focused about the RUL estimation and the unavailability influenced by operational environment of a wind turbine. We have established a wind turbine simulator with a deteriorating hydraulic pitch system for data simulation. We have proposed a long-term continuous wind speed model for the environment simulation. Then, we have proposed RUL estimation methods for different timescales and studied the unavailability caused by the maintenance delay and failure of a wind turbine.

In Chapter 2, a wind turbine simulator embedded with a deteriorating hydraulic pitch system is proposed. The deterioration of hydraulic pitch system is related to wind speed which is a random phenomenon. This randomness lead us to model the deterioration by stochastic process.

In Chapter 3, a continuous wind speed generation method based on a 2-level Markov chain and stochastic differential equations is proposed. Two stochastic differential equations are discussed in this model framework This model is capable of generating wind speed with different time scales. For example, a one-second step wind speed generation can be performed during 10 minutes or for a few hours based on SDE. In line with the short time generation, a long-term generation for a few months or years can be based on the outer Markov chain. The developed model is particularly suitable to be merged with a deterioration model of wind turbine's key component, like blade-pitch system.

In Chapter 4, a RUL prediction method for a dynamic system which operates under changing environment are proposed, cases about wind turbine are studied. The research work also responses the question about RUL prediction timescale. According to the numerical results, the environment state where the prediction is

carried out has significant influence on the prediction results. Hence, in order to obtain convincing prediction results on the deterioration of dynamic system, it demands that the CMS provides accurate information about the current environment.

In Chapter 5, an unavailability model based on maintenance delay and deterioration is discussed.

## 6.2 Perspective

Normally, the designed service life of a wind turbine is 20 years. However, it is a challenge to ensure that wind turbine operates safely and reliability under harsh operational environment for a long period. Hence, providing efficient maintenance planning is an efficient way to keep wind turbines in good conditions.

Besides, the maintenance policy based on RUL estimation is helpful for grid dispatch. The commercial market share occupied by wind energy grows rapidly. For instance, renewable energy will provide 45% power that 23% of them is transformed from wind energy for France in the year of 2030 [140]. Because of the inherent random characteristic of renewable energies, the growth of renewable energies brings a challenge for the dispatch of grid. However, an annual production of a wind farm can be estimated as a selection of the wind farm is based on statistical wind resource information. With accurate weather forecasts, the future wind condition can be known, hence, the production of the wind farm can be estimated. More accurate production can be estimated if the health conditions of wind turbine are well known, this point can be achieved with the help of the RUL estimation and maintenance policy.

The final aim of a wind farm is to obtain profit for its owner. Ensuring the safe operation of wind turbines, transferring as much as possible generated wind energy to the grid, and minimizing the operation and maintenance (O&M) cost of wind farm are the methods to increase owner's profit. Scheduling maintenance keeps the wind turbine in good condition. However, when an RUL is estimated for wind turbines, the owner has several choices for making a maintenance decision:

- perform a preventive maintenance at the first opportunity
- let the wind turbines deteriorates, and making a balance between the expense and revenue, then choose a time to carry out a maintenance
- do nothing, let the wind turbine fail and then carry out a corrective maintenance

Maintenance itself has costs, such as the cost of labor, the cost for renting special vehicles, the cost of replacement pieces and the profit loss of shutting down wind turbine caused by maintenance. Moreover, once the warranties provided by the manufacture lapse, the cost of wind farm's operation and maintenance significantly

goes up. According to a RUL estimation value, the scheduled maintenance time directly influences the revenue for the wind farm.

Hence, the future work can focus on the points following:

### 1. Improvement about the deterioration model

As components of wind turbine have different structure designs, different movements and made by different materials, it is very difficult to describe their deterioration processes through the same stochastic process. In our opinions, a convincing RUL estimation will require a probabilistic deterioration model based on wind conditions, loads of component, and material-degradation, and it can reflect the inspection report. In the future, one shall try to merge loads of component and material degradation to the deterioration model.

### 2. Maintenance policy and its optimization for wind farm

For a wind farm consisting of several wind turbines, similar failures or deteriorations may occur to wind turbines at the same moment, and due to the quality individual deviation of each wind turbine, some wind turbines may deteriorate more quickly than others. Considering the constraints caused by environment, wind turbine location on the farm, special vehicles etc, it is not possible anytime we require. Therefore, some wind turbine should be prioritized. However, the priorities depends on the concerned profit plan, maintenance cost, demand of electric grid and etc. Form this point of view, the maintenance policy for a wind farm is interesting and one can address, for instance, the maintenance itinerary optimization.

### 3. Warranty

Wind turbine is valuable and vulnerable. Warranty policy is important for the wind farm owner and also important for the provider. In the future, warranty policy for wind turbine will be studied.

# Chapter 7

## Résumé de Thèse en Français

### 7.1 Introduction

Les éoliennes étaient des éoliennes à régulation passive de la charge par décrochage, fonctionnant dans une plage de vitesse du vent étroite. Paul La Cour a conçu la première éolienne pour la production de courant continu en 1891 [11]. Après la Première Guerre mondiale, grâce à l'expérience de la conception d'hélices d'avions, la compréhension scientifique de la conception des éoliennes a fait un grand pas en avant en Europe. Avec le nouveau contexte théorique des éoliennes, de nombreuses méthodes prometteuses pour la conception moderne des éoliennes ont émergé. L'éolienne WIME D-30 d'un diamètre de 30 m et d'une puissance de 100 kW a fonctionné de 1931 à 1942 en Crimée [12] et a produit de l'électricité dans un petit réseau de 20 MW. Cependant, le début de la Seconde Guerre mondiale a ruiné ces modèles. Avec la reconstruction de l'Europe après la guerre, le développement des éoliennes a de nouveau attiré l'intérêt des chercheurs. Certains prototypes d'éoliennes ont été fabriqués et ont fourni de l'électricité au réseau. Après 1980, la renaissance de l'énergie éolienne a commencé énormément en Europe et aux États-Unis. Après près de 40 ans, l'éolienne se partage une grande partie du marché de l'électricité. Il est nécessaire de résumer les évolutions concernant le site, la taille, la puissance et le contrôle de l'éolienne pour que le contexte de recherche de cette thèse puisse être développé.

- **Evolution du site**

Afin de capter d'énergie éolienne que possible, des éoliennes terrestres sont érigées dans des endroits éloignés où les ressources éoliennes sont abondantes. Aujourd'hui, l'énergie éolienne en mer suscite l'intérêt de pays populaires comme le Danemark, la Chine, le Royaume-Uni, les Pays-Bas et l'Allemagne, en raison de ses excellentes ressources éoliennes et de l'évitement des problèmes d'utilisation des terres. Avec le développement des technologies de soutien, les éoliennes sont construites en eau peu profonde (pour les éoliennes à fondation fixe) et en eau plus profonde (pour les éoliennes flottantes).

- **Evolution de la taille**

Si l'Airbus A380 de 79,75 m d'envergure est considéré comme un avion géant, les éoliennes commerciales d'aujourd'hui devraient être qualifiées de super géantes, car le diamètre de leur rotor dépasse facilement 100 m. La puissance du vent  $P$  qui traverse une zone  $A$  à une vitesse  $v$  est

$$P = \frac{1}{2}\rho Av^3 \quad (7.1)$$

où  $\rho$  est la densité de l'air. L'amélioration de la surface du rotor est donc un moyen efficace de capter beaucoup plus d'énergie à la même vitesse du vent ( $v$ ). Le diamètre du rotor de la toute nouvelle éolienne offshore SG 10.0-193D de Simens est de 193 m [13]. De nos jours, la taille limite d'une éolienne est inconnue. Avec l'ambition de capter une énorme quantité d'énergie, de plus grandes éoliennes pourraient voir le jour.

- **Evolution de la puissance nominale**

Selon Yang et al. [14], les éoliennes deviennent de plus en plus grandes en puissance nominale, comme le montre le tableau 7.1.

Table 7.1: Évolution de la puissance nominale des éoliennes

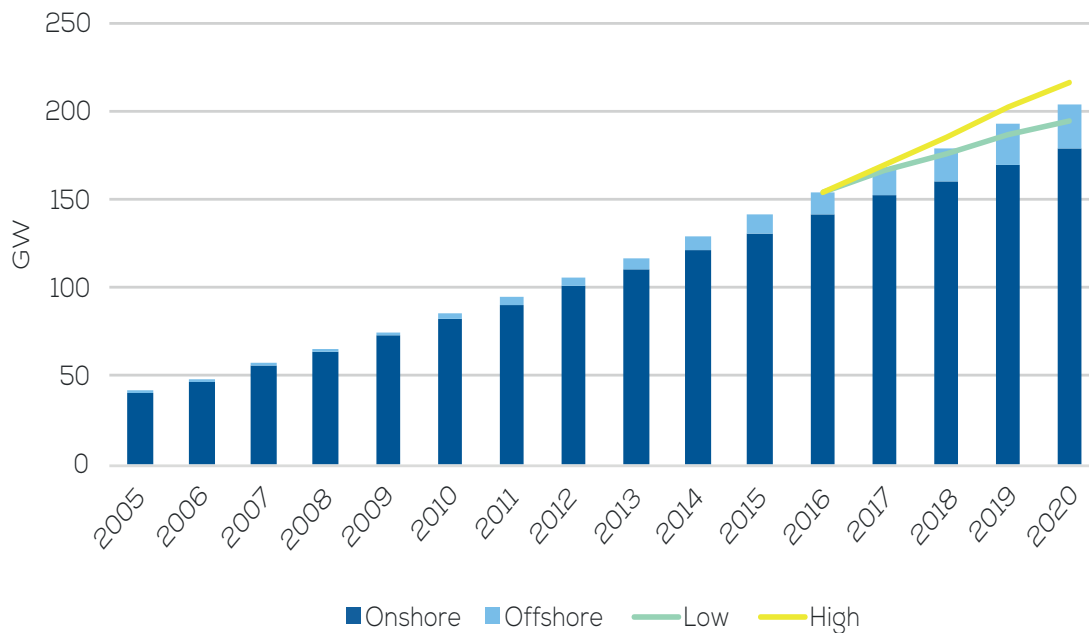
Fabricant	Modèle d'éolienne	Puissance nominale
Repower	M104	3.4 MW
GE	4.0-110	4.0MW
Gamesa	G-128	4.5MW
Enercon	E-126	7MW
Wind Power Ltd	Aerogenerator X	10MW (in development)

- **Evolution du contrôle**

Au début, les éoliennes étaient des éoliennes passives à régulation de charge par décrochage, à vitesse de rotation fixe, fonctionnant dans une plage de vitesse du vent étroite. C'est alors qu'est apparue l'éolienne à vitesse variable avec contrôle actif de la pale. L'application de la commande de la pale des pales a permis aux éoliennes modernes d'être plus grandes et de fonctionner sur de plus grandes plages de vitesse du vent. Cependant, les chercheurs essaient de mettre au point une pale intelligente qui peut mesurer la vitesse du vent et s'adapter automatiquement aux conditions du vent. On croit qu'avec une pale intelligente, la fiabilité et l'efficacité de l'éolienne peuvent être améliorées.

- **Evolution de la capacité installée cumulative**

Selon le rapport de Wind EUROPE [16], la capacité installée totale cumulée en Europe atteindra 204 GW en 2020, comme le montre la figure 7.1.



Source: WindEurope

Capacité installée cumulée prévue jusqu'en 2020

Par conséquent, il peut conclure que les éoliennes sont des machines géantes qui fonctionnent automatiquement à des endroits éloignés ou en mer dans un environnement hostile et aléatoire sans la superviser humain. En tant que producteur d'électricité coûteux et sa contribution croissante au réseau, la fiabilité de l'éolienne est un enjeu important. Cependant, son environnement d'exploitation, l'emplacement du site et la taille de l'éolienne posent de nombreux défis à la fiabilité de l'éolienne et à sa maintenance :

- **Défis causés par le site**

Le site éloigné du parc éolien peut ne pas être accessible à tout moment. Par conséquent, les activités d'entretien des éoliennes ne peuvent être effectuées que pendant une période de temps accessible. Il faut donc prévoir et planifier. Les composants détériorés qui sont susceptibles de tomber en panne pendant la période de temps non accessible doivent être réparés / remplacés à l'avance pour éviter des temps d'arrêt indésirables.

- **Défis causés par la taille**

Pour effectuer les activités de maintenance, la taille croissante des éoliennes peut nécessiter des véhicules ou des équipements spéciaux. De plus, la croissance rapide de la taille de la conception, qui manque d'expérience opérationnelle pratique, peut entraîner des défaillances inattendues.

- **Défis causés par le système de contrôle**

Les systèmes de contrôle utilisés pour le pitch, le générateur et le convertisseur sont de plus en plus sophistiqués. Cependant, les composants

électriques et électroniques montrent qu'ils sont moins fiables que les composants mécaniques. De plus, le système de surveillance de l'état actuel n'est pas efficace pour détecter les pannes électriques et électroniques. Les temps d'arrêt causés par les pannes de composants électriques et électroniques sont plus importants dans les régions éloignées et en mer en raison de l'accessibilité réduite.

Pour améliorer la fiabilité des éoliennes, plusieurs méthodes peuvent être envisagées :

1. Amélioration de la théorie de conception et de la technologie d'agrandissement des éoliennes.
2. Développement d'un système avancé de surveillance de l'état des éoliennes.
3. Article prévoir la durée de vie utile restante des éoliennes et établir un calendrier de maintenance raisonnable et économique pour les éoliennes en service.

Les travaux de cette thèse peuvent être classés dans la dernière méthode. Mais c'est aussi un élément critique pour les systèmes modernes de surveillances, car ce dernier doit fusionner un module pronostic.

### 7.1.1 Fiabilité des éoliennes et influence du vent

De nombreux efforts ont été déployés pour recueillir des données sur la fiabilité des éoliennes [17, 18, 19, 20, 21, 22, 23].

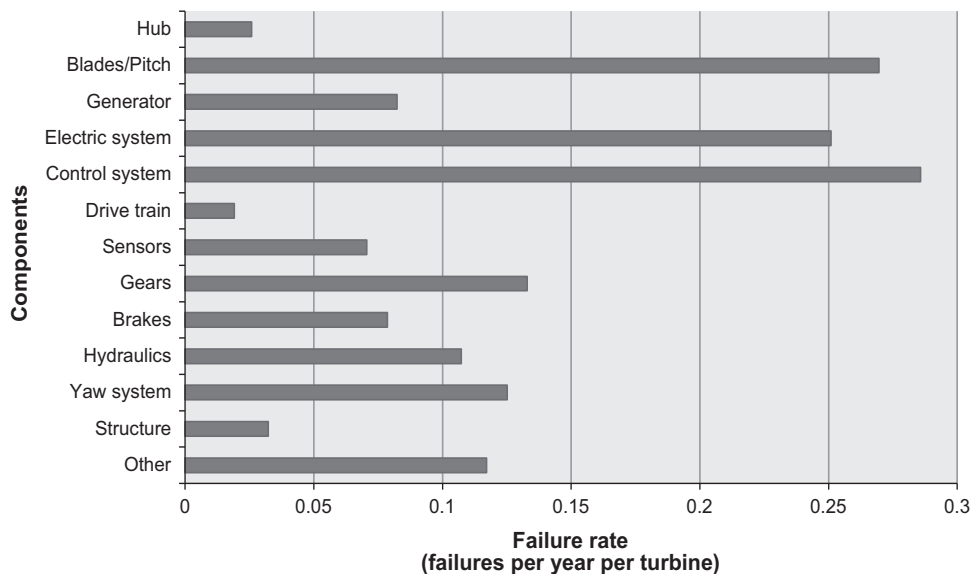


Figure 7.1: Taux de défaillance moyen des composants d'éolienne VS (Source [8])

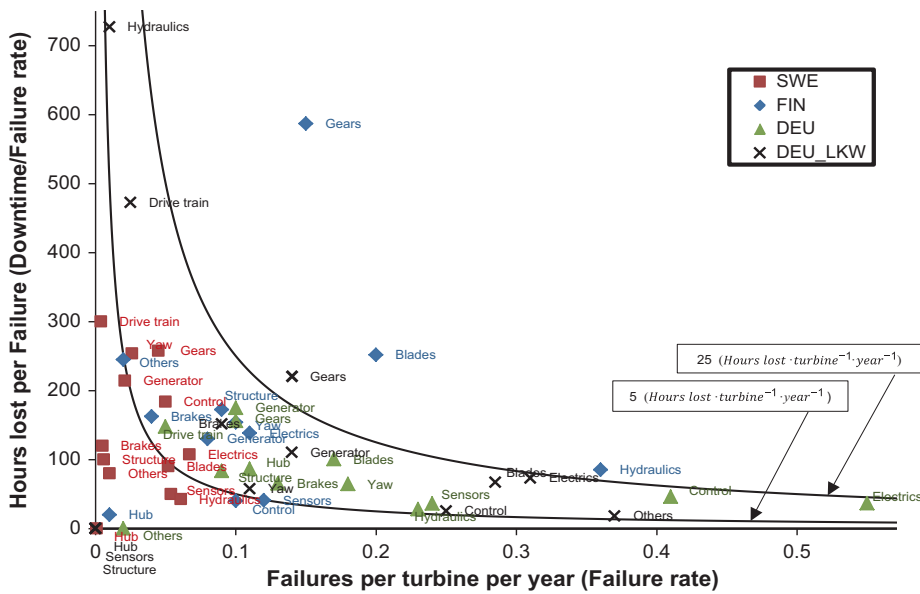


Figure 7.2: Taux d'échec VS heures perdues par échec : Suède(SWE), Finlande(FIN), (DEU) et Allemagne(DEU\_LKW) (Source [8])

Selon la Figure 7.1 et 7.2, les systèmes de commande, électriques et de contrôle ont des taux de défaillance élevés ; la défaillance des boîtes de vitesses, des pales et des générateurs entraînent des temps d'arrêt plus longs. J.M. Pinar Pérez et al [8] ont également conclu que les grandes éoliennes avaient tendance à subir plus de pannes que les petites.

**L'influence du vent sur la fiabilité des éoliennes**

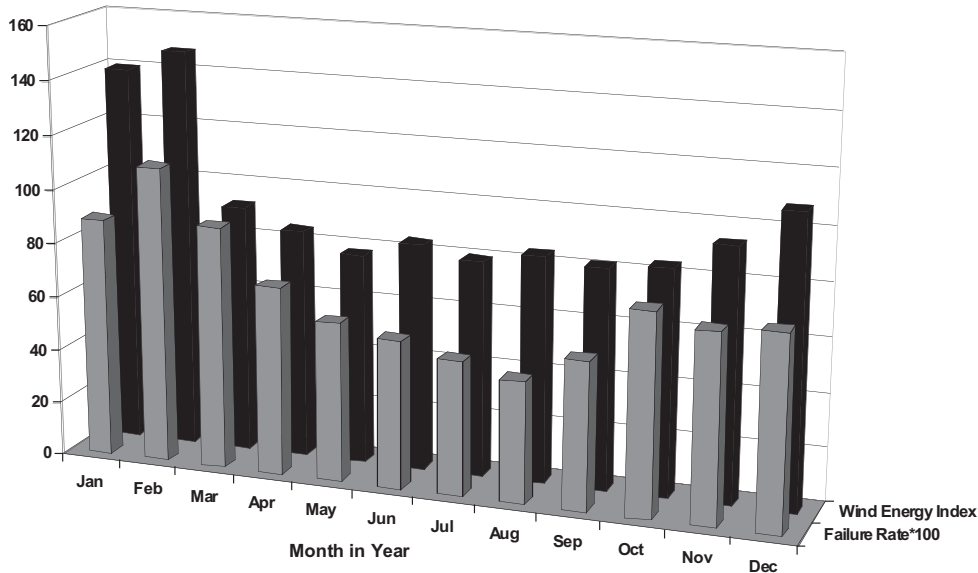


Figure 7.3: Taux d'échec mensuel moyen et IFE pour chacun des 12 mois de la période de l'enquête 1994-2004(source: [9])

Contrairement aux autres turbines à gaz/vapeur, les éoliennes sont fortement in-

fluencée par le vent, en particulier la vitesse du vent. P.Tavner et al [9] s'intéresse à l'influence de la vitesse du vent sur la fiabilité d'éolienne. Cette recherche quantifie les données sur la vitesse du vent sous forme d'indice de l'énergie éolienne (WEI) qui est défini comme suit

$$WEI = \frac{\text{(Actual monthly energy production from a collection of wind turbines)}}{\text{(Long term expected monthly energy production from those turbines in the presence of average weather)}}$$

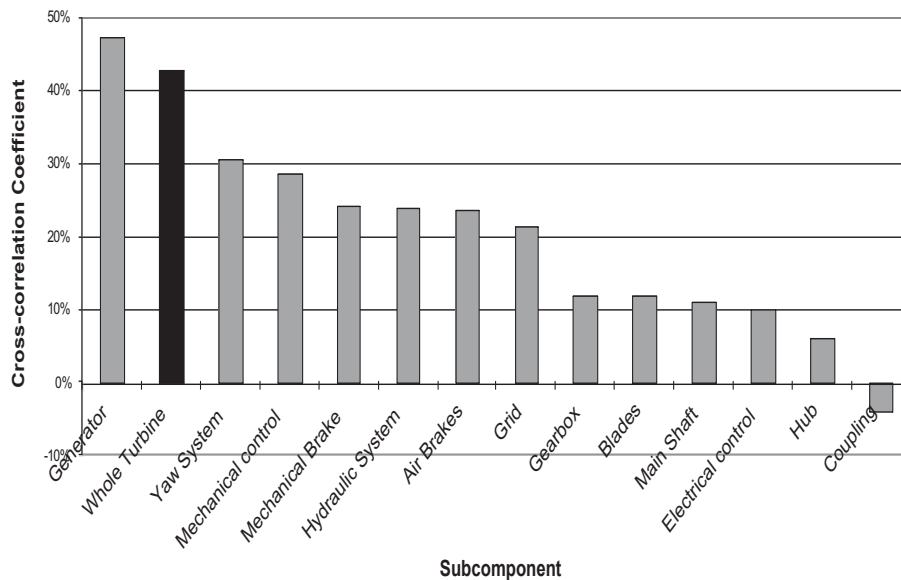


Figure 7.4: Résumé des corrélogrammes croisés des taux de défaillance des sous-composantes de l'IFE, 1994-2004 (source: [9])

La figure 7.3 montre la relation entre le taux d'échec et l'IFE. D'après ce chiffre et les résultats de l'étude de [19], il est évident que les conditions météorologiques et la vitesse du vent ont une influence significative sur la détérioration et la défaillance des composants d'éolienne. De plus, ils soulignent que certains composants d'éolienne sont plus affectés par la vitesse du vent que d'autres, comme le système hydraulique, la génératrice, la commande de lacet et le frein mécanique (voir Figure 7.3). D'après l'auteur, ces composants ne sont pas conçues avec les effets changeants les changeants rapides de la variation de la vitesse du vent. Un rapport chinois sur la défaillance du système de tangage WT affirme que la plupart des défaillances du système de tangage surviennent pendant les saisons venteuses en raison d'une variation importante de la vitesse du vent, etc. Les recherches menées à [25] montrent que des vitesses de vent différentes ont des effets différents sur les dommages de fatigue de l'engrenage appliqué à une éolienne. Ceci est dû au fait que la plage de contrainte du pignon est fonction de la vitesse de rotation du pignon, qui est fondamentalement déterminée par la vitesse du vent.

## 7.2 Modèle de génération de la vitesse du vent

Ce chapitre propose un modèle mathématique qui permet de générer des séquences de vitesse du vent satisfaisantes pour l'étude RUL des composants d'éoliennes et pour une estimation précise de la puissance de sortie, la vitesse du vent générée par ce modèle a les propriétés suivantes :

- peut refléter la tendance du vent à long terme
- peut contenir des informations de turbulence à petite échelle de temps
- peut correspondre à la distribution de probabilité des données de la vitesse réelle du vent
- peut rapidement générer les données

### 7.2.1 Description du modèle de vent

#### 7.2.1.1 Description générale

Reynolds doit être prise en compte pour analyser les effets de la turbulence [125]. La série temporelle de la vitesse du vent  $U(t)$  peut être décomposée en sa valeur moyenne  $\bar{U}(t)$  et la fluctuation  $u(t)$ .

$$U(t) = \bar{U}(t) + u(t) \quad (7.2)$$

Cette décomposition nous donne une idée pour modéliser séparément la vitesse moyenne du vent et la fluctuation de la vitesse du vent. Comme il est mentionné dans [10],  $\bar{U}(t)$  peut être considéré comme un filtre passe-bas correspondant aux effets horaires, quotidiens, mensuels, saisonniers ou annuels ; turbulence  $u(t)$ , qui a une valeur moyenne nulle, peut être considéré comme un filtre passe-haut correspondant aux impacts turbulents.

Dans cet article, nous proposons un modèle de chaîne de Markov à deux niveaux incorporant des SDE. La figure 7.5 montre le modèle global avec la chaîne de Markov et le modèle SDE. Ce modèle est très flexible grâce aux propriétés suivantes :

- La chaîne de Markov extérieure est utilisée pour modéliser la tendance macroscopique (générale) de la vitesse du vent. Il peut avoir plusieurs significations, telles que la vitesse moyenne du vent pour une échelle de temps spécifique ou différentes classes de vitesse du vent.
- Les SDE embarqués sont principalement utilisés pour modéliser des séquences continues de vitesse du vent à court terme (comme une seconde) en fonction de l'environnement des états qui est défini par la chaîne de Markov externe. Différents réglages de paramètres et différents SDEs donnent une grande variété de modèles de vitesse du vent en continu.

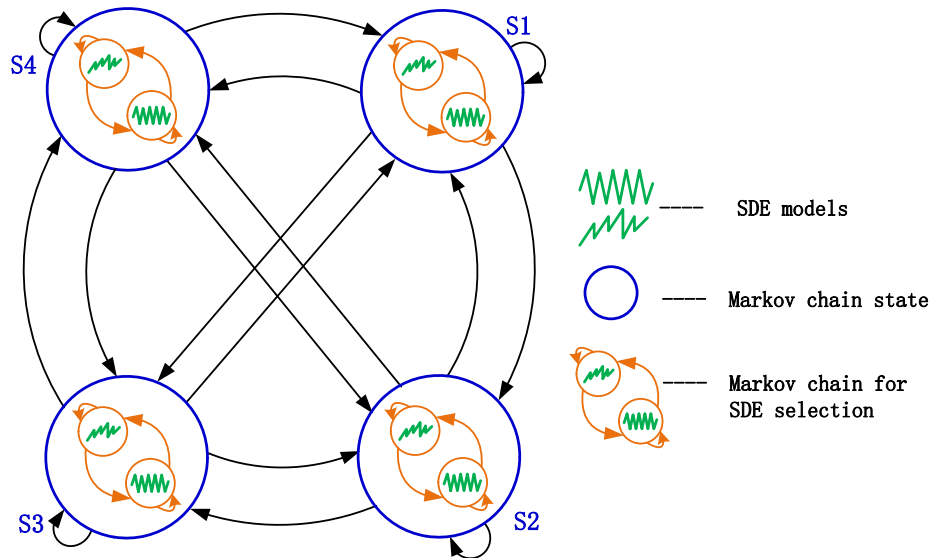


Figure 7.5: Wind speed generation model — 2-level Markov chain model embedded with SDE

- Pour différentes conditions de simulations telles que rafales ou conditions météorologiques extrêmes, d'autres SDEs peuvent être complétées. Pour ces raisons, ce modèle est facilement modifiable en fonction des besoins de l'utilisateur.

### 7.2.1.2 Chaîne de Markov intégrée avec SDE

#### La chaîne de Markov comme modèle macroscopique de vitesse du vent

Une chaîne de Markov est définie de façon unique par son espace d'état, sa matrice de transition et sa distribution initiale. La modélisation de la vitesse du vent en chaîne de Markov comprend quatre étapes principales : définition de l'état, estimation de la matrice de transition, simulation de l'état et simulation de la vitesse du vent. La définition de l'état est liée à un problème de classification et dépend de l'objectif. Il correspond au choix de l'intervalle sur la plage de vitesse du vent, qui peut dépendre de la fréquence d'occurrence des valeurs de vitesse. Soit  $S = [s_1, s_2, \dots, s_N]$  l'espace d'état de la chaîne de Markov externe correspondant aux différents états possibles de la vitesse du vent. Soit  $\{X_t\}_{t \geq 0}$  représente la série temporelle de la vitesse du vent. L'événement " $X_0 = s_5$ " signifie qu'au temps  $t = 0$ , la vitesse du vent est en état  $s_5$ . Le tableau 3.1 montre un exemple d'affectation d'état. La distribution initiale est estimée en divisant l'ensemble de données en cellules selon les états. Les vecteurs d'occurrences obtenus peuvent alors être normalisés dans chaque bin. Soit  $p_i^0 = \mathbb{P}\{X_0 = s_i\}$  indique la probabilité que le premier élément de la série temporelle du vent soit dans l'intervalle  $s_i$ . Pour l'estimer, comptez le nombre de fois qu'il y a une valeur appartenant à l'état  $s_i$  dans toute la série chronologique enregistrée et divisez-la par le nombre total de valeurs enregistrées.

Soit la probabilité de transition comme suit :

$$\begin{aligned} p_{ij} &= \mathbb{P}(X_{n+1} = s_j | X_n = s_i, X_{n-1} = s_{i_{n-1}}, \dots, X_0 = s_{i_0}) \\ &= \mathbb{P}(X_{n+1} = s_j | X_n = s_i) \end{aligned} \quad (7.3)$$

où  $s_i, s_j \in S$ . La probabilité  $p_{ij}$  peut être estimée en comptant le nombre de fois qu'une valeur dans l'état  $s_i$  suivi d'une fois dans l'état  $s_j$  dans la série temporelle du vent, normalisée par le nombre total d'occurrences des valeurs dans l'état  $s_i$ . La matrice de transition de la chaîne de Markov est définie comme suit :

$$\pi = \begin{bmatrix} p_{1,1} & p_{1,2} & \cdots & p_{1,n} \\ p_{2,1} & p_{2,2} & \cdots & p_{2,n} \\ \vdots & \vdots & \ddots & \vdots \\ p_{m,1} & p_{m,2} & \cdots & p_{m,n} \end{bmatrix}.$$

### SDEs for continuous short-term wind speed modeling

L'auteur de [10] conclut qu'en gros, il existe trois classes de distributions de turbulence de la vitesse du vent. L'analyse montre que 90 à 10 % de la turbulence de la vitesse du vent suit une sorte de fonction de distribution de probabilités monomodale symétrique (PDF) qui est bien ajustée par une PDF gaussienne. 9% de la turbulence de la vitesse du vent suit une sorte de PDF mono-modal dissymétrique qui peut être décrite par la série Gram-Charlier. Et le reste 1% suit une sorte de PDF bimodal qui est équipé d'un mélange de PDF gaussiens. Considérons les deux premières classes indiquées par [10] qui représentent 99% de toutes les distributions de turbulences. L'objectif est d'associer un SDE à chaque classe. Pour considérer que la dynamique de la vitesse du vent est influencée par un bruit gaussien, on considère un processus de diffusion qui est une équation différentielle stochastique particulière comme suit :

$$dZ(t) = a(Z(t), t) dt + b(Z(t), t) dW(t), \quad t \in [0, T] \quad (7.4)$$

où  $a(Z(t), t)$  et  $b(Z(t), t)$  sont les termes dérive et diffusion, respectivement.

$W(t)$  est le processus standard de Wiener défini comme suit :

- $W(0) = 0$ , avec probabilité 1.
- Pour  $0 \leq t_i < t_{i+1} \leq T$ , l'incrément  $\Delta W_i = W(t_{i+1}) - W(t_i)$  est une distribution gaussienne avec zéro moyenne et  $\sigma = t_{i+1} - t_i$ , soit,  $\Delta W_i \sim N(0, \sigma)$ .
- Pour  $0 \leq t_i < t_{i+1} < t_{i+1} < t_{i+2} \leq T$ , les incréments non chevauchants  $\Delta W_i = W(t_{i+1}) - W(t_i)$  et  $\Delta W_{i+1} = W(t_{i+2}) - W(t_{i+1})$  sont indépendants.

En d'autres termes, le processus de Wiener (ou mouvement brownien standard) est un processus continu dont les incréments sont normalement distribués. Un grand nombre de processus stochastiques définis par l'équation (7.4) sont disponibles.

Certains d'entre eux sont de bons candidats pour s'adapter aux données de vitesse du vent.

Combiné aux résultats de recherche de [10], un procédé de diffusion à inversion de moyenne semble être un candidat approprié. Pour de tels processus de diffusion, les fluctuations des enregistrements de dégradation d'une tendance générale à la dégradation sont auto-corrélées et l'espérance de  $Z(t)$  tend à dériver vers sa moyenne à long terme avec le temps. La propriété de retour à la moyenne fait en sorte que la volatilité n'est pas "explosive".

### 7.2.1.3 Processus d'OU pour la production d'énergie éolienne

Les processus OU sont utilisés pour modéliser les deux premières classes sur la turbulence de la vitesse du vent présentées par [10]. En d'autres termes, pour chaque classe de vitesse du vent à court terme, un processus OU est utilisé. Ce modèle permet de générer une vitesse de vent continue pendant une courte période, par exemple

#### Processus OU pour la classe 1

Pour l'équation (1.17), Soit  $\zeta = 0, a = -\alpha, b = \beta$ . Afin d'éviter toute confusion avec le cas général,  $Y(t)$  est utilisé au lieu de  $Z(t)$ . Le processus OU choisi pour décrire l'incrément de la séquence de vitesse du vent lorsque la turbulence est bien ajustée par PDF gaussien est le suivant :

$$dY(t) = aY(t)dt + b dW(t), t \in [0, T] \quad Y(0) = 0 \quad (7.5)$$

où  $a$  est une constante strictement négative pour tous les  $Y(t)$  et  $b$  est constante.  $Y(t)$  est la turbulence de la vitesse du vent au temps  $t$  et  $c$ 'est un processus de diffusion autocorrélé stationnaire.  $W(t)$  est un mouvement brownien standard.

Selon l'équation (1.18), l'approximation de la log-vraisemblance basée sur la probabilité de transition est définie comme suit :

$$\begin{aligned} \log L(\mathbf{a}, \mathbf{b}) &= \log \prod_{i=1}^N \mathbb{P}(Y(t_{i+1}), t_{i+1} | Y(t_i), t_i; \mathbf{a}, \mathbf{b}) \\ &= -\frac{n}{2} (\log(b^2) + \log(v(a))) + \frac{1}{2b^2v(a)} \sum_{i=0}^{n-1} (Y_{t_{i+1}} - \exp(a\Delta)Y_{t_i})^2 \end{aligned} \quad (7.6)$$

où  $\Delta = t_{i+1} - t_i, t_i = i\Delta, (i = 1, \dots, n)$  et  $v(a) = \frac{\exp(2a\Delta)-1}{2a}$ .

Par conséquent, les estimateurs de paramètres de  $a$  et  $b$  sont les suivants :

$$\hat{a} = \frac{1}{\Delta} \log\left(\frac{\sum_{i=1}^n Y_{t_{i-1}} Y_{t_i}}{\sum_{i=1}^n Y_{t_{i-1}}^2}\right) \quad (7.7)$$

$$\hat{b}^2 = \frac{1}{nv(\hat{a})} \sum_{i=1}^n (Y_{t_i} - \exp(\hat{a}\Delta)Y_{t_{i-1}})^2 \quad (7.8)$$

### Processus OU pour la classe 2

Pour la classe 2, la turbulence de la vitesse du vent se présente sous la forme d'un PDF mono-modal dissymétrique. Le processus OU choisi pour décrire la vitesse du vent est le suivant : un autre modèle de SDE proposé par Antoine

$$dY(t) = -(Y(t) - \mu)dt + \sigma dW(t), \quad ; Y(0) = 0 \quad (7.9)$$

où  $Y(t)$  est la vitesse du vent au temps  $t$ ,  $\mu$  et  $\sigma$  sont des paramètres constants et  $W(t)$  est le mouvement brownien standard. Avec  $\Delta t = t_i - t_{i-1}$  selon l'équation (1.18) et [97] la fonction densité est la suivante :

$$\begin{aligned} & \mathbb{P}(Y(t_i), t_i | Y(t_{i-1}), t_{i-1}; \boldsymbol{\mu}, \boldsymbol{\sigma}) \\ &= \frac{e^{\Delta t}}{\sqrt{\pi \cdot \sigma^2 (e^{2\Delta t} - 1)}} \exp\left(-\frac{(Y(t_i) \cdot e^{\Delta t} + \mu(1 - e^{\Delta t}) - Y(t_{i-1}))^2}{\sigma^2 (e^{2\Delta t} - 1)}\right) \end{aligned} \quad (7.10)$$

Ainsi, en minimisant numériquement la fonction de log-vraisemblance suivante, les valeurs estimées de  $\hat{\mu}$  et  $\hat{\sigma}$  peuvent être obtenues.

$$\log L(\boldsymbol{\mu}, \boldsymbol{\sigma}) = \log \prod_{i=1}^N \mathbb{P}(Y(t_i), t_i | Y(t_{i-1}), t_{i-1}; \boldsymbol{\mu}, \boldsymbol{\sigma}) \quad (7.11)$$

#### 7.2.1.4 Modèle de chaîne de Markov pour deux classes de vent de commutation

Afin de basculer aléatoirement entre les deux classes, une chaîne de Markov interne est considérée à l'intérieur de chaque état de la chaîne de Markov externe. Pour éviter toute confusion entre la chaîne de Markov externe et la chaîne de Markov interne, cette dernière est désignée ci-après comme un modèle de sélection SDE (SSM). Selon les statistiques fournies par [10] et avec respectivement 90% et 10% de turbulence de vitesse du vent pour les classes 1 et 2, la probabilité de transition indiquée dans le tableau 7.2 est attribuée au SSM.

class	$Class_1$	$Class_2$
$Class_1$	0.9	0.1
$Class_2$	0.9	0.1

Table 7.2: Probabilité de transition pour SSM

## 7.2.2 Procédure de génération de la vitesse du vent

Il y a deux difficultés à estimer la matrice de probabilité de transition du modèle de la chaîne de Markov à partir des données sur la vitesse réelle du vent :

- Markov chaîne avec beaucoup d'états pourrait être construite résultant en une matrice de transition énorme qui pourrait causer des difficultés supplémentaires dans l'estimation ;
- Le nombre d'éléments dans certains états pourrait être beaucoup plus faible que dans d'autres, ce qui donnerait un grand nombre de probabilités proches de 0 dans la matrice des probabilités de transition.

Afin d'éviter les phénomènes ci-dessus, le nombre d'États devrait être déterminé relativement plus petit. Elle pourrait être déterminée par les utilisateurs ou en fonction d'un critère. Les auteurs de [127] recommandent de déterminer l'intervalle avec les quantiles empiriques. Supposons que la série chronologique de la vitesse du vent soit stationnaire et ergodique. Par conséquent, la fonction de distribution cumulative empirique est un estimateur cohérent de la distribution cumulative de la mesure invariante de cette série chronologique. Les limites sont prises pour être  $\hat{F}_N^{-1}(j/k)$ ,  $j = 1, 2, \dots, k$ , où  $k \in N$  est le nombre d'états,  $N$  est le nombre d'états de la chaîne Markov externe, et  $\hat{F}_N$  est la fonction de distribution cumulative empirique.

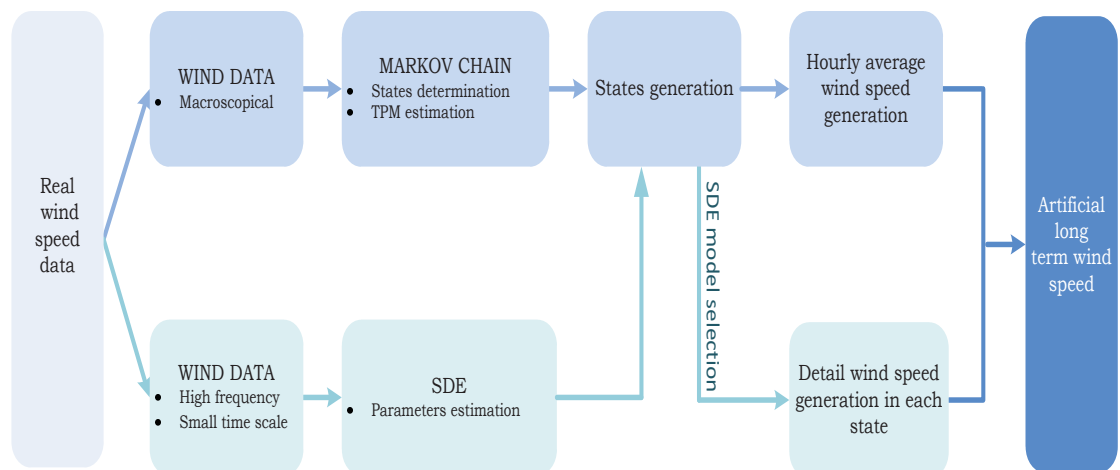


Figure 7.6: Étapes pour la génération de la vitesse du vent

Les principales étapes de production de données artificielles sur la vitesse du vent (illustrées à la figure 7.6) sont les suivantes :

- step 1 Choisir les données de vitesse du vent pour l'estimation de la chaîne de Markov et des SDEs séparément
- step 2
- Déterminer les états de la chaîne de Markov externe
  - Estimer la matrice de probabilité de transition de la chaîne de Markov à partir des données de vitesse du vent réel
  - Estimer les paramètres des SDE à partir des données de vitesse du vent réel
- step 3 Générer la vitesse moyenne horaire du vent
- step 4 Utilisez SSM pour sélectionner SDE et générer des données continues de vitesse du vent par rapport à l'état de la chaîne de Markov externe. Si l'état extérieur n'est pas le dernier, revenir à l'étape 3, sinon, terminer.

## 7.3 Estimation de la durée de vie utile résiduelle

Selon les recherches effectuées par A.R. Nejad et al. [25], l'éolienne résiste à différentes charges associées à la vitesse du vent. En fait, des charges plus élevées génèrent généralement des vibrations plus élevées pour le groupe motopropulseur de l'éolienne. Les vibrations excessives sont une cause connue de détérioration des composants en rotation. De plus, les vibrations peuvent être transmises à d'autres composants par l'intermédiaire de la structure de connexion, ce qui a pour effet de détériorer l'état de fonctionnement des autres composants en cas de vibrations trop importantes. Il mentionne également qu'en saison venteuse, les systèmes à poix ont un taux d'échec plus élevé dans [24]. Par conséquent, ce que l'on peut conclure est énuméré comme suit :

- (1) L'environnement opérationnel de l'éolienne change de façon aléatoire.
- (2) L'environnement opérationnel de l'élément a une incidence sur l'état de santé de l'éolienne et la détérioration de celle-ci.
- (3) Le taux de détérioration varie selon les environnements opérationnels.

### 7.3.1 Simplification et description du modèle pour le système en détérioration

Afin de simplifier le problème d'ingénierie réel et de proposer des modèles mathématiques, faire les hypothèses suivantes :

- (1) Article L'environnement opérationnel peut être classé en fonction d'un paramètre et peut être classé dans un nombre fini d'états opérationnels différents. Par exemple, l'environnement opérationnel d'une éolienne peut être classé en fonction de la vitesse du vent ; l'environnement opérationnel des véhicules peut être classé en fonction de la vitesse de rotation du moteur.

- (2) Le passage à l'état d'environnement opérationnel suivant dépend uniquement de l'état actuel de l'environnement opérationnel.
- (3) Supposons que seul l'environnement opérationnel influe sur la détérioration. Il est vrai qu'un système dynamique se dégrade plus sévèrement dans les environnements opérationnels difficiles que dans les environnements opérationnels stables. Par conséquent, le taux de détérioration est corrélé à l'environnement opérationnel. Par conséquent, la détérioration du système peut être considérée comme un processus stochastique dont les paramètres sont constants par morceaux.
- (4) L'indicateur de détérioration est l'information provenant du système de surveillance.

### Modèle pour les états de l'environnement opérationnel

Les chaînes de Markov décrivent généralement les mouvements d'un système entre différents états [132], une chaîne de Markov à temps discret est très appropriée pour la modélisation de l'environnement opérationnel considérée dans ce chapitre. A chaque étape, l'environnement opérationnel peut soit rester dans l'état où il se trouve, soit passer à un autre état d'environnement opérationnel.

Soit  $E = \{e_1, e_2, \dots, e_n\}$  l'ensemble des états d'environnement opérationnel. Définissez  $P = [p_{ij}] ; (1 \leq i \leq n, 1 \leq j \leq n)$  comme matrice de transition, c'est-à-dire,  $p_{ij}$  est la probabilité de passer de l'état opérationnel actuel  $e_i$  au suivant  $e_j$ . Les variables aléatoires de la séquence  $(OE_n)$  prennent des valeurs en  $E$ .

$(OE_n)_{0 \leq n \leq N}$  est une chaîne de Markov spatiale d'état discrète à temps discret si et seulement si,

- $\mathbb{P}(OE_0 = e_{i_0}) = \lambda_{i_0}$
- $\mathbb{P}(OE_{n+1} = e_{i_{n+1}} \mid OE_0 = e_{i_0}, \dots, OE_n = e_{i_n}) = \mathbb{P}(OE_{n+1} = e_{i_{n+1}} \mid OE_n = e_{i_n}) = p_{i_n i_{n+1}}$

Où  $\lambda_{i_0}, i_0 \in \mathbb{N}^+$  est la distribution initiale de l'état initial  $e_{i_0}$ .

### Modèle pour l'indicateur de détérioration dans divers états d'environnement opérationnel.

Soit  $\{D(t); t \geq 0\}$  un processus stochastique continu, monotone et croissant qui représente le processus de détérioration d'un système dynamique. Si la détérioration augmente

$$\Delta D_{(t, \delta_t)} = D(t + \delta_t) - D(t) \quad (t > 0, \delta_t > 0)$$

dépend seulement du présent et non du passé, le processus est markovien. En particulier,  $\Delta D_{(t, \delta_t)}$  dépend de l'heure actuelle  $t$  et de  $\delta_t$ , un modèle généralement accepté pour la modélisation de la dégradation est le processus gamma non homogène.

En d'autres termes, le processus gamma non-homogène est un processus stochastique dont l'incrément est indépendant, non négatif et suivant une distribution gamma, il convient de modéliser la détérioration monotone progressive s'accumulant dans le temps, telle que fatigue, usure, corrosion, formation de fissures, etc.

Rappeler les propriétés d'un processus gamma non homogène  $D(t)_{t \geq 0}$  comme suit.

- $D(0) = 0$  avec probabilité 1.
- $D(t)$  a des incréments indépendants.
- $\Delta D_{(t, \delta_t)} = D(t + \delta_t) - D(t)$ , pour tous les  $\delta_t > 0, t \geq 0$ , suit une distribution Gamma avec le paramètre forme  $\alpha_{(t, \delta_t)} = a(t + \delta_t) - a(t)$  et la paramètre échelle  $\beta > 0$  donné par

$$f_{\Delta D_{t, \delta_t}}(x | \alpha_{(t, \delta_t)}, \beta) = \frac{\left(\frac{x}{\beta}\right)^{\alpha_{(t, \delta_t)} - 1}}{\beta \Gamma(\alpha_{(t, \delta_t)})} e^{-\frac{x}{\beta}} \quad (7.12)$$

où,  $\Gamma(a) = \int_{z=0}^{\infty} z^{a-1} e^{-z} dz$  est la fonction gamma.

Pour modéliser différents taux de détérioration en fonction des différents environnements opérationnels, la détérioration du système peut être considérée comme un processus gamma dont les paramètres sont constants par morceaux et liés aux environnements opérationnels, comme le tableau 7.3.

Table 7.3: Paramètres du procédé gamma qui sont constants par morceaux et en relation avec les environnements opérationnels

Environnement opérationnel	$e_1$	$e_2$	$\dots$	$e_i$	$\dots$	$e_n$
Paramètres du procédé gamma	$\alpha_1, \beta_1$	$\alpha_2, \beta_2$	$\dots$	$\alpha_i, \beta_i$	$\dots$	$\alpha_n, \beta_n$

### 7.3.2 Prédiction de la durée de vie utile restante

La valeur de détérioration  $D(t + \tau)$  au temps  $t + \tau$  est la somme de la valeur de détérioration connue  $D(t)$  au temps  $t$  et de l'incrément de détérioration  $\Delta D_{(t, \tau)}$  entre temps  $t$  et  $\tau$  :

$$\Delta D(t + \tau) = D(t) + \Delta D_{(t, \tau)}$$

Apparemment, connaître la valeur de détérioration  $D(t + \tau)$  au temps  $t + \tau$  est le principal problème à résoudre pour la prédiction RUL (voir équation (1.8)). Puisque la valeur de détérioration  $D(t)$  est connue, estimer l'incrément de détérioration entre temps  $t$  et  $t + \tau$  est la solution. Compte tenu des incertitudes, il aborde la question de la distribution de probabilité de l'incrément  $\Delta D_{(t, \tau)}$ , illustrée à la Figure ??.

Le calcul d'environ  $D(t + \tau)$  concerne l'échelle de temps, c'est-à-dire la longueur de  $\tau$ . Un intérêt d'estimation RUL se concentre sur l'influence causée par la condition

actuelle pour le futur proche. Un autre se concentre sur un  $\tau$  suffisamment long pour que l'influence actuelle puisse être négligée. Par conséquent, deux méthodes de calcul différentes sont mises au point pour l'estimation du RUL ci-après.

### 7.3.2.1 Cas1 : Estimation RUL pour une étiquette assez longue $\tau$

Si le  $\tau$  est assez long, l'éolienne subit tout l'environnement opérationnel pendant le  $\tau$ . Pour dire simplement, si une chaîne de Markov peut se manifester dans la matrice de transition, elle est ergodique.

Pour une telle chaîne de Markov, il existe une distribution stable unique  $\pi = \{\pi_1, \pi_2, \dots, \pi_n\}$  ( $n$  est le nombre d'états) qui est indépendante de l'état initial, et satisfait

$$\pi^\infty P = \pi^\infty \quad \sum \pi_i^\infty = 1.$$

Dans ce cas, l'estimation du RUL est basée sur la valeur moyenne attendue de la détérioration sur une longue période. Comme  $\tau$  est assez long, il peut inclure tous les états de l'environnement opérationnel. Ainsi, selon la distribution stationnaire, on peut estimer un temps de séjour moyen dans chaque état de l'environnement opérationnel. De plus, il est possible d'estimer un incrément de détérioration moyen  $\mathbb{E}(\Delta D_{i(t,\tau)})$  dans chaque état d'environnement opérationnel  $e_i$ . Par conséquent, l'incrément de détérioration du système dynamique entre le temps  $t$  et  $\tau$  est le suivant

$$\mathbb{E}(\Delta D_{(t,\tau)}) \approx \sum_i \mathbb{E}(\Delta D_{i(t,\tau_i)}) \quad (\sum \tau_i = \tau) \quad (7.13)$$

où,  $\mathbb{E}(\Delta D_{i(t,\tau_i)})$  est l'incrément moyen de détérioration de l'état d'environnement opérationnel  $e_i$  entre temps  $t$  et  $\tau$ .

Indiquez  $\pi_i$  comme la proportion du temps passé dans l'environnement opérationnel indique  $e_i$ . De  $e_i$ , l'environnement opérationnel passe à l'état  $e_j$  avec la probabilité  $p_{ij}$ .

$$\pi_j = \sum_i \pi_i p_{ij} \quad (7.14)$$

Évidemment, il est vrai que

$$\sum_j \pi_j = 1 \quad (7.15)$$

Le temps moyen passé par  $\bar{\tau}_i$  dépensé dans l'état  $e_i$  sur la durée  $\tau$  est

$$\bar{\tau}_i = \pi_i \times \tau \quad (7.16)$$

La distribution de l'incrément de détérioration accumulé dans l'état  $e_i$  entre  $t$  et  $t + \tau$  est la suivante

$$\Delta D_{i(t,\tau)} \sim \Gamma(\alpha_{e_i}(\bar{\tau}_i), \beta_{e_i}) \quad (7.17)$$

Par conséquent, l'espérance asymptotique de l'incrément de détérioration de l'état

$e_i$  entre  $t$  et  $t + \tau$  est la suivante

$$\mathbb{E}(\Delta D_{i(t,\tau)}) = \alpha_{e_i} \times \bar{\tau}_i \quad (7.18)$$

Du point de vue de la prédiction, le PDF/CDF de l'incrément de détérioration  $\Delta D_{(t,\tau)}$  au temps  $t + \tau$  est également intéressant. Selon la propriété additive du processus gamma, il est simple d'obtenir la distribution de probabilité de l'incrément de détérioration moyen  $\Delta \bar{D}_{(t,\tau)}$  pour un système dynamique. Représente  $\bar{\alpha}$  comme paramètre de forme moyenne du procédé gamma avec formule

$$\bar{\alpha} = \sum_i \alpha_{e_i}(\bar{\tau}_i) \quad (7.19)$$

En conséquence, pour  $\tau \rightarrow \infty$ , let  $\beta = \beta_{e_i}$ , le pdf de  $\Delta \bar{D}_{(t,\tau)}$  et le rapprochement du RUL CDF sont comme suit,

$$\Delta \bar{D}_{(t,\tau)} \sim \Gamma(\bar{\alpha}(\tau), \beta) \quad (7.20)$$

$$F_{RUL(t)}(\tau) \simeq \frac{\Gamma(\bar{\alpha}(\tau), (L - D(t))\beta)}{\Gamma(\bar{\alpha}(\tau))} \quad (7.21)$$

où,  $\Gamma(m, n) = \int_{z=n}^{\infty} z^{m-1} e^{-z} dz$  est la fonction gamma incomplète.

### 7.3.2.2 Cas 2 : Estimation RUL tenant compte de l'état actuel de l'environnement opérationnel

Dans ce cas, l'estimation RUL dépend étroitement du dernier état de l'environnement opérationnel et de l'échelle de temps de prévision. Dans cette section, la prédiction en une seule étape est donnée au début, et à la fin, une méthode générale de prédiction en N étapes sera présentée.

Tout d'abord, donnez les illustrations comme suit :

- l'échelle de temps d'une étape est de la même longueur que  $l$ . Pour simplifier la notation,  $t + 1, t + 2, \dots, t + N$  représente un pas, tow-step,  $\dots$ , N-step forward from time  $t$ , respectivement.
- entre temps  $t - 1$  et  $t$ , l'état de fonctionnement est indiqué par  $e_i$ .

**Prédiction RUL d'un pas en avant** En supposant que l'heure actuelle est  $t$ ,

$$\begin{aligned} & \mathbb{P}(D(t+1) < d | D(t) = d_t, \text{OE}_t = e_{i_t}) \\ &= \mathbb{P}(\Delta D_{(t,1)} < d - d_t | D(t) = d_t, \text{OE}_t = e_{i_t}) \\ &= \sum_{i_{t+1}=1}^n \mathbb{P}(\Delta D_{(t,1)} < d - d_t | \text{OE}_t = e_{i_t}) \mathbb{P}(\text{OE}_{t+1} = e_{i_{t+1}}) \\ &= \sum_{i_{t+1}=1}^n p_{i_t i_{t+1}} \int_0^{d-d_t} f_{\alpha_{i_{t+1}}, \beta}(x) dx \end{aligned} \quad (7.22)$$

où,  $f_{\alpha_{i_{t+1}},\beta}(x)$  est le PDF d'une distribution gamma avec le paramètre de forme  $\alpha_{i_{t+1}}$  et le paramètre d'échelle  $\beta$ ,  $n$  est le nombre total des états des environnements opérationnels.

### 7.3.2.3 Prédiction RUL en deux étapes

$$\begin{aligned}
& \mathbb{P}(D(t+2) < d | D_t = d_t, \text{OE}_t = e_{i_t}) & (7.23) \\
& = \mathbb{P}(\Delta D_{(t,1)} + \Delta D_{(t+1,2)} < d - d_t | \text{OE}_t = e_{i_t}) \\
& = \int_0^{d-d_t} \mathbb{P}(\Delta D_{(t,1)} + \Delta D_{(t+1,2)} < d - d_t | \text{OE}_{t+1} = e_{i_{t+1}}, \text{OE}_t = e_{i_t}, \Delta D_{(t,1)} = x) f_{\Delta D_{(t,1)}}(x) dx \\
& \quad \times \mathbb{P}(\text{OE}_{t+1} | \text{OE}_t) \\
& = \int_0^{d-d_t} \sum_{i_{t+1}=1}^n \mathbb{P}(\Delta D_{(t+1,2)} < d - d_t - x | \Delta D_{(t,1)} = x, \text{OE}_t = e_{i_t}) p_{i_t i_{t+1}} f_{\Delta D_{(t,1)}}(x) dx \\
& = \int_0^{d-d_t} \mathbb{P}(\Delta D_{(t+1,2)} < d - d_t - x) \sum_{i_{t+1}=1}^n p_{i_t i_{t+1}} f_{\Delta D_{(t,1)}}(x) dx \\
& = \sum_{i_{t+1}=1}^n \sum_{i_{t+2}=1}^n p_{i_t i_{t+1}} p_{i_{t+1} i_{t+2}} \int_0^{d-d_t} F_{\alpha_{i_{t+2}},\beta}(d - d_t - x) f_{\Delta D_{(t,1)}}(x) dx
\end{aligned}$$

où,  $n$  est le nombre total d'états de l'environnement opérationnel.  $F_{\alpha_{i_{t+2}},\beta}$  est le CDF d'une distribution gamma avec le paramètre de forme  $\alpha_{i_{t+2}}$  et le paramètre d'échelle  $\beta$ .  $f_{\Delta D_{(t,1)}}$  est le PDF d'une distribution gamma avec le paramètre de forme  $\alpha_{i_{t+1}}$  et le paramètre d'échelle  $\beta$ .

### Approximation de la prédiction RUL à N pas en avant par matrices de calcul.

$$\begin{aligned}
& \mathbb{P}(D(t+N) < d | D_t = d_t, \text{OE}_t = e_{i_t}) & (7.24) \\
& = \mathbb{P}(\Delta D_{(t,1)} + \Delta D_{(t+1,2)} + \dots + \Delta D_{(t+(N-1),N)} < d - d_t | \text{OE}_t = e_{i_t})
\end{aligned}$$

L'équation (7.24) est difficile à calculer alors que  $N$  devient grand. Si les incréments indépendants de détérioration suivent les distributions gamma avec le même paramètre d'échelle  $\beta$  mais des paramètres de forme différents, la somme de l'incrément suit une distribution gamma avec un paramètre de forme qui est la somme des différents paramètres de forme et du paramètre d'échelle, soit

$$\sum_{m=1}^N \Delta X_m \sim \Gamma\left(\sum_{m=1}^N \alpha_m, \beta\right)$$

Cette propriété est très pratique pour le calcul. Pour une prédiction RUL à  $N$  pas en avant, considérant que l'incrément de détérioration de chaque pas est indépendant l'un de l'autre, la prédiction RUL à  $N$  pas en avant peut être exprimée comme suit :

$$\begin{aligned} & \mathbb{P}(D(t+N) < d | D_t = d_t, \text{OE}_t = e_{i_t}) \\ &= \int_0^{d-d_t} f_{\alpha_s, \beta}(x) dx \end{aligned} \quad (7.25)$$

où,

$$\alpha_s = (0 \cdots 1 \cdots 0)_{1 \times n} \left( \sum_{m=1}^N P^m \right) A \mathbb{I}_{n \times 1} \quad (7.26)$$

$f_{\alpha_s, \beta}$  est le PDF d'une distribution gamma avec le paramètre de forme  $\alpha_s$  et le paramètre d'échelle  $\beta$ ;  $N$  est l'étape de prédiction;  $(0 \cdots 1 \cdots 0)_{1 \times n}$  représente l'état initial du fonctionnement;  $P$  est la matrice de transition de probabilité de l'environnement opérationnel;  $A$  est une matrice diagonale de  $\alpha$  pour différents environnements opérationnels, et  $\mathbb{I}_{n \times 1}$  avec la valeur 1.

## 7.4 Modèle d'indisponibilité pour éolienne

Comme mentionné précédemment, l'éolienne fonctionne automatiquement dans divers environnements, il est important de trouver une méthode pour mesurer sa fiabilité. De plus, la connaissance de ses informations de fiabilité est utile pour la planification de la maintenance qui joue un rôle important dans l'exploitation du parc éolien et la production d'énergie. Compte tenu de l'environnement opérationnel de l'éolienne et du délai d'exécution des travaux de maintenance, il est nécessaire de trouver un seuil d'alarme de détérioration pour les éoliennes afin de programmer correctement les travaux de maintenance. Ce chapitre se concentre sur l'étude de l'indisponibilité des éoliennes. Une méthode pour proposer le seuil d'alarme dépend de la politique de maintenance et l'estimation de l'indisponibilité de l'éolienne causée par les pannes et la maintenance est également étudiée dans cette section.

### 7.4.1 Simplifications, hypothèses et politique de maintenance

#### 7.4.1.1 Simplification de l'environnement opérationnel

La vitesse moyenne du vent pour l'entretien est inférieure à 11 m/s. Et l'environnement opérationnel est considéré comme une chaîne de Markov discrète. Par conséquent, pour simplifier la question traitée dans ce chapitre, classez l'environnement opérationnel  $E$  en deux sous-ensembles : un sous-ensemble  $\overline{E}_M$  dans lequel la vitesse moyenne du vent est inférieure à 11 m/s, un autre  $\overline{\overline{E}}_M$  dans lequel la vitesse moyenne du vent est supérieure à 11 m/s. Indiquez-les par  $E_M = \{e_1, ; e_2, e_3, e_4\}$ ,  $\overline{\overline{E}}_M = \{e_5, ; e_6, e_7, e_8\}$ , respectivement.

#### 7.4.1.1.a Maintenance policy

Nous considérons l'éolienne comme un système réparable, et l'action de maintenance proposée est conforme au schéma suivant :

- Si l'indicateur de détérioration  $D_t$  est supérieur au seuil de défaillance  $L_F$ , le système échoue. Le moment où l'indicateur de détérioration arrive ou traverse  $L_F$  est donné par  $\sigma_F$ .

$$\sigma_F = \inf(t | D_t \geq L_F) \quad (7.27)$$

- Lorsque l'indicateur de détérioration  $D_t$  devient supérieur ou égal au seuil d'alarme  $L_A$ , un entretien est prévu. Le moment où  $D(t)$  arrive ou traverse  $L_A$  est donné par  $\sigma_A$ .

$$\sigma_A = \inf(t | D_t \geq L_A) \quad (7.28)$$

- Seuls les environnements opérationnels  $e_1, ; e_2, e_3, ; e_4$  permettent de mettre en œuvre la maintenance. Ainsi, l'opération de maintenance a un temps de retard radôme  $\tau$  lorsque l'environnement opérationnel appartient à  $\overline{E_M}$ .
- Nous supposons que l'entretien peut être effectué immédiatement lorsque l'environnement le permet. L'opération de maintenance a une durée  $\rho$ .
- Entre  $\sigma_A$  et  $\sigma_A + \tau$ , l'éolienne se détériore et une panne peut apparaître avant la maintenance. En fonction de l'apparition d'une panne, une action de maintenance préventive ou corrective doit être effectuée.
  - Si une panne survient dans l'intervalle de temps, à savoir,  $\sigma_F \leq \sigma_A + \tau$ , l'éolienne est indisponible du moment de la panne jusqu'au moment de la fin de l'opération de maintenance  $\sigma_A + \tau + \rho$
  - Si une panne ne survient pas dans l'intervalle de temps, à savoir,  $\sigma_A + \tau$ , l'éolienne est indisponible à partir du moment où  $\sigma_A + \tau$  est indisponible jusqu'à la fin de l'opération de maintenance  $\sigma_A + \tau + \rho$ .
- A la fin de l'entretien, l'éolienne est supposée être " comme neuve " (as-good-as new).

#### 7.4.1.2 Hypothèse stationnaire

Selon l'hypothèse d'environnement opérationnel à deux sous-ensembles ci-dessus et le schéma de maintenance, à long terme, le processus de détérioration de l'éolienne peut être considéré comme un processus régénératif. En d'autres termes, l'éolienne est mise en service et fonctionne au temps  $T_0$ . Lorsqu'il échoue, au moment  $T_1$ , il sera restauré à l'état "comme neuf". Lorsque l'éolienne tombe de nouveau en panne au moment  $T_1 + T_2$ , elle est de nouveau restaurée, et ainsi de suite. Les temps restaurés  $T_1, T_2, \dots$  sont indépendants les uns des autres. Pour simplifier, l'indisponibilité est considérée dans un cycle de vie, par exemple, le cycle de vie de temps en temps  $T_0$  à temps  $T_1$ . Le modèle d'indisponibilité asymptotique des

éoliennes est basé sur la distribution stationnaire des états de l'environnement opérationnel.

### 7.4.2 Modèle d'indisponibilité asymptotique pour les éoliennes

L'indisponibilité d'une éolienne a deux significations : l'une est l'indisponibilité causée par une détérioration ou une panne entraînant un temps d'arrêt ; l'autre signifie que l'éolienne est en état d'arrêt, qui n'est causée que par une vitesse de vent inappropriée, par exemple, un vent à basse vitesse ne peut entraîner l'éolienne au travail. Ce chapitre ne s'intéresse qu'à l'indisponibilité causée par les détériorations et les pannes. Indiquez  $T_1 = \sigma_A + \tau + \rho$  comme premier temps de renouvellement (première réparation). Soit  $U_\infty$  l'indisponibilité asymptotique de l'éolienne,  $U(t)$  la durée d'indisponibilité avant temps  $t$ . Nous avons  $U_\infty$ ,  $U(t)$  respectivement comme suit,

$$U_\infty = \frac{\mathbb{E}(U(T_1))}{\mathbb{E}(T_1)} \quad (7.29)$$

$$U(t) = \begin{cases} 0 & (t \in [T_0, \sigma_A)) \\ \rho & (t \in [\sigma_A, T_1] \text{ and } \sigma_F \geq \sigma_A + \tau) \\ (\sigma_A + \tau + \rho) - \sigma_F & (t \in [\sigma_A, T_1] \text{ and } \sigma_F < \sigma_A + \tau) \end{cases} \quad (7.30)$$

Ainsi, pour le premier cycle de vie, la durée d'indisponibilité  $U(T_1)$  de l'éolienne est

$$U(T_1) = \rho \mathbb{I}_{\{\sigma_F \geq \sigma_A + \tau\}} + ((\sigma_A + \tau + \rho) - \sigma_F) \mathbb{I}_{\{\sigma_F \leq \sigma_A + \tau\}} \quad (7.31)$$

où,  $\mathbb{I}_{\{A\}} = 1$  si  $A$  est vrai et 0 sinon.

L'éolienne peut être considérée comme le système à long terme, compte tenu de sa performance moyenne, nous avons

$$\begin{aligned} U_\infty &= \frac{\mathbb{E}(\rho \mathbb{I}_{\{\sigma_F \geq \sigma_A + \tau\}}) + ((\sigma_A + \tau + \rho) - \sigma_F) \mathbb{I}_{\{\sigma_F \leq \sigma_A + \tau\}}}{\mathbb{E}(\sigma_A + \tau + \rho)} \\ &= \frac{\mathbb{E}(\rho) + \mathbb{E}(\tau \mathbb{I}_{\{\sigma_F - \sigma_A > \tau\}}) + \mathbb{E}((\sigma_F - \sigma_A) \mathbb{I}_{\{\sigma_F - \sigma_A \leq \tau\}})}{\mathbb{E}(\sigma_A) + \mathbb{E}(\tau) + \mathbb{E}(\rho)} \end{aligned} \quad (7.32)$$

Par conséquent, le modèle d'indisponibilité est,

$$U_\infty = \frac{\rho + \mathbb{E}(\tau \mathbb{I}_{\{\sigma_F - \sigma_A > \tau\}}) + \mathbb{E}((\sigma_F - \sigma_A) \mathbb{I}_{\{\sigma_F - \sigma_A \leq \tau\}})}{\mathbb{E}(\sigma_A) + \mathbb{E}(\tau) + \rho} \quad (7.33)$$

### 7.4.3 Temps d'activation dans le seuil d'alarme $\mathbb{E}(\sigma_A)$

Ce terme peut être facilement obtenu à partir du modèle de détérioration proposé au chapitre 4.

$$\mathbb{E}(\sigma_A) = \int_0^\infty \left( \sum_{i=1}^8 \mathbb{P}(\text{OE}_i = e_i) \int_0^{L_A} f_{\alpha_i t, \beta}(x) dx \right) dt \quad (7.34)$$

Où,  $f_{\alpha_i t, \beta}$  est une fonction gamma pdf, avec le paramètre de forme  $\alpha_i t$  et le paramètre de gamme  $\beta$ .

### 7.4.4 Maintenance attente $\mathbb{E}(\tau)$

Pour une chaîne Markov discrète, l'attente de maintenance  $\tau$  est en fait le temps de séjour passé dans l'environnement opérationnel  $\overline{E_M}$ , ou le premier temps de frappe dans  $E_M$  depuis un état  $\overline{E_M}$ . Soit  $T$  le temps de frappe dans un état d'environnement opérationnel du sous-ensemble  $E_M$ , lorsque l'état d'environnement opérationnel est initialement dans un état  $\overline{E_M}$ . Nous l'avons fait,

$$T = \inf\{k > \lceil \frac{\sigma_A}{\delta t} \rceil; \text{OE}_k = e_i, e_i \in E_M\} \quad (7.35)$$

La seule hypothèse est que le sous-ensemble  $\overline{E_M}$  doit être transitoire à tout moment  $t \geq \sigma_A$ . Le sous-ensemble  $E_M$  sera considéré comme la classe de terminal. Maintenant, nous allons donner l'expression explicite de l'attente de retard de maintenance  $\mathbb{E}(\tau)$ . La matrice de transition  $P$  de la chaîne de Markov représentant l'environnement opérationnel est divisée comme suit :

$$P = \begin{bmatrix} \mathbf{p}^{\overline{E_M}} & \mathbf{p}^{\overline{E_M}E_M} \\ \mathbf{p}^{E_M\overline{E_M}} & \mathbf{p}^{E_M} \end{bmatrix}$$

Où,  $\mathbf{p}^{\overline{E_M}}$  est la probabilité que l'environnement opérationnel reste dans le sous-ensemble  $\overline{E_M}$  lui-même ;  $\mathbf{p}^{\overline{E_M}E_M}$  est la probabilité du sous-ensemble  $\overline{E_M}$  à  $E_M$ ;  $\mathbf{p}^{E_M\overline{E_M}}$  est la probabilité du sous-ensemble  $E_M$  à  $\overline{E_M}$ , et  $\mathbf{p}^{E_M}$  est la probabilité restant dans  $E_M$  lui-même.

Définir une autre chaîne de Markov  $Y$  dont l'espace d'états est  $E_Y = \overline{E_M} \cup E_{M_\Delta}$ , où  $E_{M_\Delta}$  contient les états de  $E_M$  qui sont directement atteints par un état opérationnel de  $\overline{E_M}$ , à savoir  $E_{M_\Delta} \subset E_M$ . La matrice de transition de la chaîne de Markov  $Y$  est donnée par

$$\mathbf{Q} = \begin{bmatrix} \mathbf{p}^{\overline{E_M}} & \mathbf{p}^{\overline{E_M}E_{M_\Delta}} \\ \mathbf{0} & \mathbf{I} \end{bmatrix} \quad (7.36)$$

Par conséquent, le temps de frappe en  $E_M$  de l'environnement opérationnel original de la chaîne de Markov est le même que le temps de frappe en  $E_{M_\Delta}$  de la chaîne de Markov  $Y$ , en faisant cela, le calcul est plus facile. Selon la recherche effectuée

par A. Platis et al. [139], la distribution du temps de frappe dans le sous-ensemble  $E_M$  au temps  $k$  est de

$$\mathbb{P}(T > k) = \mathbb{P}(\forall i, i \leq n, OE_i \in \overline{E_M}) = \alpha_{\overline{E_M}}(\mathbf{p}^{\overline{E_M}})^{k-1} \mathbf{1}_d \quad (7.37)$$

Où,  $\alpha_{\overline{E_M}}$  est la distribution initiale. Et le temps de frappe attendu est donné par

$$\begin{aligned} \mathbb{E}(T) &= \sum_{k \geq 0} k \times \mathbb{P}(T = k) = \sum_{k \geq 0} \mathbb{P}(T > k) \\ &= \alpha_{\overline{E_M}}(\mathbf{I} + \sum_{k \geq 1} (\mathbf{p}^{\overline{E_M}})^{k-1}) \mathbf{1}_d \end{aligned} \quad (7.38)$$

Par conséquent, l'attente de maintenance attendu  $\mathbb{E}(\tau)$  est le suivant

$$\begin{aligned} \mathbb{E}(\tau) & \\ &= \mathbb{E}(\tau | OE_{\sigma_A} \in \overline{E_M}) \mathbb{P}(OE_{\sigma_A} \in \overline{E_M}) + \mathbb{E}(\tau | OE_{\sigma_A} \in E_M) \mathbb{P}(OE_{\sigma_A} \in E_M) \\ &= \alpha_{\overline{E_M}}(\mathbf{I} + \sum_{k \geq 1} (\mathbf{p}^{\overline{E_M}})^{k-1}) \mathbf{1}_d \left( \sum_{i=5}^8 \mathbb{P}(e_i \in \overline{E_M}) \right) \end{aligned} \quad (7.39)$$

### 7.4.5 Temps indisponible dû à un entretien ou à une panne

$$\begin{aligned} &\mathbb{E}(\tau \mathbb{I}_{\{\sigma_F - \sigma_A > \tau\}}) + (\sigma_F - \sigma_A) \mathbb{I}_{\{\sigma_F - \sigma_A \leq \tau\}} \\ &= \mathbb{E}(\tau \mathbb{I}_{\{\sigma_F - \sigma_A > \tau\}}) + \mathbb{E}((\sigma_F - \sigma_A) \mathbb{I}_{\{\sigma_F - \sigma_A \leq \tau\}}) \end{aligned} \quad (7.40)$$

Remplacer  $\sigma_{F-A}$  par  $\sigma_{F-\mathbb{E}(D_{\sigma_A})}$ , et notez la durée  $\sigma_F - \sigma_A$  comme  $t_{AL}$ , Premièrement, regardez l'expression  $\mathbb{E}((\sigma_F - \sigma_A) \mathbb{I}_{\{\sigma_F - \sigma_A \leq \tau\}})$

$$\begin{aligned} &\mathbb{E}((\sigma_F - \sigma_A) \mathbb{I}_{\{\sigma_F - \sigma_A \leq \tau\}}) \\ &= \mathbb{E}(\sigma_F - \sigma_A) \\ &\approx \mathbb{E}(\sigma_{F-\mathbb{E}(D_{\sigma_A})}) \\ &= \int_0^{+\infty} \sum_{i=1}^8 \mathbb{P}(OE_i = e_i) f_{\alpha_i t, \beta}(L_F - \mathbb{E}(D_{\sigma_A})) dt \end{aligned} \quad (7.41)$$

# Bibliography

- [1] Wind energy barometer 2017. <https://www.eurobserv-er.org/\wind-energy-barometer-2017/>, 2017. Accessed: 2017-11-21.
- [2] Wind energy in europe, scenarios for 2030. <https://windeurope.org/about-wind/reports/wind-energy\in-europe-scenarios-for-2030/>, 2017. Accessed: 2017-11-21.
- [3] Marcelo Gustavo Molina and Juan Gimenez Alvarez. Technical and regulatory exigencies for grid connection of wind generation. In *Wind Farm-Technical Regulations, Potential Estimation and Siting Assessment*. InTech, 2011.
- [4] Wei Teng, Rui Jiang, Xian Ding, Yibing Liu, and Zhiyong Ma. Detection and quantization of bearing fault in direct drive wind turbine via comparative analysis. *Shock and Vibration*, 2016:1–12, 01 2016.
- [5] The gedser wind turbine. [http://mstudioblackboard.tudelft.nl/duwind/Wind%20energy%20online%20reader/Static\\_pages/wind\\_pioneers.htm](http://mstudioblackboard.tudelft.nl/duwind/Wind%20energy%20online%20reader/Static_pages/wind_pioneers.htm). Online, Accessed: 2019-1-19.
- [6] Tvind prototype. <https://en.wind-turbine-models.com/turbines/39-tvind-prototype>. Online, Accessed: 2019-1-19.
- [7] German onshore wind power ? output, business and perspectives. <https://www.cleanenergywire.org/factsheets/german-onshore-wind-power-output-business-and-perspectives>. Online, Accessed: 2019-1-16.
- [8] Jesús María Pinar Pérez, Fausto Pedro García Márquez, Andrew Tobias, and Mayorkinos Papaelias. Wind turbine reliability analysis. *Renewable and Sustainable Energy Reviews*, 23:463–472, 2013.
- [9] Peter Tavner, Clare Edwards, Andy Brinkman, and Fabio Spinato. Influence of wind speed on wind turbine reliability. *Wind Engineering*, 30(1):55–72, 2006.
- [10] Rudy Calif. Pdf models and synthetic model for the wind speed fluctuations based on the resolution of langevin equation. *Applied energy*, 99:173–182, 2012.

- [11] Flemming Petersen, Birger Svenningsen, Jytte Thorndahl, and Birgitte Wistoft. *Som vinden blæser*. KLO, 1994.
- [12] Krasnovsky wime d-30. <https://www.en.wind-turbine-models.com/turbines/1035-krasnovsky-wime-d-30>. Online, Accessed: 2019-1-19.
- [13] Wind turbine sg 10.0-193 dd. <https://www.siemensgamesa.com/en-int/products-and-services/offshore/wind-turbine-sg-10-0-193-dd>. Online, Accessed: 2019-1-19.
- [14] Wenxian Yang, Peter J Tavner, Christopher J Crabtree, Y Feng, and Y Qiu. Wind turbine condition monitoring: technical and commercial challenges. *Wind Energy*, 17(5):673–693, 2014.
- [15] Can intelligent blades sense the wind and adapt? <https://www.windpowerengineering.com/mechanical/blades/can-intelligent-blades-sense-the-wind-and-adapt/>. Online, Accessed: 2019-1-19.
- [16] Nghiem Aloys, Fraile Daniel, Mbistrova Ariola, and Remy Tom. Wind energy in Europe: Outlook to 2020. Technical report, Wind EUROPE, 09 2017.
- [17] GJW Van Bussel and MB Zaaijer. Reliability, availability and maintenance aspects of large-scale offshore wind farms, a concepts study. In *Proceedings of MAREC*, volume 2001, 2001.
- [18] GJW Van Bussel and MB Zaaijer. Estimation of turbine reliability figures within the dowec project. *DOWEC Report*, 10048(4), 2003.
- [19] PJ Tavner, DM Greenwood, MWG Whittle, R Gindele, S Faulstich, and B Hahn. Study of weather and location effects on wind turbine failure rates. *Wind Energy*, 16(2):175–187, 2013.
- [20] Johan Ribrant and Lina Bertling. Survey of failures in wind power systems with focus on swedish wind power plants during 1997-2005. In *Power Engineering Society General Meeting, 2007. IEEE*, pages 1–8. IEEE, 2007.
- [21] Johan Ribrant. Reliability performance and maintenance? a survey of failures in wind power systems. *KTH School of Electrical Engineering*, pages 59–72, 2006.
- [22] F Spinato, Peter J Tavner, GJW Van Bussel, and E Koutoulakos. Reliability of wind turbine subassemblies. *IET Renewable Power Generation*, 3(4):387–401, 2009.
- [23] Shuangwen Sheng. Report on wind turbine subsystem reliability? a survey of various databases. *National renewable energy laboratory-NREL/PR-5000-59111*, 2013.
- [24] LI Lin. S11500 series wind turbine pitch system failure analysis. *China Wind Power Production and Operation Management (2013) (in Chinese)*, 2013.

- [25] Amir Rasekhi Nejad, Zhen Gao, and Torgeir Moan. On long-term fatigue damage and reliability analysis of gears under wind loads in offshore wind turbine drivetrains. *International Journal of Fatigue*, 61:116–128, 2014.
- [26] ZR Shu, QS Li, YC He, and PW Chan. Observations of offshore wind characteristics by doppler-lidar for wind energy applications. *Applied Energy*, 169:150–163, 2016.
- [27] Ali Naci Celik. A statistical analysis of wind power density based on the weibull and rayleigh models at the southern region of turkey. *Renewable energy*, 29(4):593–604, 2004.
- [28] Rebecca Barthelmie, Ole Frost Hansen, Karen Enevoldsen, Jørgen Højstrup, Sten Frandsen, Sara Pryor, Søren Larsen, Maurizio Motta, and Peter Sanderhoff. Ten years of meteorological measurements for offshore wind farms. *Journal of Solar Energy Engineering*, 127(2):170–176, 2005.
- [29] H Saleh, A Abou El-Azm Aly, and S Abdel-Hady. Assessment of different methods used to estimate weibull distribution parameters for wind speed in zafarana wind farm, sues gulf, egypt. *Energy*, 44(1):710–719, 2012.
- [30] Cristina Herrero-Novoa, Isidro A Pérez, M Luisa Sánchez, Ma Ángeles García, Nuria Pardo, and Beatriz Fernández-Duque. Wind speed description and power density in northern spain. *Energy*, 138:967–976, 2017.
- [31] Teresa Scholz, Vitor V Lopes, and Ana Estanqueiro. A cyclic time-dependent markov process to model daily patterns in wind turbine power production. *Energy*, 67:557–568, 2014.
- [32] Christopher Lennard. Simulating an extreme wind event in a topographically complex region. *Boundary-layer meteorology*, 153(2):237–250, 2014.
- [33] MA Baseer, JP Meyer, S Rehman, and Md Mahbub Alam. Wind power characteristics of seven data collection sites in jubail, saudi arabia using weibull parameters. *Renewable Energy*, 102:35–49, 2017.
- [34] Nilay Sezer-Uzol and Lyle N Long. 3-d time-accurate cfd simulations of wind turbine rotor flow fields. *AIAA paper*, 394:2006, 2006.
- [35] Lars Landberg, Gregor Giebel, Henrik Aalborg Nielsen, Torben Nielsen, and Henrik Madsen. Short-term prediction—an overview. *Wind Energy*, 6(3):273–280, 2003.
- [36] Philippe Poggi, Marc Muselli, Gilles Notton, Christian Cristofari, and Alain Louche. Forecasting and simulating wind speed in corsica by using an autoregressive model. *Energy conversion and management*, 44(20):3177–3196, 2003.
- [37] Rajesh G Kavasseri and Krithika Seetharaman. Day-ahead wind speed forecasting using f-arima models. *Renewable Energy*, 34(5):1388–1393, 2009.

- [38] Heping Liu, Ergin Erdem, and Jing Shi. Comprehensive evaluation of arma-garch (-m) approaches for modeling the mean and volatility of wind speed. *Applied Energy*, 88(3):724–732, 2011.
- [39] Yousef MK Ali. *Forecasting power and wind speed using artificial and wavelet neural networks for Prince Edward Island (PEI)*. PhD thesis, Dalhousie University, 2010.
- [40] Haiyan Lub Jianzhou Wanga, Tong Niua. An analysis-forecast system for uncertainty modeling of wind speed: A case study of large-scale wind farms. *Applied Energy*, 211(5):492–512, 2018.
- [41] Ruey S Tsay. *Analysis of financial time series*, volume 543. John Wiley & Sons, 2005.
- [42] Barbara G Brown, Richard W Katz, and Allan H Murphy. Time series models to simulate and forecast wind speed and wind power. *Journal of climate and applied meteorology*, 23(8):1184–1195, 1984.
- [43] U Schlink and G Tetzlaff. Wind speed forecasting from 1 to 30 minutes. *Theoretical and applied climatology*, 60(1-4):191–198, 1998.
- [44] Tilmann Gneiting, Kristin Larson, Kenneth Westrick, Marc G Genton, and Eric Aldrich. Calibrated probabilistic forecasting at the stateline wind energy center: The regime-switching space-time method. *Journal of the American Statistical Association*, 101(475):968–979, 2006.
- [45] Lalarukh Kamal and Yasmin Zahra Jafri. Time series models to simulate and forecast hourly averaged wind speed in quetta, pakistan. *Solar Energy*, 61(1):23–32, 1997.
- [46] A Sfetsos. A novel approach for the forecasting of mean hourly wind speed time series. *Renewable energy*, 27(2):163–174, 2002.
- [47] EA Bossanyi. Short-term wind prediction using kalman filters. *Wind Engineering*, 9(1):1–8, 1985.
- [48] Petroula Louka, Georges Galanis, Nils Siebert, Georges Kariniotakis, Petros Katsafados, Ioannis Pytharoulis, and George Kallos. Improvements in wind speed forecasts for wind power prediction purposes using kalman filtering. *Journal of Wind Engineering and Industrial Aerodynamics*, 96(12):2348–2362, 2008.
- [49] Philippe Crochet. Adaptive kalman filtering of 2-metre temperature and 10-metre wind-speed forecasts in iceland. *Meteorological Applications*, 11(2):173–187, 2004.
- [50] Pedro M Fonte and JC Quadrado. Ann approach to wecs power forecast. In *Emerging Technologies and Factory Automation, 2005. ETFA 2005. 10th IEEE Conference on*, volume 1, pages 4–pp. IEEE, 2005.

- [51] MC Alexiadis, PS Dokopoulos, HS Sahsamanoglou, and IM Manousaridis. Short-term forecasting of wind speed and related electrical power. *Solar Energy*, 63(1):61–68, 1998.
- [52] Shuhui Li. Wind power prediction using recurrent multilayer perceptron neural networks. In *Power Engineering Society General Meeting, 2003, IEEE*, volume 4, pages 2325–2330. IEEE, 2003.
- [53] Mehmet Bilgili, Besir Sahin, and Abdulkadir Yasar. Application of artificial neural networks for the wind speed prediction of target station using reference stations data. *Renewable Energy*, 32(14):2350–2360, 2007.
- [54] Guo-Rui Ji, Pu Han, and Yong-Jie Zhai. Wind speed forecasting based on support vector machine with forecasting error estimation. In *Machine Learning and Cybernetics, 2007 International Conference on*, volume 5, pages 2735–2739. IEEE, 2007.
- [55] Junmo Koo, Gwon Deok Han, Hyung Jong Choi, and Joon Hyung Shim. Wind-speed prediction and analysis based on geological and distance variables using an artificial neural network: A case study in south korea. *Energy*, 93:1296–1302, 2015.
- [56] Erasmo Cadenas and Wilfrido Rivera. Short term wind speed forecasting in la venta, oaxaca, méxico, using artificial neural networks. *Renewable Energy*, 34(1):274–278, 2009.
- [57] Christopher J Crabtree, Donatella Zappalá, and Peter J Tavner. Survey of commercially available condition monitoring systems for wind turbines. 2014.
- [58] Jannis Tautz-Weinert and Simon J Watson. Using scada data for wind turbine condition monitoring—a review. *IET Renewable Power Generation*, 11(4):382–394, 2016.
- [59] Jung-Hun Park, Hyun-Yong Park, Seok-Yong Jeong, Sang-Il Lee, Young-Ho Shin, and Jong-Po Park. Linear vibration analysis of rotating wind-turbine blade. *Current applied physics*, 10(2):S332–S334, 2010.
- [60] Shuangwen Sheng and Paul S Veers. *Wind turbine drivetrain condition monitoring—an overview*. National Renewable Energy Laboratory Golden, Colo, USA, 2011.
- [61] TW Verbruggen. Wind turbine operation & maintenance based on condition monitoring wt- $\omega$ . *Final Report, April*, 2003.
- [62] Renaldas Raišutis, Elena Jasiūnienė, and Egidijus Žukauskas. Ultrasonic ndt of wind turbine blades using guided waves. *Ultragarsas*, 63(1):7–11, 2008.
- [63] Li Zhen, He Zhengjia, Zi Yanyang, and Chen Xuefeng. Bearing condition monitoring based on shock pulse method and improved redundant lifting scheme. *Mathematics and computers in simulation*, 79(3):318–338, 2008.

- [64] Randy R Schoen, Brian K Lin, Thomas G Habetler, Jay H Schlag, and Samir Farag. An unsupervised, on-line system for induction motor fault detection using stator current monitoring. *IEEE Transactions on Industry Applications*, 31(6):1280–1286, 1995.
- [65] Jun Wei and Joe McCarty. Acoustic emission evaluation of composite wind turbine blades during fatigue testing. *Wind Engineering*, pages 266–274, 1993.
- [66] Mahmood Shafiee and Maxim Finkelstein. An optimal age-based group maintenance policy for multi-unit degrading systems. *Reliability Engineering & System Safety*, 134:230–238, 2015.
- [67] Bryant Le and John Andrews. Modelling wind turbine degradation and maintenance. *Wind Energy*, 19(4):571–591, 2016.
- [68] Mahmood Shafiee, Maxim Finkelstein, and Christophe Bérenguer. An opportunistic condition-based maintenance policy for offshore wind turbine blades subjected to degradation and environmental shocks. *Reliability Engineering & System Safety*, 142:463–471, 2015.
- [69] JZ Sikorska, Melinda Hodkiewicz, and Lin Ma. Prognostic modelling options for remaining useful life estimation by industry. *Mechanical Systems and Signal Processing*, 25(5):1803–1836, 2011.
- [70] Dragan Banjevic. Remaining useful life in theory and practice. *Metrika*, 69(2-3):337–349, 2009.
- [71] Ariane Lorton, Mitra Fouladirad, and Antoine Grall. A methodology for probabilistic model-based prognosis. *European Journal of Operational Research*, 225(3):443–454, 2013.
- [72] Khanh Le Son, Mitra Fouladirad, Anne Barros, Eric Levrat, and Benoît Iung. Remaining useful life estimation based on stochastic deterioration models: A comparative study. *Reliability Engineering & System Safety*, 112:165–175, 2013.
- [73] Yaogang Hu, Hui Li, Pingping Shi, Zhaosen Chai, Kun Wang, Xiangjie Xie, and Zhe Chen. A prediction method for the real-time remaining useful life of wind turbine bearings based on the wiener process. *Renewable Energy*, 127:452–460, 2018.
- [74] YS Sherif and ML Smith. Optimal maintenance models for systems subject to failure—a review. *Naval research logistics quarterly*, 28(1):47–74, 1981.
- [75] Khanh Le Son, Mitra Fouladirad, and Anne Barros. Remaining useful life-time estimation and noisy gamma deterioration process. *Reliability Engineering & System Safety*, 149:76–87, 2016.
- [76] Bruno Castanier, Antoine Grall, and Christophe Bérenguer. A condition-based maintenance policy with non-periodic inspections for a two-unit series system. *Reliability Engineering & System Safety*, 87(1):109–120, 2005.

- [77] Christophe Bérenguer, Antoine Grall, Laurence Dieulle, and Michel Roussignol. Maintenance policy for a continuously monitored deteriorating system. *Probability in the Engineering and Informational Sciences*, 17(2):235–250, 2003.
- [78] Antoine Grall, Laurence Dieulle, Christophe Bérenguer, and Michel Roussignol. Continuous-time predictive-maintenance scheduling for a deteriorating system. *IEEE transactions on reliability*, 51(2):141–150, 2002.
- [79] Xiaojun Zhou, Lifeng Xi, and Jay Lee. Reliability-centered predictive maintenance scheduling for a continuously monitored system subject to degradation. *Reliability Engineering & System Safety*, 92(4):530–534, 2007.
- [80] Joeri Poppe, Robert N. Boute, and Marc R. Lambrecht. A hybrid condition-based maintenance policy for continuously monitored components with two degradation thresholds. *European Journal of Operational Research*, 268(2):515 – 532, 2018.
- [81] Sheldon M Ross. *Introduction to probability models*. Academic press, 2014.
- [82] Jinrui Ma, Mitra Fouladirad, and Antoine Grall. Flexible wind speed generation model: Markov chain with an embedded diffusion process. *Energy*, 164:316–328, 2018.
- [83] Nima Gorjian, Lin Ma, Murthy Mittinty, Prasad Yarlagadda, and Yong Sun. A review on degradation models in reliability analysis. In *Engineering Asset Lifecycle Management*, pages 369–384. Springer, 2010.
- [84] Hal Caswell. Matrix population models. *Encyclopedia of Environmetrics*, 3, 2006.
- [85] Rafael Pérez-Ocón, Juan Eloy Ruiz-Castro, and M Luz Gámiz-Pérez. A piecewise markov process for analysing survival from breast cancer in different risk groups. *Statistics in medicine*, 20(1):109–122, 2001.
- [86] Syed Waqar Haider, Karim Chatti, and Gilbert Y Baladi. Long-term pavement performance effectiveness of preventive maintenance treatments using markov chain algorithm. *Engineering Journal*, 16(4):149–158, 2012.
- [87] Meng-Lai Yin, John E Angus, and Kishor S Trivedi. Optimal preventive maintenance rate for best availability with hypo-exponential failure distribution. *IEEE Transactions on reliability*, 62(2):351–361, 2013.
- [88] Chongquan Zhong and Haibo Jin. A novel optimal preventive maintenance policy for a cold standby system based on semi-markov theory. *European Journal of Operational Research*, 232(2):405–411, 2014.
- [89] Jeffrey P Kharoufeh and Steven M Cox. Stochastic models for degradation-based reliability. *IIE Transactions*, 37(6):533–542, 2005.
- [90] Mohamed Abdel-Hameed. A gamma wear process. *IEEE transactions on Reliability*, 24(2):152–153, 1975.

- [91] Hanene Louahem M'Sabah, Azzedine Bouzaouit, and Ouafae Bennis. Simulation of bearing degradation by the use of the gamma stochastic process. *Mechanics and Mechanical Engineering*, 22(4):1309–1317, 2018.
- [92] JM van Noortwijk. Gamma process model for time-dependent structural reliability analysis. In *Numerical Modelling of Discrete Materials in Geotechnical Engineering, Civil Engineering and Earth Sciences: Proceedings of the First International UDEC/3DEC Symposium, Bochum, Germany, 29 September-1 October 2004*, page 101. CRC Press, 2004.
- [93] JM Van Noortwijk. A survey of the application of gamma processes in maintenance. *Reliability Engineering & System Safety*, 94(1):2–21, 2009.
- [94] Christian Thierfelder. The trending ornstein-uhlenbeck process and its applications in mathematical finance. *Mathematical Finance*, 2015.
- [95] Donald A Darling and AJF Siegert. The first passage problem for a continuous markov process. *The Annals of Mathematical Statistics*, pages 624–639, 1953.
- [96] PCB Phillips. The structural estimation of a stochastic differential equation system. *Econometrica: Journal of the Econometric Society*, pages 1021–1041, 1972.
- [97] Yingjun Deng, Anne Barros, and Antoine Grall. Degradation modeling based on a time-dependent ornstein-uhlenbeck process and residual useful lifetime estimation. *IEEE Transactions on Reliability*, 65(1):126–140, 2016.
- [98] Odd O Aalen and Håkon K Gjessing. Survival models based on the ornstein-uhlenbeck process. *Lifetime data analysis*, 10(4):407–423, 2004.
- [99] HB Hendriks, BH Bulder, JJ Heijdra, JTG Pierik, GJW Van Bussel, RPJOM van Rooij, M Zaaier, WAAM Bierbooms, D Th Den Hoed, GJ De Vilder, et al. Dowec concept study: Evaluation of wind turbine concepts for large scale offshore application. In *Proceedings of OWEMES*, volume 211, 2000.
- [100] HJT Kooijman, C Lindenburg, D Winkelaar, and EL Van der Hooft. Dowec 6 mw pre-design. *Energy Research Center of the Netherlands (ECN)*, 2003.
- [101] C Lindenburg. Aeroelastic modelling of the lmh64-5 blade. *Energy Research Center of the Netherlands, Technical Report No. DOWEC-02-KL-083/0, DOWEC 10083\_001*, 2002.
- [102] David J Malcolm and A Craig Hansen. Windpact turbine rotor design study: June 2000–june 2002 (revised). Technical report, National Renewable Energy Lab.(NREL), Golden, CO (United States), 2006.
- [103] Kevin Smith. Windpact turbine design scaling studies technical area 2: turbine, rotor, and blade logistics. *National Renewable Energy Laboratory, NREL/SR-500-29439*, 2001.
- [104] Repower 5m wind turbine. [https://www.thewindpower.net/turbine\\_en\\_14\\_repower\\_5m.php](https://www.thewindpower.net/turbine_en_14_repower_5m.php). Online, Accessed: 2019-1-07.

- [105] Offshore windpower m5000. <http://lumma.org/energy/specs/ArevaM5000.pdf>. Online, Accessed: 2019-1-07.
- [106] Jason Jonkman, Sandy Butterfield, Walter Musial, and George Scott. Definition of a 5-mw reference wind turbine for offshore system development. Technical report, National Renewable Energy Lab.(NREL), Golden, CO (United States), 2009.
- [107] Shashikanth Suryanarayanan and Amit Dixit. Control of large wind turbines: Review and suggested approach to multivariable design. In *Proc. of the American Control Conference*, pages 686–690. Citeseer, 2005.
- [108] Herbert E Merritt. *Hydraulic control systems*. John Wiley & Sons, 1967.
- [109] Peter Fogh Odgaard, Jakob Stoustrup, and Michel Kinnaert. Fault-tolerant control of wind turbines: A benchmark model. *IEEE Transactions on Control Systems Technology*, 21(4):1168–1182, 2013.
- [110] Peter F Odgaard and Kathryn E Johnson. Wind turbine fault detection and fault tolerant control-an enhanced benchmark challenge. In *American Control Conference (ACC), 2013*, pages 4447–4452. IEEE, 2013.
- [111] Laurent Rakoto, Julien Schorsch, and Michel Kinnaert. Modelling hydraulic pitch actuator for wind turbine simulation under healthy and faulty conditions? *IFAC-PapersOnLine*, 48(21):577–582, 2015.
- [112] H Nfaoui, H Essiarab, and AAM Sayigh. A stochastic markov chain model for simulating wind speed time series at tangiers, morocco. *Renewable Energy*, 29(8):1407–1418, 2004.
- [113] F Youcef Ettoumi, H Sauvageot, and A-E-H Adane. Statistical bivariate modelling of wind using first-order markov chain and weibull distribution. *Renewable energy*, 28(11):1787–1802, 2003.
- [114] Hongxing Yang, Yutong Li, Lin Lu, and Ronghui Qi. First order multivariate markov chain model for generating annual weather data for hong kong. *Energy and Buildings*, 43(9):2371–2377, 2011.
- [115] Roberto Carapellucci and Lorena Giordano. A new approach for synthetically generating wind speeds: A comparison with the markov chains method. *Energy*, 49:298–305, 2013.
- [116] Kevin Brokish and James Kirtley. Pitfalls of modeling wind power using markov chains. In *Power Systems Conference and Exposition, 2009. PSCE'09. IEEE/PES*, pages 1–6. IEEE, 2009.
- [117] Guglielmo D’Amico, Filippo Petroni, and Flavio Prattico. First and second order semi-markov chains for wind speed modeling. *Physica A: Statistical Mechanics and its Applications*, 392(5):1194–1201, 2013.
- [118] Rafael Zárata-Miñano, Marian Anghel, and Federico Milano. Continuous wind speed models based on stochastic differential equations. *Applied Energy*, 104:42–49, 2013.

- [119] Dennis L Elliott and Jack B Cadogan. Effects of wind shear and turbulence on wind turbine power curves. Technical report, Pacific Northwest Lab., Richland, WA (USA), 1990.
- [120] S Frandsen, I Antoniou, JC Hansen, L Kristensen, H Aa Madsen, B Chaviaropoulos, D Douvikas, JA Dahlberg, A Derrick, P Dunbabin, et al. Redefinition power curve for more accurate performance assessment of wind farms. *Wind Energy*, 3(2):81–111, 2000.
- [121] Julia Gottschall, Edgar Anahua, Stephan Barth, and Joachim Peinke. Stochastic modelling of wind speed power production correlations. *PAMM*, pages 665–666, 2006.
- [122] Julia Gottschall and Joachim Peinke. Stochastic modelling of a wind turbine’s power output with special respect to turbulent dynamics. In *Journal of Physics: Conference Series*, volume 75, page 012045. IOP Publishing, 2007.
- [123] Klaus Kaiser, W Langreder, H Hohlen, and J Højstrup. Turbulence correction for power curves. *Wind Energy*, pages 159–162, 2007.
- [124] William David Lubitz. Impact of ambient turbulence on performance of a small wind turbine. *Renewable Energy*, 61:69–73, 2014.
- [125] RJ Adrian, KT Christensen, and Z-C Liu. Analysis and interpretation of instantaneous turbulent velocity fields. *Experiments in fluids*, 29(3):275–290, 2000.
- [126] International Electrotechnical Commission et al. Iec 61400-1: Wind turbines part 1: Design requirements. *International Electrotechnical Commission*, 2005.
- [127] Jie Tang, Alexandre Brouste, and Kwok Leung Tsui. Some improvements of wind speed markov chain modeling. *Renewable Energy*, 81:52–56, 2015.
- [128] E Branlard. Generation of time series from a spectrum: Generation of wind time series from the kaimal spectrum, generation of wave time series from jonswap spectrum. *Technical University of Denmark*, 2010.
- [129] Jose A Carta, Penelope Ramirez, and Sergio Velazquez. A review of wind speed probability distributions used in wind energy analysis: Case studies in the canary islands. *Renewable and Sustainable Energy Reviews*, 13(5):933–955, 2009.
- [130] D Bocchetti, Massimiliano Giorgio, Maurizio Guida, and Gianpaolo Pulcini. A competing risk model for the reliability of cylinder liners in marine diesel engines. *Reliability Engineering & System Safety*, 94(8):1299–1307, 2009.
- [131] Haitao Liao and Zhigang Tian. A framework for predicting the remaining useful life of a single unit under time-varying operating conditions. *Iie Transactions*, 45(9):964–980, 2013.

- [132] Xuejing Zhao, Mitra Fouladirad, Christophe Bérenguer, and Laurent Bordes. Condition-based inspection/replacement policies for non-monotone deteriorating systems with environmental covariates. *Reliability Engineering & System Safety*, 95(8):921–934, 2010.
- [133] CHAD CASAROTTO. Markov chains and the ergodic theorem. 2007.
- [134] Linda Kaufman. Matrix methods for queuing problems. *SIAM Journal on Scientific and Statistical Computing*, 4(3):525–552, 1983.
- [135] RE Funderlic and JB Mankin. Solution of homogeneous systems of linear equations arising from compartmental models. *SIAM Journal on Scientific and Statistical Computing*, 2(4):375–383, 1981.
- [136] Luciano Galeone. The use of positive matrices for the analysis of the large time behavior of the numerical solution of reaction-diffusion systems. *mathematics of computation*, 41(164):461–472, 1983.
- [137] P. G. Moschopoulos. The distribution of the sum of independent gamma random variables. *Ann. Inst. Statist. Math.*, 37(Part A):541–544, 1985.
- [138] Mohamed Akkouchi. On the convolution of gamma distributions. *Soochow Journal of Mathematics*, 31(2):205–211, 2005.
- [139] A Platis, N Limnios, and M Le Du. Hitting time in a finite non-homogeneous markov chain with applications. *Applied stochastic models and data analysis*, 14(3):241–253, 1998.
- [140] L'éolien dans la transition (in french). <https://fee.asso.fr/la-transition-energetique/>. Online, Accessed: 2019-2-25.

# Jinrui MA

## Doctorat : Optimisation et Sûreté des Systèmes

### Année 2019

#### Modélisation pour le pronostic et la maintenance des éoliennes

De plus en plus d'éoliennes sont exploitées pour produire de l'énergie électrique. Les éoliennes de grande taille fonctionnent de manière automatique dans des conditions environnementales souvent difficiles. Il en résulte des dégradations et des défaillances provoquant des arrêts indésirables. En conséquence, les recherches sur la fiabilité des éoliennes attirent beaucoup d'attention. Le principal composant étudié dans cette thèse est un composant crucial pour les éoliennes à vitesse variable : le système hydraulique d'orientation des pales. Trois sujets sont abordés : la modélisation de la détérioration du système hydraulique de contrôle de l'angle de tangage, l'estimation de sa durée de vie utile restante et une politique de maintenance. La principale contribution de la thèse est la prise en compte de l'influence de l'environnement caractérisé par la vitesse du vent. Un modèle continu à long terme d'évolution de la vitesse du vent est proposé. Un simulateur d'éolienne avec système hydraulique de contrôle de tangage se détériorant est établi pour effectuer les simulations numériques. Cette thèse illustre l'intérêt des processus stochastiques pour la modélisation dans le domaine de l'énergie éolienne. Le modèle de vitesse du vent s'appuie sur une chaîne de Markov à deux niveaux avec diffusion intégrée. Le processus de détérioration du système hydraulique de contrôle est modélisé par un processus gamma couplé à une chaîne de Markov. Sur cette base, la durée de vie et l'indisponibilité de l'éolienne sont modélisées, évaluées et utilisées pour l'aide à la décision de maintenance.

Mots clés : éoliennes – vents, vitesse – entretien – processus stochastiques – durée de vie (ingénierie).

#### Prognosis and Maintenance Modelling for Wind Turbines

Nowadays, more and more wind turbines are erected on-shore or off-shore to generate electric energy from wind. Since the valuable big-size wind turbines automatically operate under harsh environment, undesirable downtime occurs from degradations and failures caused by the environment. Therefore, the research about the reliability of wind turbine attract a lot of attention.

The main component studied in this thesis is the hydraulic pitch system. It is a crucial component for variable-speed wind turbines. Three subjects are addressed: the hydraulic pitch system deteriorating modelling, its remaining useful lifetime estimation, and its maintenance. The methods proposed are not only limited to the hydraulic pitch system, but also can be extended to the dynamic systems that operate under various environment.

The main contribution of the thesis is that the influence of the environment (wind speed) is always taken into account. A continuous long-term wind speed model is proposed as a research by product. A wind turbine simulator is established to carry out the numerical simulations. It specifically includes a deteriorating model for hydraulic pitch system.

This thesis highlights the relevance of stochastic processes in the field of wind energy modelling. The wind speed model is based on a two-level Markov chain with embedded diffusion processes. The deterioration process of hydraulic pitch system is modelled by a gamma process driven by a Markov chain. On these bases, the remaining useful life and the unavailability of wind turbine are discussed and used for maintenance decision-making.

Keywords: wind turbines – winds, speed – maintenance – stochastic processes – service life (engineering).

Thèse réalisée en partenariat entre :

